United Arab Emirates University
Scholarworks@UAEU

Theses | Electronic Theses and Dissertations

4-2016

Sand Area Changes in the Emirate of Abu Dhabi, United Arab Emirates between 1992 and 2013 Using a Time Series of Satellite Imagery

Rami W A Saeed

Follow this and additional works at: https://scholarworks.uaeu.ac.ae/all_theses

Part of the Education Commons

Recommended Citation

A Saeed, Rami W, "Sand Area Changes in the Emirate of Abu Dhabi, United Arab Emirates between 1992 and 2013 Using a Time Series of Satellite Imagery" (2016). *Theses*. 281.
https://scholarworks.uaeu.ac.ae/all_theses/281

This Thesis is brought to you for free and open access by the Electronic Theses and Dissertations at Scholarworks@UAEU. It has been accepted for inclusion in Theses by an authorized administrator of Scholarworks@UAEU. For more information, please contact fadl.musa@uaeu.ac.ae.

United Arab Emirates University

College of Humanities and Social Sciences

Department of Geography & Urban Planning

SAND AREA CHANGES IN THE EMIRATE OF ABU DHABI, UNITED ARAB EMIRATES BETWEEN 1992 AND 2013 USING A TIME SERIES OF SATELLITE IMAGERY

Rami W A Saeed

This thesis is submitted in partial fulfilment of the requirements for the degree of Master of Science in Remote Sensing and Geographic Information Systems

Under the Supervision of Dr. Nazmi Saleous

April 2016

Declaration of Original Work

I, Rami W A Saeed, the undersigned, a graduate student at the United Arab Emirates University (UAEU), and the author of this thesis entitled "*Sand area changes in the emirate of Abu Dhabi, United Arab Emirates between 1992 and 2013 using a time series of satellite imagery*", hereby, solemnly declare that this thesis is my own original research work that has been done and prepared by me under the supervision of Dr. Nazmi Saleous, in the College of Humanities and Social Sciences at UAEU. This work has not previously been presented or published, or formed the basis for the award of any academic degree, diploma or a similar title at this or any other university. Any materials borrowed from other sources (whether published or unpublished) and relied upon or included in my thesis have been properly cited and acknowledged in accordance with appropriate academic conventions. I further declare that there is no potential conflict of interest with respect to the research, data collection, authorship, presentation and/or publication of this thesis.

Student's Signature: 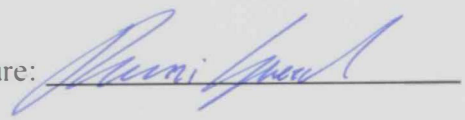 Date: 31- 5- 2016

Copyright © 2016 Rami W A Saeed
All Rights Reserved

Advisory Committee

1) Advisor: Dr. Nazmi Zeidan Saleous

Title: Associate Professor

Department of Geography & Urban Planning

College of Humanities and Social Sciences

2) Co-advisor: Dr. Salem Mohammed Ghaleb Issa

Title: Associate Professor

Department of Geology

College of Science

Approval of the Master Thesis

This Master Thesis is approved by the following Examining Committee Members:

1) Advisor (Committee Chair): Dr. Nazmi Saleous
   Title: Associate Professor
   Department of Geography and Urban Planning
   College of Humanities and Social Sciences
   Signature _____ Date 15.5.16

2) Member: Dr. Shahrazad Abu Ghazleh
   Title: Assistant Professor
   Department of Geography and Urban Planning
   College of Humanities and Social Sciences
   Signature _____ Date 15.5.16

3) Member: N/A
   Title:
   Department of ...
   College of ...
   Signature _____ Date _____

4) Member (External Examiner):
   Title: Dr. Marouane Temimi
   Department of Water and Environmental Engineering
   Institution: Masdar Institute of Science and Technology
   Signature _____ Date 15.5.16

This Master Thesis is accepted by:

Dean of the College of Humanities and Social Sciences: Professor Saif Salim Al-Qaydi

Signature _____ Date 18.5.16

Dean of the College of the Graduate Studies: Professor Nagi T. Wakim

Signature _____ Date 31/5/2016

Copy 1 of 11

Abstract

Sand encroachment is a major problem that affects arid countries and has severe consequences on their infrastructure. It poses a threat to the environment, roads, habitats, farms and plantations thus requiring human intervention for the removal of the encroaching sands. Tracking sand dune movement and sand changes in such regions and studying their trajectories in time is very important. It allows governments to plan better counter measures to prevent their occurrence and minimize their danger.

The Emirate of Abu Dhabi underwent significant socioeconomic changes during the study period, which resulted in an unprecedented boom in population growth, reflected by increased demand for new infrastructures and urban development. Sand movements are accelerated by anthropogenic activities, as witnessed through their encroachment onto farms and interstate roadways. In this study, we used remote sensing data to map sand movement and its effect on urban and agricultural areas.

Using six individual Landsat scenes to create a mosaic for each of the study dates of 1992, 2002, and 2013, we created land cover thematic maps using supervised classification. The resulted maps were checked and evaluated using higher resolution imagery, namely SPOT, IKONOS, and RapidEye. They were then imported into GIS where change analysis was run using the post classification procedure. Change analysis results indicated an increase in sand cover, between 1992 and 2013, by 1.26%. The using of Landsat imagery to track changes in land cover features over a large region and across time proved to be very useful for better understanding of changes, their trajectories, and their causes and impacts.

Keywords: Remote Sensing, GIS, Land cover classification, Sand area change, Abu Dhabi, UAE.

Title and Abstract (in Arabic)

مساحة تغيير الاراضي الرملية في إمارة أبو ظبي، الإمارات العربية المتحدة بين عام 1992 وعام 2013 باستخدام سلسلة زمنية من صور الأقمار الصناعية

الملخص

زحف الرمال هى مشكلة رئيسة تؤثر على البلدان الصحراوية و لها عواقب وخيمة تؤثر على بنيتها التحتية. حيث انها تشكل خطرا على البيئة والطرق والمواطن الطبيعية والمزارع والمناطق الحضرية مما يتطلب التدخل البشري لوقف وا زالة زحف الرمال. ومن المهم جدا تتبع حركة الكثبان الرملية ومراقبة مساراتها ودراستها لاتاحة الفرصة للحكومات لوضع الخطط المناسبة لمنع وقوعها والحد من خطورتها.

خلال فترة الدراسة شهدت إمارة أبو ظبي تغييرات كبيرة في النواحي الاجتماعية والاقتصادية والتنمية الحضرية، مما أدى إلى طفرة غير مسبوقة في النمو السكاني نتج عنه زيادة العبء على البنية التحتية الجديدة. وساهمت الأنشطة البشرية والحركة فى المزارع والطرق الصحراوية في زيادة تحركات الرمال وفي هذه الدراسة تم استخدام بيانات الاستشعار عن بعد لرسم خريطة تبين حركة الرمال وتأثيرها على المناطق الحضرية والزراعية.

باستخدام لاندسات (Landsat) قمنا بعمل فسيفساء من ستة مشاهد للفترة التى تغطيها الدراسة عن عام 1992، 2002 و 2013 وأنشأنا الخرائط الموضعية التي تبين الغطاء الأرضي بالتصنيف الاشرافى. و تم فحص ومقارنة هذه الخرائط وتقييمها باستخدام أعلى مستويات الاستبانة بواسطة معلومات من الاقمار الصناعية IKONOS و Spot و RapidEye وتم ادخال هذه المعلومات الى نظم المعلومات الجغرافية (GIS) حيث تم إجراء تحليل التغيرات باستخدام اجرآت ما بعد التصنيف. وأشارت النتائج الى زيادة في غطاء الرمال بين عامي 1992 و 2013 بنسبة 1.26٪.

أثبتت الدراسة ان استخدام التصويرعن طريق لاندسات لتعقب التغييرات في ملامح الغطاء الأرضي على منطقة كبيرة وعبر فترة زمنية محددة أنه مفيد جدا لمعرفة هذه التغيرات و مساراتها وأسبابها وآثارها.

مفاهيم البحث الرئيسية: الاستشعارعن بعد، نظم المعلومات الجغرافية، حركة الرمال مساحة تغيير الاراضي الرملية، أبو ظبي، الإمارات العربية المتحدة.

Acknowledgements

My thanks go to both my professors, Dr. Nazmi Saleous and Dr. Salem Issa whose support and teachings led me to better understand the field of remote sensing & GIS, our discussions taught me a great deal.

Special thanks go to my mother, father, brothers, sisters, and my significant other who helped me along the way.

To all my relatives who waited eagerly for my dissertation, especially Uncles Sultan & Samer.

I am sure they suspected it was endless, but here we are now.

Told you I'd get it done ☺

Dedication

To my beloved parents and family

Thank you for your support

Table of Contents

Title i
Declaration of Original Work ii
Copyright iii
Advisory Committee iv
Approval of the Master Thesis v
Abstract vii
Title and Abstract (in Arabic) ix
Acknowledgements xi
Dedication xii
Table of Contents xiii
List of Tables xv
List of Figures xvii
List of Abbreviations xix
Chapter 1: Introduction 1
1.1 Background 1
1.2 The Study Area 2
1.2.1 Physical Setting 6
1.2.2 Climate 10
1.2.3 Socio-Economic 11
1.3 Scope of the Research 12
1.4 Aim & Objectives 12
1.5 Hypotheses and Assumptions 13
1.6 Thesis Structure 13
1.7 Summary 14
Chapter 2: Sand Dunes and Remote Sensing 16
2.1 Background 16
2.2 Benefits and Limitations of Remote Sensing of Sand Dunes 16
2.3 Multispectral Classification & Mapping of Sand Dunes 20
2.4 Change Analysis Techniques 24
2.5 Summary 26
Chapter 3: Research Methodology 27
3.1 Introduction 27
3.2 Spatial Datasets & Software 28
3.3 Data preparation 30

3.4 Classification Scheme 32
3.5 Determining LULC classes 34
3.6 Image Classification & Post Processing 38
3.7 Extracting sand dunes from satellite images (MSS 1992, ETM+ 2002, OLI 2013) 39
3.8 Accuracy Assessment 39
3.9 Dune change analysis techniques 41

Chapter 4: Results & Discussion 46
4.1 Training Site Class Identification 46
4.2 Training Site Selection 48
4.3 1992 LULC Map 49
4.4 2002 LULC Map 51
4.5 2013 LULC Map 53
4.6 Accuracy Assessment 55
4.7 Change Analysis 58
4.8 Discussion 70

Chapter 5: Conclusion & Recommendations 81

Bibliography 84

Appendix 89

List of Tables

Table 1.1: Mineralogy of the UAE 6

Table 3.1: Summary of Dates and Scenes Used.....90

Table 3.2: Comparison between CDR of Landsat 4 -7 and Landsat 8.....32

Table 3.3: Themes as per Anderson 1976.....33

Table 3.4: Revised Anderson 1976 Themes as per Region of Study Area.....33

Table 3.5: Original Image.....91

Table 3.6: Inverse PCA.....91

Table 3.7: List of accuracy assessment sites.....95

Table 3.8: Imagery used for accuracy assessment.....90

Table 3.9: Union of three years.....43

Table 3.10: Final Product of from – to change across three years.....43

Table 3.11: Change trajectories between two years.....44

Table 3.12: Change trajectories for sand and non-sand between two years.....44

Table 3.13: Change trajectories for sand and non-sand across three years.....45

Table 4.1: Statistical Classifiable Classes.....48

Table 4.2: 1992 feature class areas.....49

Table 4.3: 2002 feature class areas.....51

Table 4.4: 2013 feature class areas.....53

Table 4.5: Accuracy Assessment of 1992 Classification.....56

Table 4.6: Accuracy Assessment of 2002 Classification.....57

Table 4.7: Accuracy Assessment of 2013 Classification.....58

Table 4.8: Changes from 1992 to 2002 statistics.....97

Table 4.9: Changes for sand features from 1992 to 2002 statistics.....97

Table 4.10: Changes from 2002 to 2013 statistics.....99

Table 4.11: Changes for sand features from 2002 to 2013 statistics.....99

Table 4.12: Sand / Non Sand change analysis statistics from 1992 -2002 -2013.....102

List of Figures

Figure 1.1: UAE's landscape in true color WorldView-2 composite (5,3,2).....4

Figure 1.2: UAE's seven Emirates boundaries.....5

Figure 1.3: Dune Faces and Wind Interactions.....7

Figure 1.4: Distribution of global deserts.....8

Figure 1.5: Relationship of Dune Pattern & Wind Directions.....89

Figure 1.6: Sand movement with wind.....10

Figure 3.1: Dissertation methodology process.....27

Figure 3.2: Landsat Path & Rows Covering the UAE.....29

Figure 3.3: The Study Area of the Dissertation inside Red Boundary.....29

Figure 3.4: Representation of mosaic Seamlines.....31

Figure 3.5: Pilot Study Area Used to Identify Classes.....34

Figure 3.6: Forward PCA of Pilot Study in First Three Principal Components (PCs).....35

Figure 3.7: Inverse PCA of the First Three PCs in True Color RGB.....36

Figure 3.8: Entropy Texture of Pilot Study Area.....37

Figure 3.9: ISODATA Results for Pilot Study.....38

Figure 3.10: Distribution of accuracy assessment sites.....40

Figure 3.11: Multi Year change detection methodology.....42

Figure 3.12: Change trajectories across three years.....45

Figure 4.1: Final Outcome after Merge of Classes.....47

Figure 4.2: Final Outcome after Merge of Classes.....47

Figure 4.3: Thematic Map of 1992.....50

Figure 4.4: 1992 Thematic Map Showing Sand & Non-Sand Classes.....50

Figure 4.5: Thematic Map of 2002.....52

Figure 4.6: 2002 Thematic Map Showing Sand & Non-Sand Classes.....52

Figure 4.7: Thematic Map of 2013.....54

Figure 4.8: 2013 Thematic Map Showing Sand & Non-Sand Classes.....54

Figure 4.9: Change Trajectory Map from 1992 to 2002.....59

Figure 4.10: Change Trajectory Map of Sand from 1992 to 2002.....60

Figure 4.11: Change Trajectory Map of Sand from 1992 to 2002.....61

Figure 4.12: Change Trajectory Map from 2002 to 2013.....62

Figure 4.13: Change Trajectory Map of Sand from 2002 to 2013.....63

Figure 4.14: Change Trajectory Map of Sand from 1992 to 2002.....64

Figure 4.15: Change trajectory from 1992 to 2002 to 2013.....65

Figure 4.16: Total of 203 change trajectories from 1992 to 2002 to 2013.....66

Figure 4.17: Changes in sand trajectories from 1992 to 2002 to 2013.....67

Figure 4.18: Total of 85 change trajectories for sand from 1992 to 2002 to 2013.....68

Figure 4.19: Change Trajectory Map of Sand / Non Sand from 1992 to 2002 to 2013.....69

Figure 4.20: Features Classed as Non-Sand.....70

Figure 4.21: Features Classed as Sand.....71

Figure 4.22: Coastal areas in 1992.....72

Figure 4.23: Coastal areas in 2013 since 1992.....73

Figure 4.24: Sate of coastal areas in 1992.....74

Figure 4.25: Coastal change in 2013 since1992.....74

Figure 4.26: Population distribution in 1992.....75

Figure 4.27: Population change in 2013 since 1992.....76

Figure 4.28: Road network limited in 1992.....77

Figure 4.29: Network enhancement allowed growth in 2013 since 1992.....77

Figure 4.30: Empty unused spaces in 1992.....78

Figure 4.31: Subsides allowed expansion in 2013 since 1992.....79

List of Abbreviations

UAE	United Arab Emirates
GIS	Geographic Information System
GDP	Gross Domestic Product
CDR	Climate Data Record
TM	Thematic Mapper
ETM+	Enhanced Thematic Mapper Plus
LULC	Land Use / Land Cover
NDVI	Normalized Difference Vegetation Index
CI	Crust Index
GSI	Grain Size Index
SAVI	Soil Adjusted Vegetation Index
PCA	Principal Component Analysis
PC	Principal Component
MSS	Multispectral Scanner System
LEDAPS	Landsat Ecosystem Disturbance Adaptive Processing Systems
MODIS	Moderate Resolution Imaging Spectroradiometer
DEM	Digital Elevation Model
TOA	Top of Atmosphere
ISODATA	Iterative Self Organizing Data Analysis Technique

Chapter 1: Introduction

1.1 Background

The United Arab Emirates (UAE) is located in the eastern region of the Arabian Peninsula, west of Asia. It border the Gulf of Oman and the Arabian Gulf, between Oman and Saudi Arabia, between coordinates of 22° 45' and 25° 45' N and 51° 45' and 56° E. Its climate is extremely arid and to semi-arid the eastern mountains of the country. Its area covers a total of 83,600 km^2 and is composed of flat, barren coastal plain merging into rolling sand dunes of vast desert making up 75% of the country (El-Sayed, 1999), and mountains in the east (*Figure 1.1*).

The country is a union of seven emirates: Abu Dhabi, Ajman, Dubai, Fujairah, Ras al Khaimah, Sharjah, and Umm al Quwain. Six of the seven emirates first came together in 1971, with the seventh, Ras al Khaimah, joining in 1972 (*Figure 1.2*). Abu Dhabi makes up 87% of the country's total surface area and hosts the capital city, Abu Dhabi.

The UAE's land boundaries extend up to 1066 Km: 609 Km of which are with Oman and 457 Km are with Saudi Arabia. The country's coastline extends to 1318 Km and is situated in a strategic location along the southern part of the Strait of Hormuz, which is a vital transit point for world crude oil transport.

Before the discovery of oil in the country, the Emirate of Abu Dhabi was one of the poorest coastal states, where its economy was limited to and primarily relied on oasis agriculture, fishing, pearling and trade with neighboring countries (Al Ahbabi 2002). However, after the discovery of the first commercial oil field (Bab

field) in 1958 followed by the first crude oil shipment in 1962. Abu Dhabi quickly became one of the richest states in the region, which allowed the funding of development projects, not just across the emirate but also across the union just within 10 years of entering the global oil market.

As the first president of the UAE, Sheikh Zayed bin Sultan Al- Nahayan immediately foresaw the need to invest in the development of the emirates' infrastructure. Plans to develop nation quickly took place and many facilities were rooted such as road networks, educational institutions, and ports. Oil revenues of the country were a major turning point, not just for the Emirate of Abu Dhabi, but the country as a whole.

By 2014, the United Nations estimated the UAE's population to be around 9,445,624, with 80% of the total population made up of immigrants, all living in a country that is vastly dunes. Coupled with the rapid urban expansion of the country, sand dunes pose a risk to road networks, human habitats, and farm lands due to their migration by winds that reach speeds between 6 – 10 m/s.

This sand movement has forced the government to continuously and vigorously invest in either setting up barriers or relocating sand dunes via heavy machinery, both being costly endeavors.

1.2 The Study Area

The Abu Dhabi emirate is located in the western southern part of the country, and is divided into three administrations: Abu Dhabi, Al Ain, and the Western Region Municipality. The emirate borders Oman to the East, Saudi Arabia to the South and West, and the Arabian Gulf to the North. It includes over 200 islands,

including major ones such as Mubarraz, Zirkyu, Delma, Sir Bani Yas, Marawah, Abu Abyadh, and Saadiat. The emirate could be divided into five different landforms: sand dunes, interdune areas, coastal sabkhas, inland sabkhas, and exposed rock (Glennie 1996).

The Abu Dhabi emirate was selected for this study because it makes up 87% of the total country in terms of land area, and the large majority of the emirate is covered with dunes, that pose a threat to farms and roads as they migrate. Furthermore, dunes, in general, have not been studied extensively in the emirate, thus presenting the opportunity to further explore how Landsat could support dune studies. Moreover, the UAE, as a whole, saw an unprecedented urban growth in the time span of 40 odd years, where the whole country changed from a nomad-like lifestyle to a brimming beacon of civilization, thus giving the opportunity to see the drastic changes in land cover over a short period of time.

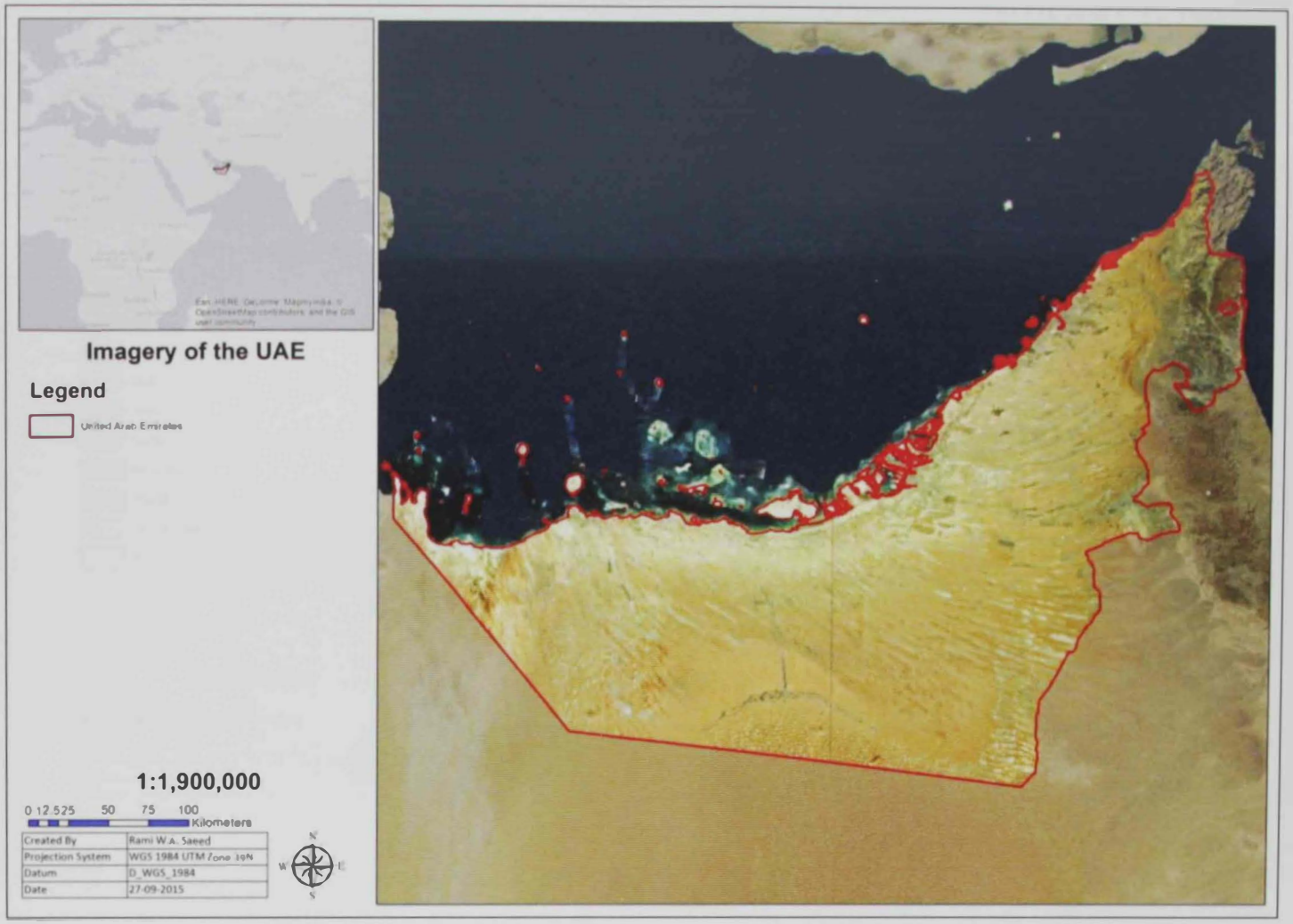

Figure 1.1: UAE's landscape in true color WorldView-2 composite (5.3.2)

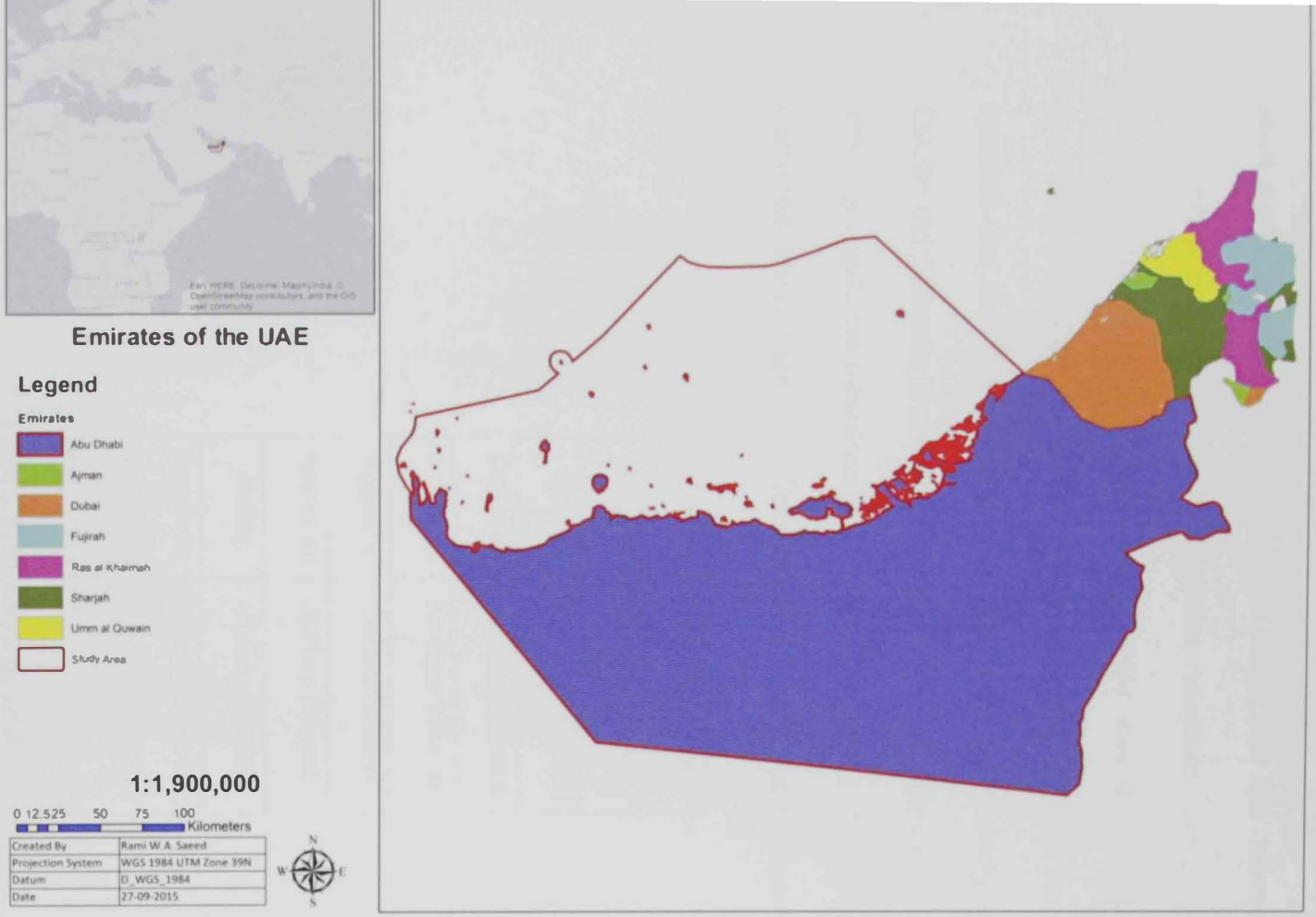

Figure 1.2: UAE's seven Emirates boundaries

1.2.1 Physical Setting

The UAE's terrain is composed of a rich variety of landforms traversing a short range of distance. Studies have noted that the minerals that could be encountered are: Quartz, Calcite, Dolomite, Anorthite, Gypsum, Anhydrite, Halite, Aragonite, and Celestite (Howari, 2007). While other studies that used Landsat and band ratio to perform land cover classification based on surface mineralogy, have revealed that the four main minerals that could be remotely sensed are Quartz, Calcite and Dolomite (carbonate minerals), and Anorthite (feldspar mineral) (Pease, 1999). As such, the minerloaogical composition of the UAE falls into five classes: Carbonate, Mixed Carbonate, Quartz, Mixed Quartz, and Feldspar (*Table 1.1*)

Mineral	Mineral Type
Quartz	Silicate Mineral
Calcite	Carbonate Mineral
Dolomite	Carbonate Mineral
Anorthite	Feldspar Mineral
Gypsum	Sulfate Mineral
Anhydrite	Sulfate Mineral
Halite	Halide Mineral
Aragonite	Carbonate Mineral
Celestite	Sulfate Mineral

Table 1.1: Mineralogy of the UAE

Dunes are frequent in desert environments, and they are an accumulation of sediments blown by wind into mounds or ridges. They have two faces, one is a gentle windward slope that is wind facing and dominated by sand depositions and sand saltation, while the other is a downwind side that is commonly a steep avalanche known as the slip face. The slip face, stands at an angle of repose, which is the maximum angle at which the material would lose stability, causing sand dune migration, and that angle lies between 30° and 34° for sand (*Figure 1.3*); Moreover, dunes can have more than one slip face (Summerfield, 1996).

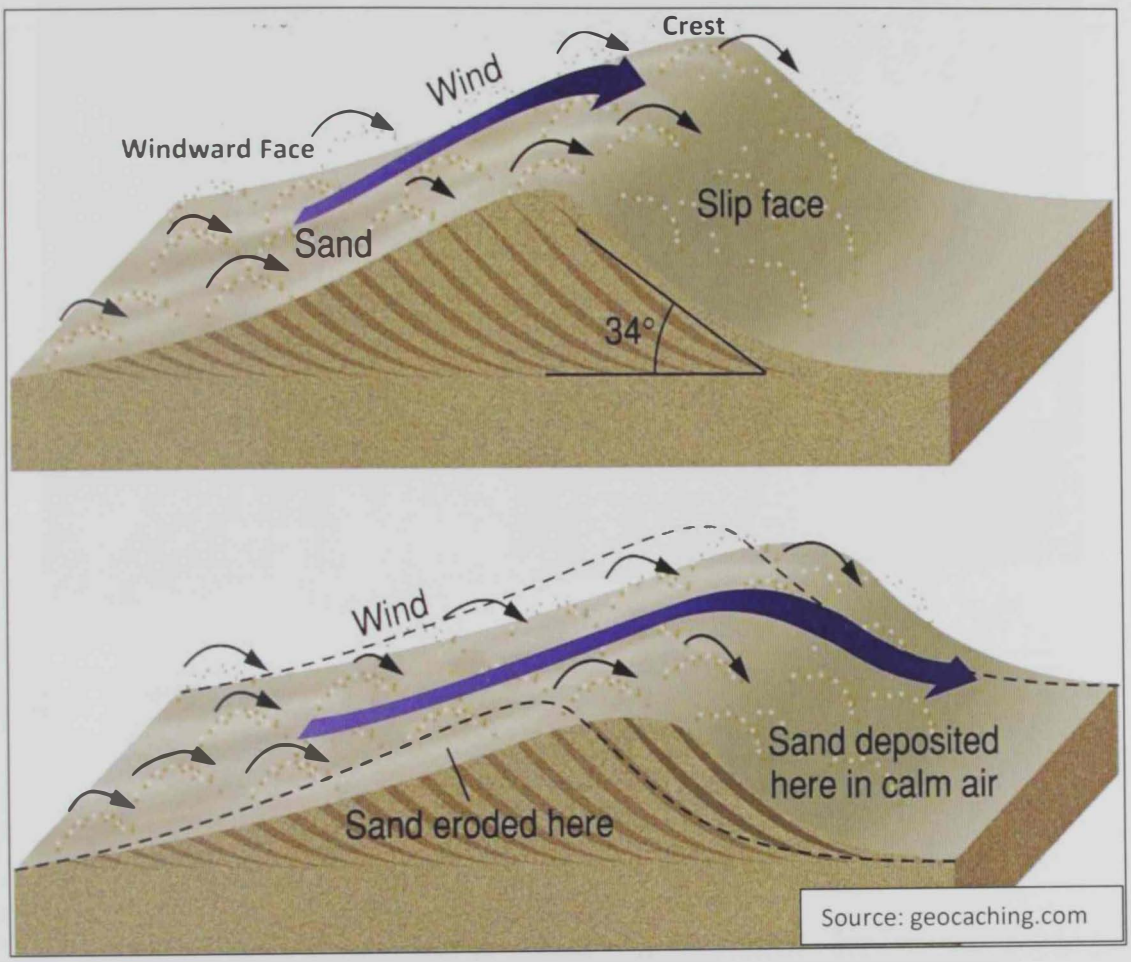

Figure 1.3: Dune Faces and Wind Interactions

Desertification, sand encroachment, and dust storms are some of the geological hazards related to the increasing climate change and anthropogenic activity found in

arid lands associated with Aeolian systems. Aeolian sand dunes are one of the most widely studied land cover features in the world. They cover almost 10% of the land between latitudes 30°N and 30°S (Sarnthein, 1978) and occupy about 75% of the United Arab Emirates' (UAE) surface area (*Figure 1.4*), thus making it one of the most important geomorphological features in the country (El-Sayed, 1999), and nearly all known types of sand dunes occur in it (Embabi, 1993).

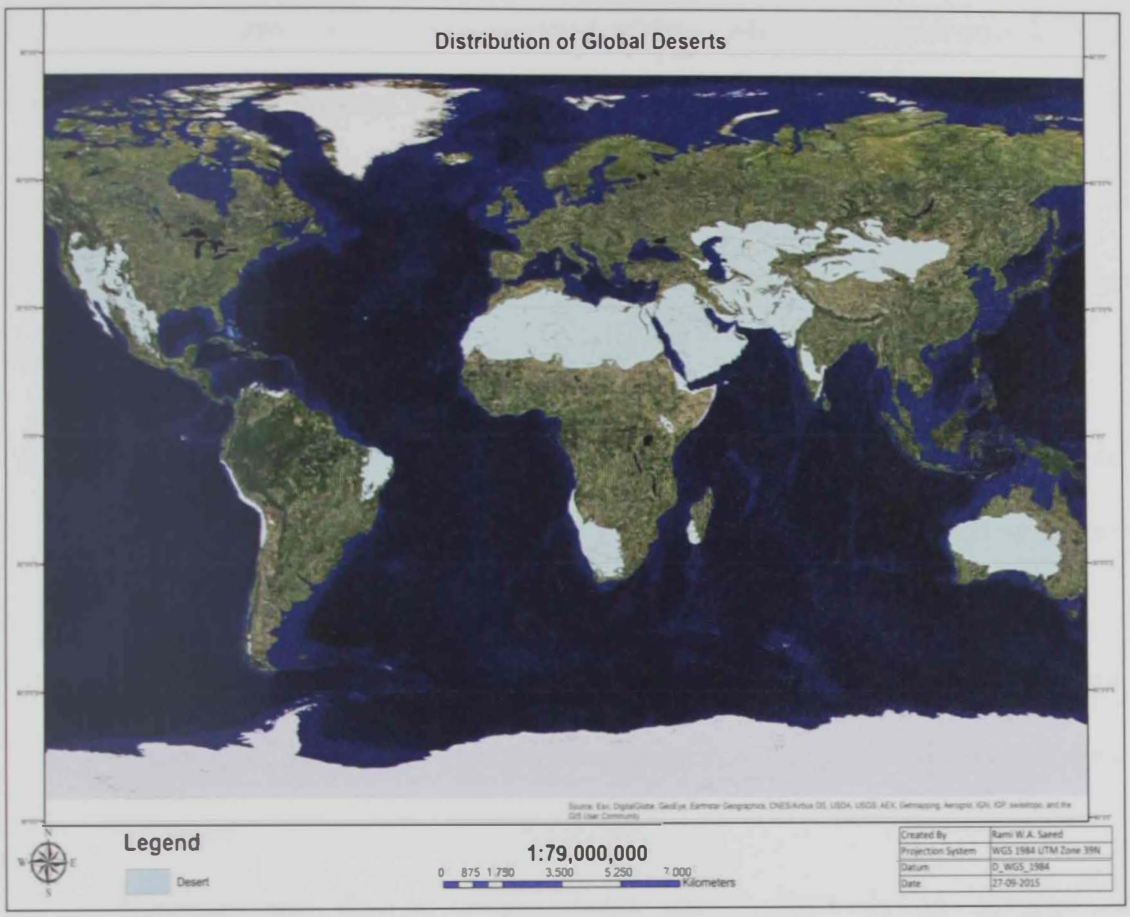

Figure 1.4: Distribution of global deserts

Aeolian sand dunes are prominent in the UAE due to the country's climatological patterns, where the lack of rainfall and summer temperatures reaching 50°C, coupled with the scarcity of vegetation cover and strong wind patterns, all

contribute to the suitable conditions that enhance sand dune movement (Glenni, 2001, Al-Awadi, 2004)

Sand dunes are dynamic in nature, with dunes changing their location, length, or height, depending on their type (Tsoar, 2001) and they are mainly influenced by wind regime, sand supply, vegetation cover, and grain size. Changes in any of the aforementioned variables would affect how dunes are formed, for example, a linear dune is formed under a bidirectional wind regime, whereas a transverse dune is formed under a unidirectional wind regime with an ample supply of sand (Wasson & Hyde, 1983)

According to Tsoar (2004), sand dunes could be classified into three distinctive groups (*Appendix A Figure 1.5*):

a) **Migrating Dunes**: where the whole dune body advances with little or no change in the shape and dimension. Transverse and crescent (barchan) dunes are examples of migrating dunes.

b) **Elongating Dunes**: where the length of the dune increases over time through a very different process than the ones that affect the migrating dunes. Linear dunes are examples of elongating dunes.

c) **Accumulating Dunes**: where dunes exhibit little or no advance or elongation. Star dunes are an example of accumulating dunes.

In the study area, the major types of dunes encountered are barchans, Barchanoid, and transverse for the migrating group, linear for the elongating, and star dunes for the accumulating (Embabi, 1991).

As for their movement, sand dunes are known to move or jump above the surface when wind speeds reach 5.5 – 6 m/sec, a process known as saltation that causes sand to be accumulated on the crest (*Figure 1.6*) (Abu Al-Khair, 1981)

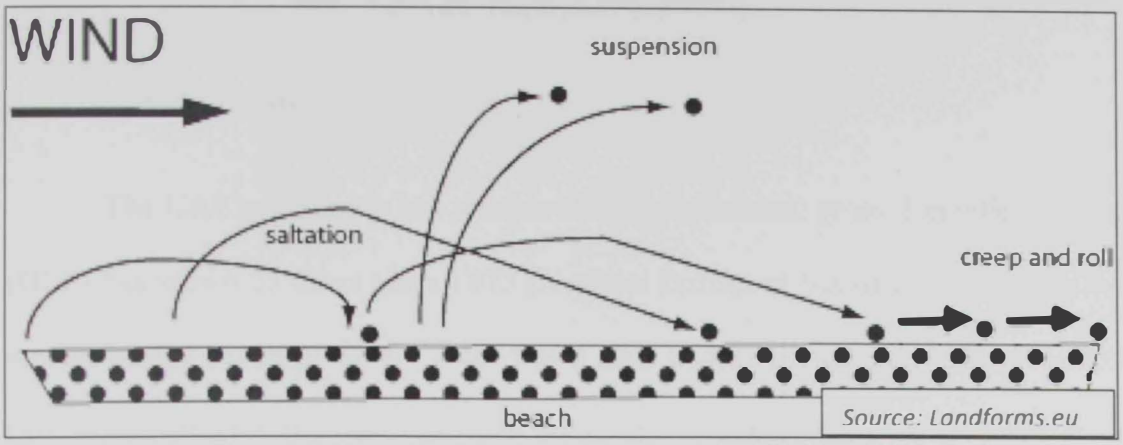

Figure 1.6: Sand movement with wind

1.2.2 Climate

The Emirates' weather during the year can be summarized into two key seasons:

Summer – Starting in May and lasts until September, the country faces extreme heat and humidity. During this period temperature could reach up to 48°C while humidity ranges between 80 – 90 %. Sandstorms regularly strike between May to early July, while rainfall is rare.

Winter – Starting in December to March, temperatures reach a high of 24°C during the day and a low of 10°C at night, and fog becomes more frequent during this period. Rainfall occurs most often between November and February and, on average, reaches 12cm per year.

On average, the annual wind speed in the Emirate of Abu Dhabi ranges between 4.63 and 5.6 m/s, with the average maximum reaching between 6 to 10 m/s. The predominant directions are North West, North North-West, and West North-West, 21.1%, 15.8%, and 14.6% of the time, respectively.

1.2.3 Socio-Economic

The UAE's economy has prospered, and its nominal gross domestic product (GDP) has grown 27 times since 1975 (National Bureau of Statistics), becoming the second largest economy in the Arab world after Saudi Arabia. This unprecedented pace of growth over the past years has been largely supported by the revenues from oil and gas exports, which the country has reinvested in itself to prepare itself for a post-oil era by diversifying its economy. These efforts have driven an increased performance in trade, financial services, tourism, real estate, logistics, communications and manufacturing. The country has a uniquely flexible, globalized labor market, and the track record of economic growth has also ensured a very high growth rate in population.

This population growth places challenges on the nation when it comes to trying to meet its demand for energy, water, and urban development. Since the country is located in the desert, where fresh water is limited and temperatures are high during the summer, the UAE's carbon footprint is one of the highest in the world (Global Footprint Network, 2010). There is a high demand for energy and many goods cannot be produced by the country, therefore, goods need to be imported, and freshwater needs to be desalinated.

1.3 Scope of the Research

Various studies were conducted worldwide using remote sensing and geographic information system (GIS) to map and understand the movement of sand dunes. This study focuses on changes in sand over time in Abu Dhabi Emirate using these technologies and methodologies.

1.4 Aim & Objectives

This study is of paramount importance as 75 % of the UAE is covered by sand dunes (El-Sayed, 1999). Their movement, aided by wind, poses a threat to the environment, roads, habitats, farms and plantations (Yao, 2007), thus requiring human intervention for the removal of the encroaching sand. Therefore, by better understanding the shifts in land cover features, better planning could be done for the future.

The objectives of this study are:

1. To create mosaics of the newly released Landsat CDR imagery covering the study area for 3 dates: 1992, 2002, and 2013.
2. To identify the classification scheme of the study area with the minimum representative land cover classes of the study area.
3. Isolate the sand class and create sand maps for the study area from Landsat imagery for the three dates.
4. Perform change analysis through the selected time periods, and discuss the findings in regards to the movement of sand in the emirate.

1.5 Hypotheses and Assumptions

We assume that dune movements are a fact of nature, accelerated by anthropogenic activities, as witnessed through their encroachment onto farms and interstate roadways. Our hypothesis is that these movements can be measured and modeled using remote sensing techniques and statistical analysis.

1.6 Thesis Structure

This dissertation is divided as follows:

- Chapter 1: Introduction

  This chapter describes the study area, the Emirate of Abu Dhabi, and provides a brief background into the geographical, physical, and economic setting of the UAE as a whole. It discusses the location, size, climate and landscape of the study area, giving a summary of the impact of dune movement onto the various land covers and its impact on the socio-economic field. Finally, it ends with the research objectives, hypothesis, and thesis structure.

- Chapter 2: Literature Review

  In this chapter, we talk about the various remote sensing and geographic information system (GIS) techniques and research methods done previously on dune movement across the globe. As well as how they are closely related to the current study area in order to analyze the most suitable methodology to utilize in studying the Abu Dhabi emirate's sand dunes.

including the various thematic map development techniques, the classification process, and the change analysis algorithms utilized.

- Chapter 3: Methodology

  Chapter three discusses the utilization of what was learned from the literature review, data collection the study was performed on, description, and pre-processing, and the various methods and techniques that were performed to analyze and explore its results to better understand the area of interest.

- Chapter 4: Result Analysis & Discussion

  This chapter explains the result of the analysis of the methodology that was followed, the accuracy assessment of the results, and the result interpretation in scientific form, while discussing the driving forces and their impacts at the same time.

- Chapter 5: Conclusion & Recommendations

  The final chapter concludes the research work done and the significant issues that are covered to set up better future research to obtain better results.

1.7 Summary

The Abu Dhabi Emirate is made up of three municipalities, Abu Dhabi, the Eastern Region, and the Western Region. The emirate has similar physical settings as the rest of the country: the same weather and landscape could be seen throughout the region, with climates being bi-seasonal: hot and humid in summer, and temperate and sunny, with sparse rain during winter.

The exploration and production of oil and gas in the emirate has led to a drastic change in the land cover of this region. Due to the continuous increase in population, coupled with the limited resources of freshwater and high temperature during the summer, the need for constant urbanization and infrastructure development is essential. These projects are slowly changing the land feature over the years, where land is exploited and transformed for human use (Gardner 2009). This study aims at mapping the sand features, and tracking their trajectory across time to better understand the process and causes of sand movement.

Chapter 2: Sand Dunes and Remote Sensing

2.1 Background

Field surveys of dune migration are difficult and expensive; they cannot be repeated sufficiently often to permit ongoing monitoring. For that reason, the use of remotely sensed data is a highly effective method that allows researchers to study and monitor wide areas of sand dunes.

There are many different methods that can be used to measure the migration rates of sand dunes, such as the change detection techniques offered by Kumar (1993), neighborhood statistics by Larue (2004) and Bishop (2008), and the vector extraction from raster as done by Liao (2009).

2.2 Benefits and Limitations of Remote Sensing of Sand Dunes

Sand dune systems are large in areas, and when sand migrates, they cover long distances and wide areas through transport pathways as indicated by previous field geochemical and remote sensing studies that will be explored in this chapter. These studies also showed that the Landsat Thematic Mapper (TM) is capable of distinguishing between active and inactive sands (Scheidt, 2008).

The characteristics of the spectral, spatial, and temporal resolutions on both the Thematic Mapper on board the Landsat 5 and the Enhanced Thematic Mapper Plus (ETM+) onboard the Landsat 7 are quite similar (Masek, 2001, Teillet, 2001). However, the main improvements of the ETM+ over the TM are the improved thermal band, the addition of the panchromatic band, and the availability of two calibration modes from radiance into DN (Levin, 2004).

The reflectance spectral signature of sand dunes as detected by space borne sensors is highly dependent on two criteria. First, the characteristics of the dunes and their surfaces, which include vegetation cover, mineralogy, texture, and the presence of a biogenic soil crust (White, 1997, Gerbermann and Neher, 1979, Karnieli and Tsoar, 1995). Second, is the geometry amongst the sun, the surface, and the sensor, and the atmospheric attenuation (Howari, 2007). It should be noted that under the TM sensor, spectra of sand would be registered as sand as long as the cell under investigation does not contain more than 30 to 40 percent vegetation (Hutchison, 1982, Tueller, 1987, Smith, 1990, Janke, 2002).

Since part of this study focuses on sand dune classification and extraction, several aspects that affect how the sensor records the dunes are investigated:

a) **Mineralogy**: Different minerals reflect differently, and in the spectral resolution of Landsat, Quartz and Carbonates show a significant difference in the Mid-Infrared (band 5 and 7). Whereas Quartz shows high reflectance, Carbonate shows half that of Quartz, therefore, using band ratio 5 / 7 helps distinguish Quartz from Carbonate (Pease, 1999), which in turn generates a gradient from back to white indicating the decreasing Carbonate and the increasing Quartz. Another band ratio s used in previous studies was the Thermal Infrared / Near-Infrared (6 / 4) ratio. This ratio plays on the temperature variation that minerals have from one another, where mafic minerals are distinguishable from Quartz and Carbonate (Pease, 1999), because of the higher absorption of the mafic minerals. However, due to subtle variations, it is coupled with the infrared band 4 to highlight them

better. This method proved useful because mafic minerals a have weaker response in band 4 than in band 6 (Hunt, 1982, Vincient, 1997, Pease, 1999).

b) **Texture**: Texture is related to the grain size that covers the top of the sand dune, and using remote sensing, the observed spectral differences between the active and inactive sand dunes is a result of grain size and composition difference. Active sand is consistently brighter and is generally expressed by a uni-modal distribution of brightness values as a result of the fine sand particles (less than 62 μm) while the inactive sand has a lower albedo due to the more coarse particles (greater than 250 μm) (Lam, 2011).

c) **Geometry**: Topographic shading and cast shadows can introduce errors into the accurate analysis of remote sensing since they mask significant spectral features, and sometimes are treated as noise that needs to be removed. However, shading also stores vital information about the topographic characteristics and in this sense, the noise becomes an important signal that could be extracted and analyzed (Levin, 2004).

d) **Atmospheric Attenuation**: Ground features measured by remote sensing platforms always include environmental phenomenon that is measured as a result of the attenuation of electromagnetic radiation through the atmosphere till it reaches the sensor. This data can be treated as either noise or a signal depending on the study subject. In other words, the absorption of radiation due to the gases in the atmosphere can be seen either as a noise masking the ground reflectance or as a signal that shows the distribution of the atmospheric gases (Gao, 1993).

Due to the nature of remote sensing data from the Landsat series sensors, it requires that solar radiation passes through the atmosphere before it is measured by

it, which in turn leads to sensed data to include information about the atmosphere as well as the surface.

This study uses images provided from the Landsat series of satellites since they provide the longest continuous record of space borne imagery that began in early 1972 with the launch of Landsat 1. However, the inherent issue that is passed along due to the use of multi-temporal images in a study is the radiometric consistency among ground features. It is difficult to maintain this consistency due to the changes in sensor characteristics, atmospheric conditions, solar angles, and sensor view angles. Therefore, radiometric correction is often performed to reduce any or all of the influences above (Chen, 2005).

There are two types of radiometric corrections that are utilized to correct satellite images: absolute and relative correction. Absolute correction aims at extracting the absolute reflectance of the target at the Earth's surface. It requires inputting simultaneous atmospheric characteristics and sensor calibration, which is difficult to acquire in many cases, especially in historical datasets, but also difficult to obtain when planned for. As for relative correction, it aims towards performing the same objectives met through absolute correction, by adjusting the radiometric properties of the target images to match a predetermined base image.

Radiometric correction is also a vital step when it comes to mosaic scene classification. Jay states that unless radiometry of the mosaicked images are of acceptable levels, then digital analysis is not suitable (Jay 2009).

2.3 Multispectral Classification & Mapping of Sand Dunes

Various methods are implemented to better enhance the captured image and then be able to extract the sand field of interest. In one study by Howari (2007), the image processing techniques used were image enhancement, band ratioing, and spectral classification. Pease (1999) stated, that using Landsat TM band ratios 6/4 and 5/7 revealed the most information for mineralogy of the sand dunes; Pease used band ratioing because it helps in reducing the detected differences in the same feature due to topography overall variation in reflectance, and brightness differences related to grain size, and all the while, enhancing the differences due to the shape of the spectral reflectance (Sultan, 1986, Sabins, 1997, Pease, 1999). Thereafter, both unsupervised and supervised classifications were performed to create the land cover thematic map based on surface mineralogy. Unsupervised classification does not require ground reflectance data because it is solely based on the natural reflectance of each pixel, while the supervised classification is used to assign an unknown pixel to one of the classes (Lillesand and Kiefer, 1994, Sabins, 1997, Richards, 2000).

Another method followed to create a thematic map of the Land Use / Land Cover (LULC) was done by Hadeel (2010), where supervised classification was used. This produced more desirable results over unsupervised classification when trying to delineate LULC based on band indices to retrieve class boundary rather than the raw band data set. The three indices used are: Normalized Difference Vegetation Index (NDVI), Crust Index (CI), and Topsoil Grain Size Index (GSI).

- **NDVI** is the most common form of vegetation index, and it is the difference between the red and near-infrared band combination divided by the sum of the red and near infra-red.

$$NDVI = \frac{NIR - R}{NIR + R}$$

However, since this study is conducted in an arid area with little continuous vegetation cover, we will utilize its counterpart the Soil Adjusted Vegetation Index (SAVI) which uses a canopy background adjustment factor that makes up for the fact that there are sparse vegetation and visible soil.

$$\frac{NIR - RED}{NIR + RED + L} * (1 + L)$$

(Where L is the factor that highlights the difference between vegetation and soil)

- **CI** is used in the study of the fine sand content in the topsoil: this is for monitoring the change of surface soil using remote sensing. Applying the index to a sand soil environment has shown the ability to detect and map the different lithological/morphologic units such as active crusted sand areas.

$$CI = 1 - \frac{R - B}{R + B}$$

- **GSI** was developed based on field survey of soil surface spectral reflectance and lab analysis of soil grain composition performed by Xiao (Xiao. 2006). High values in the GSI correspond to high content of fine sand, 0 for vegetated area, and negative values for water bodies.

$$GSI = \frac{R - B}{R + B + G}$$

Other authors used simple classification methods to extract the sand dunes that varied between supervised and unsupervised processes. Ghadiry (2010) extracted the sand dunes and then transformed them into vector data to calculate the dune movement. On the other hand, Al-Hajri (2009) performed supervised

classification based on field samples, and the resultant image led up to on-screen digitization where their movement was calculated.

One of the most widely used remote sensing techniques to classify and image that contains several bands of information is the multispectral supervised classification. This method proved to be reliable and robust over the past decades of its implementation. The supervised multispectral classification process relies on the probabilities of assigning each pixel in the image to a defined class (Otazu, 2000).

Another method was the use of spatial filters to delineate the boundaries of the sand dunes, thus enabling them better extraction either with the use of supervised classification with an image add-back (Janke, 2002) or with the use of on-screen digitization (Al-Dabi, 1997). After that, the movement was calculated based on a subtraction change detection algorithm that extracted the change between the two images.

Unlike the previously mentioned methods, one author, Chang (2006), used texture analysis. Texture analysis is an approach used to identify the characteristics of a feature from the relationship among the proximate pixels rather than the reflection values on a per pixel basis. Simple naked eye inspection of texture does not allow distinguishing the sand dunes from the other land use, except the linear pattern of the long axis of sand dune area. For that, the use of filters assists in delineating these features from one another. The most common filter is the high pass filter, which is designed to ignore trivial variance by multiplying higher values to a matrix, the distortion problem of the high pass filter was pointed out by Goodchild (1993), for that, the use of other filters is more appropriate. The area covered by sand proved to have one homogeneity value; therefore, the homogeneity filter is good for

extraction of sand dunes. On the other hand, the dissimilarity values showed zero for the sand dunes, which means dissimilarity value is also a good filter for extraction of certain objects which have continuous values. Moreover, the Kruskal-Wallis statistics of texture analysis shows a significant difference in the polygons of sand dunes.

Then there is the Principal Component Analysis (PCA), where the analysis of satellite imagery has repeatedly demonstrated its capability in identifying the interrelation between the features based on their lithology, structure, and landforms (Pu and Gong, 2000, Krishnamurthy and Srinivas, 1996). Using the PCA method, six Principal Components (PC) are generated from the Landsat ETM+ sensor, following a maximum likelihood classification algorithm, and an 82% accuracy map was developed (Rajesh, 2008). Fung and LeDrew (1987) used PCA to detect LCLU changes using the multi-temporal MSS and TM images, and Gong (1993) used band pair image differencing for each spectral band, and then used PCA for the multispectral difference image, which proved to be better than the simple image differencing.

In multispectral remote sensing, the large number spectral bands being collected would sometimes lead to redundancy in the data being collected as some ground objects hardly vary over certain wavelength ranges. Since not all multispectral bands contribute the same amount of information, it is necessary to reduce these redundancies to improve data storage and image processing performance. (Richards and Jai, 1999)

Data redundancy is usually visualized by plotting a scatterplot of two bands, if the distribution of pixels within the plot form along a line then it is said that the

two bands are highly correlated, and if the scattering of the pixels is wide, it is said that the information within these two bands are uncorrelated (Amdev Ren, 2005).

Another method followed is the calculation of the PCA. PCA is used to produce uncorrelated output bands which segregate noise components and reduces dataset dimensionality by finding new sets of orthogonal axes that have their origin at the data mean and that are rotated so that data variance is maximized (Ifarraguerri and Chang, 2000), and it has the following advantages (Sabins, 1987):

1. Most of the variance in a multispectral dataset is compressed into one or two PC images.

2. Noise may be relegated to the less correlated PC images.

3. Spectral difference between materials may be more apparent in PC images than in individual bands.

PCs were derived from the solar reflective spectral bands of the selected imagery, and, as it is expected, the first three components provide almost the whole of the explained variance, therefore, we consider PCs up to the third component.

2.4 Change Analysis Techniques

Change analysis is the process of identifying the differences in the state of an object or a phenomenon by observing it at different times (Singh, 1989). To better understand the relationships and interactions between the human and the natural processes and to better manage and utilize the resources available, timely and accurate change detection of the Earth's surface features is required (Lu, Mausel, Brondizio, & Moran, 2004). The use of remotely sensed data to map LULC changes

started as early as land remote sensing imagery were made available in the 1970s (Huang, 2009) and since then, many LULC change detection techniques have been developed (Jensen, 1996):

- Post Classification
- Write Function Memory
- Multi Date Composite Image
- Image Algebra
- Binary Mask
- Using Ancillary Data
- Manual On Screen Digitization
- Spectral Change Vector
- Knowledge Based

In this study, we will be following the post classification method to meet the set objectives. Before implementing the change detection analysis, several conditions must be met, according to Al Kuwari (2011):

- Precise registration of multi-temporal images
- Precise radiometric and atmospheric calibration
- Similar phonological states between multi-temporal images
- Selection of the same spatial and spectral resolution images to produce high-quality change detection results

2.5 Summary

Overall, upon examining various techniques and methods previously used to identify LULC of desert environments using remote sensing, we can identify which method is the easiest and most suitable to recreate over three years. Therefore, we will be able to produce constant results with minimum interference and errors, and to analyze the change and meet the objects set by this study.

We will be using maximum likelihood to classify the image followed by the post classification change detection algorithm. With this, we should be able to track the movement of sand and study its change across time.

Chapter 3: Research Methodology

3.1 Introduction

After reviewing the literature and previous research performed on dunes and the UAE, and to meet the requirements of the study, it was decided that the following steps would be taken (*Figure 3.1*):

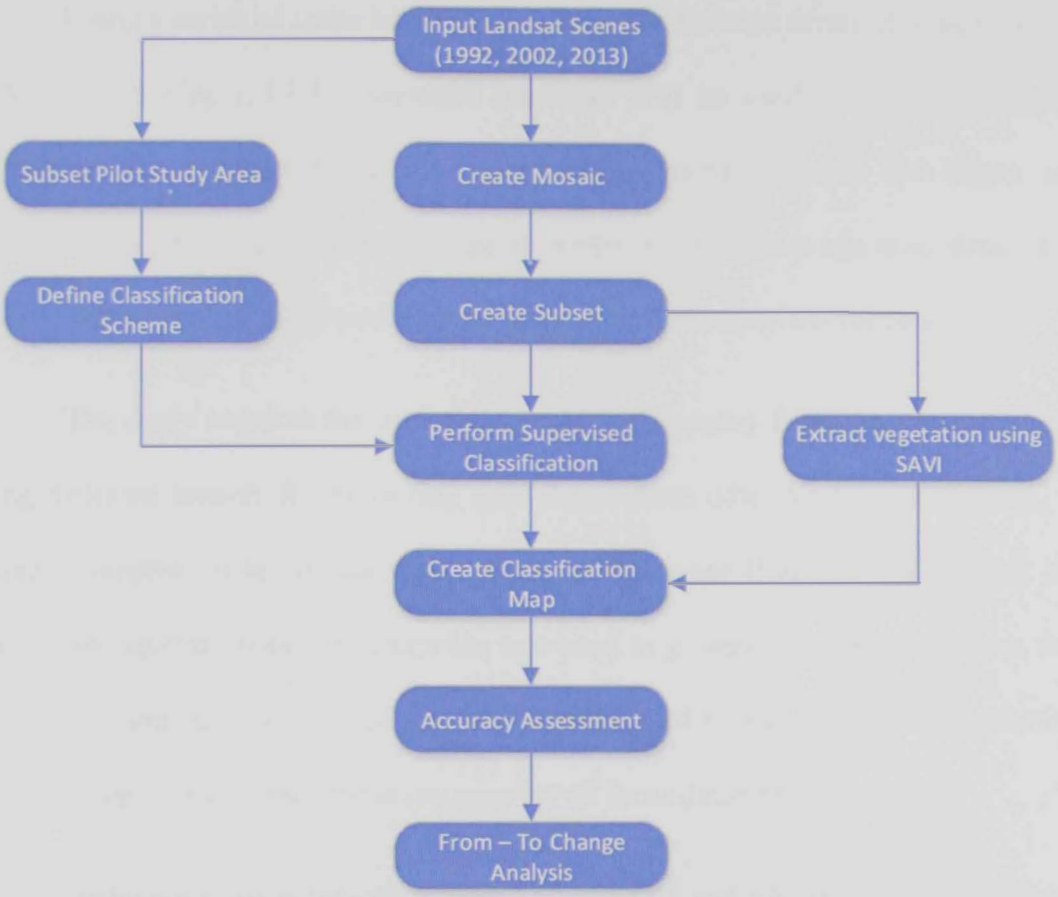

Figure 3.1: Dissertation methodology process

In short, we would create a mosaic from 6 scenes of the study years, have its vegetation extracted using SAVI, and then perform the supervised classification using the scheme derived from the pilot study. Using higher resolution imagery, we would check for the accuracy of the classification before the post classification change analysis.

3.2 Spatial Datasets & Software

This chapter considers a set of methods for sand dune classification, and assesses their results over the pilot study area. The best method that meets the study objectives is selected for implementation and is used to process the data for the entire study area.

Using a series of space borne images from the Landsat series, this section will look at developing a LULC thematic map that will be used in change detection calculations to determine the direction of movement, whether the dunes are expanding or receding, and the change in terms of area coverage over time, thus allowing us to predict what would occur in the future based on earlier years.

The study requires the use of six scenes of imagery from the Landsat series using different sensors for extracting sand dunes from other land cover features, to create a complete image for the three time frames that are 1992, 2002, and 2013. An Abu Dhabi Emirate boundary shapefile was used to generate an area of interest that spans over both land and water and was implemented in Exelis Visual Information System ENVI 5.3 to subset the study area for all three datasets.

Using a six scene mosaic of path 160 rows 43 and 44, path 161 rows 43 and 44, and path 162 rows 43 and 44 (*Figure 3.2*) for the years 1992, 2002, and 2013 (*Appendix A Table 3.1*), the study area is covered for the region that lies from Al Ain (eastern UAE-Oman border) to Bayah al Sila (western UAE-Saudi border) (*Figure 3.3*). A remote sensing image dataset covering the study area was produced for all future LULC classification.

As for the software, this study uses ENVI 5.3, which was used for all digital image processing needs, following by ESRI's ArcGIS 10.3 for map production needs.

Figure 3.2: Landsat Path & Rows Covering the UAE

Figure 3.3: The Study Area of the Dissertation inside Red Boundary

3.3 Data preparation

As part of this dissertation, the data that will be used in the study was subjected to the following data preparation tasks:

Step 1: Upload and stack the bands of each scene into one usable file.

Step 2: Perform a georeferenced mosaic process that is supported through ENVI 5.3 to get a full image for each of the 1992, 2002, and 2013 datasets. The mosaic process was done using the "Seamless Mosaic" tool in stages, since paths 161 and 162 would perfectly mosaic with each other, as they have very similar land cover features. However, path 160 has the inclusion of the mountain regions in the East. If all six scenes were to be performed at one shot, then color balancing issues would arise. That is why, paths 161 and 162 are mosaicked first, and their outcome is again mosaicked with path 160. At each stage data ignore values are set and that is to remove the image boundary from the picture, with color correction of histogram matching from overlap were it would, and cuts were done along the seamlines that were automatically generated by the system (Figure 3.4).

Step 3: Using the study area AOI that covers both the waters and the land of the emirate, a subset was created to focus the analysis on the areas of interest.

Furthermore, it should be mentioned that no radiometric correction was performed since the images used are already Surface Reflectance products from the Landsat Ecosystem Disturbance Adaptive Processing System (LEDAPS) Climate Data Record (CDR) repository that is provided by the USGS for Landsats 4, 7, and 8.

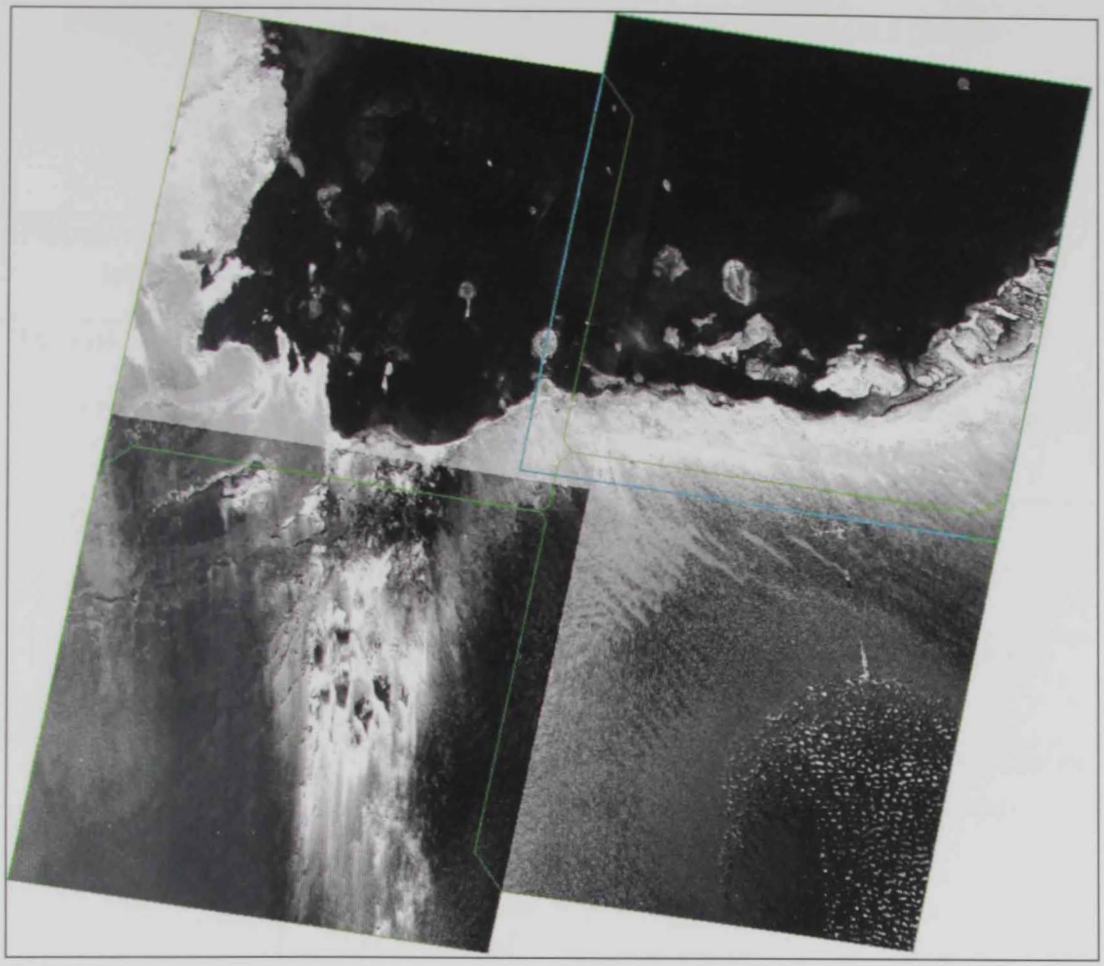

Figure 3.4: Representation of mosaic Seamlines

The Software applies moderate resolution imaging spectroradiometer (MODIS) atmospheric correction routines to level 1 Landsat TM and ETM+. Water vapor, ozone, geopotential height, aerosol optical thickness, and digital elevation model (DEM) are inputted into the 6S (Second Simulation of a Satellite Signal in the Solar Spectrum) radiative transfer models to generate the surface reflectance; this applies to the series from 4 to 7. As for Landsat 8, surface reflectance is generated using a specialized software called L8SR, that uses an internal algorithm rather than the 6S, and its inputs come from either on-board calculations, such as geopotential height, or from MODIS CMA, such as water vapor and ozone (*Table 3.2*).

Parameter	Landsat 4 -5, 7 (LEDAPS)	Landsat 8 OLI (L8SR)
Radiative transfer model	6S	Internal algorithm
Thermal correction level	TOA only	TOA only
Thermal band units	Kelvin	Kelvin
Pressure	NCEP Grid	Surface pressure is calculated internally based on the elevation
Water vapor	NCEP Grid	MODIS CMA
Air temperature	NCEP Grid	MODIS CMA
DEM	Global Climate Model DEM	Global Climate Model DEM
Ozone	OMI/TOMS	MODIS CMG Coarse resolution ozone
AOT	Correlation between chlorophyll absorption and bound water absorption of scene	MODIS CMA
Sun angle	Scene center from input metadata	Scene center from input metadata
View zenith angle	From input metadata	Hard-coded to 0
Brightness temperature calculated	Yes (Band 6 TM/ETM+)	Yes (Bands 10 & 11 TIRS)

Table 3.2: Comparison between CDR of Landsat 4 -7 and Landsat 8

3.4 Classification Scheme

A classification scheme is a list of all potential land cover types that are present in a study area that could be identified from a satellite image, and this list should be comprehensive as to encompass all the cover. Therefore, a sound classification scheme should make sure that one cover should not fit into another

class. Table 3.3 is the most popular scheme devised by Anderson (1976), and it is used by the U.S. Geological Survey (USGS) Land Use / Cover classification.

Level 1
Urban or built-up land
Agricultural land
Rangeland
Forest land
Water
Wetland
Barren land
Tundra
Perennial snow or ice

Table 3.3: Themes as per Anderson 1976

However, due to some classes being none existent in the study area, such as the perennial snow or ice, the list has been revised as follows (*Table 3.4*)

Level 1
Urban or built-up land
Agricultural land
Water
Wetland
Barren land

Table 3.4: Revised Anderson 1976 Themes as per Region of Study Area

Furthermore, to reduce the size of the data to be classified and to improve the class discrimination, a vegetation mask SAVI with a 0.5 factor was implemented to identify vegetation covered areas and exclude them from the classification process.

3.5 Determining LULC classes

Before commissioning the supervised maximum likelihood, it is imperative to determine the classifiable LULC of the Abu Dhabi Emirate. For that, unsupervised Iterative Self-Organizing Data Analysis Technique (ISODATA) classification was performed on three different datasets: multispectral, Inverse PCA, and Texture with Multispectral.

This pilot study, to determine the classifiable features, was done on a single scene. The representative was from path 160 row 43 since it was the most diversified image covering water, urban, wet lands, desert, vegetation, and the mountains (*Figure 3 5*).

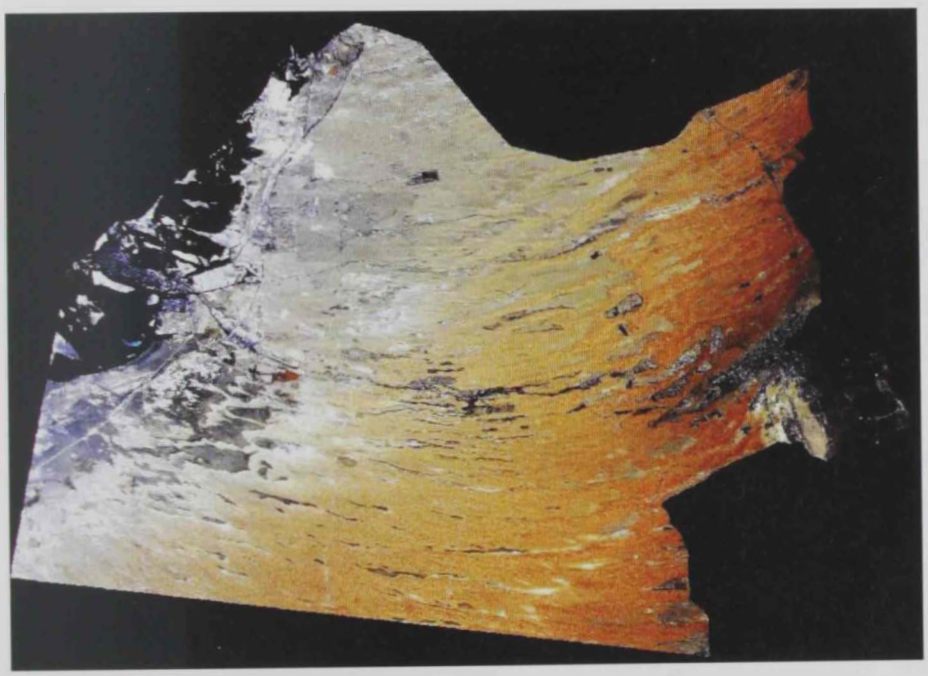

Figure 3.5: Pilot Study Area Used to Identify Classes

The first dataset tested was the standard six multispectral bands (*Figure 3.4*). The second dataset was the inverse PCA, where this dataset was derived by performing the forward principle components (PC) rotation on the multispectral bands to produce uncorrelated output bands that allowed the segregation of the noise components in the original image thus reducing the dimensionality of the dataset. After identifying the most informative 3 PC, inverse PC rotation was performed using the statistics from the forward PC rotation, therefore, giving us an image with reduced noise (*Figures 3.6 & 3.7 and Appendix A Tables 3.5 & 3.6*).

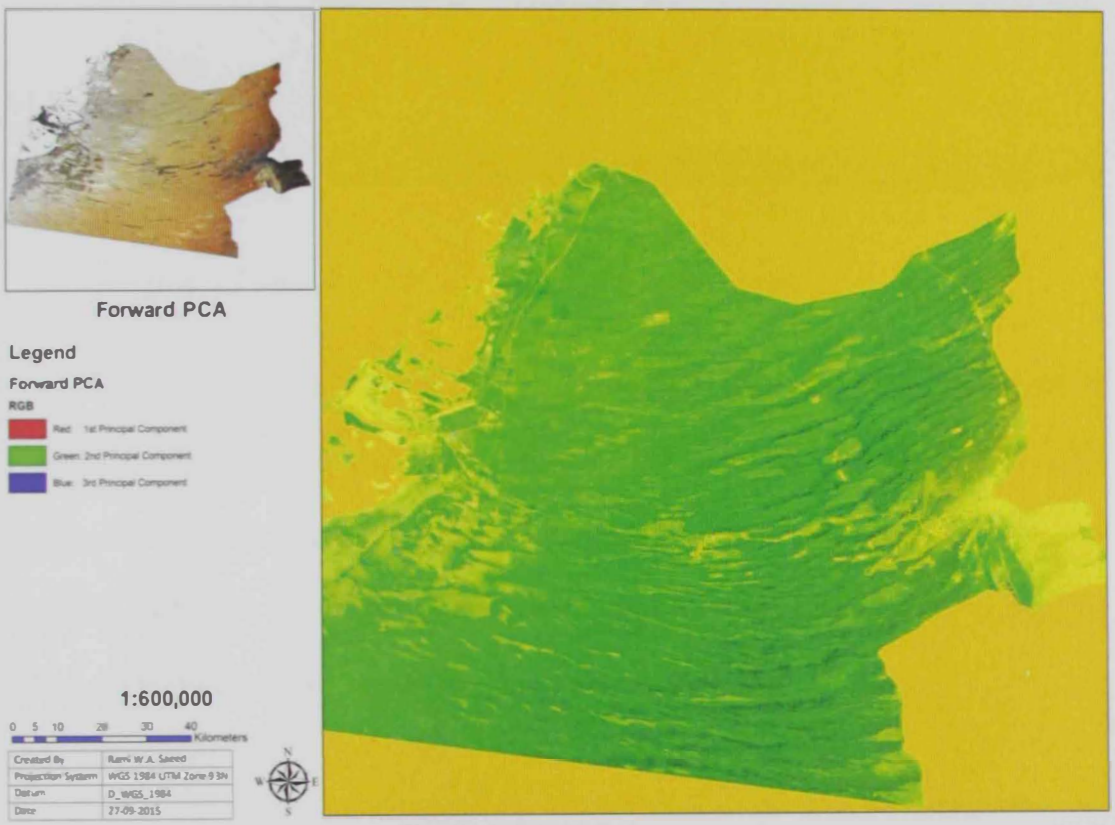

Figure 3.6: Forward PCA of Pilot Study in First Three Principal Components (PCs)

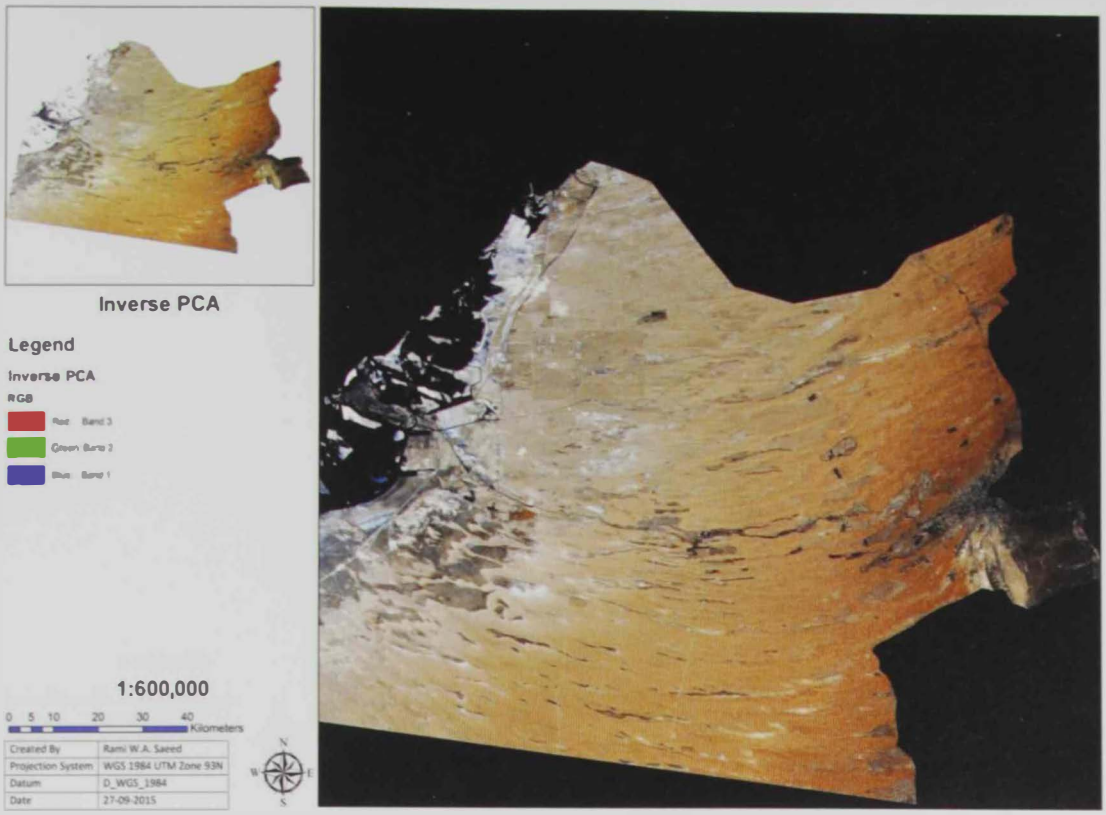

Figure 3.7: Inverse PCA of the First Three PCs in True Color RGB

The third dataset that got tested was texture (*Figure 3.8*) and multispectral (*Figure 3.5*) datasets combined into a single set. The texture was derived from the entropy of the pilot image that showed the areas of heterogeneity (areas that are texturally different) thus allowing to further enhance the multispectral image by adding the texture of the features as an add-in into the image.

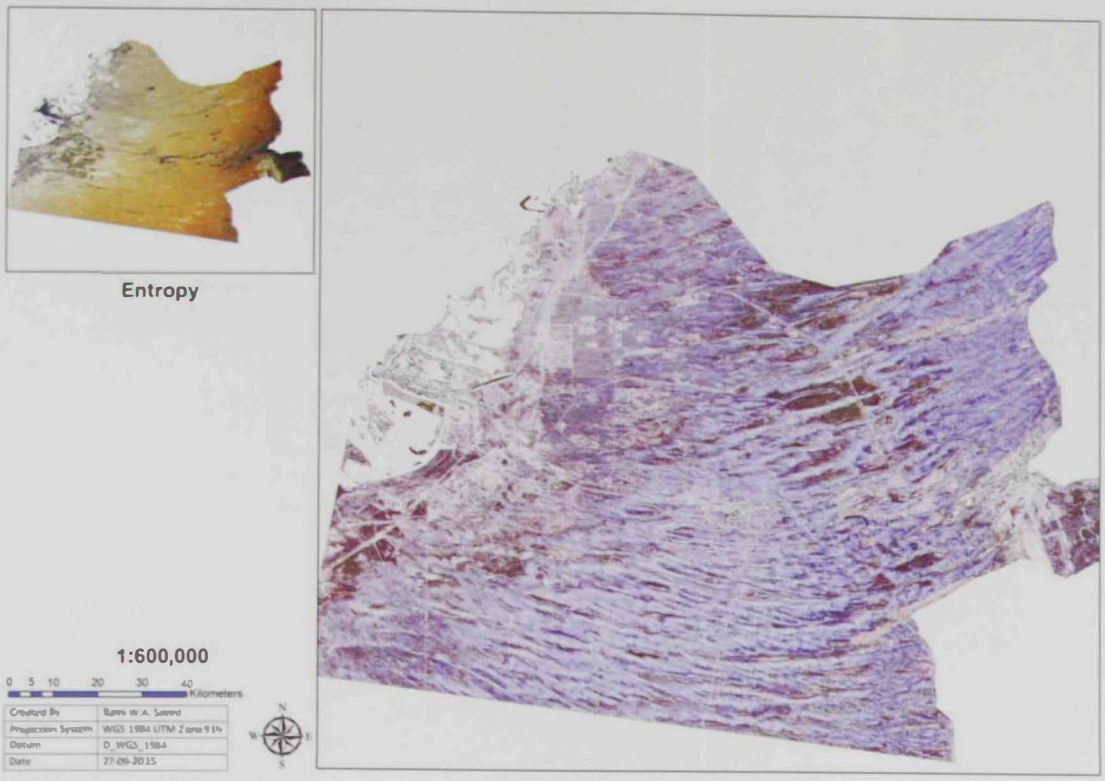

Figure 3.8: Entropy Texture of Pilot Study Area

The parameters that were used are as follows:

- The study area has no less than 30 and no more than 300 different classes
- The minimum area for each class to be considered as such is one km^2 (i.e. 11,111 pixels)
- The clustering will run to a maximum of 100 iterations

Upon that, it was noted that there is a significant difference between the number of spectral classes between the multi spectral (31 Classes), texture + multispectral (41 Classes), and the PCA (295 Classes) (*Figure 3.9*). Then to reduce the number of features classes, class merging was performed using high-resolution imagery from IKONOS 2006 and RapidEye 2012 to confirm invariant sites.

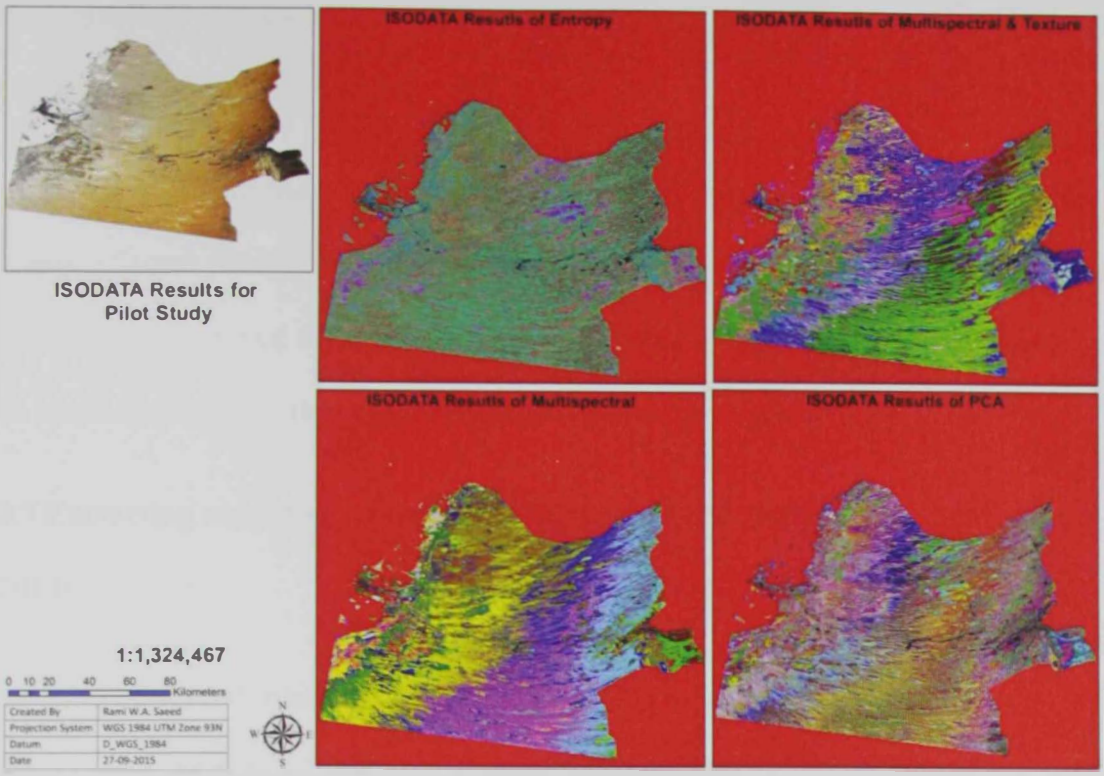

Figure 3.9: ISODATA Results for Pilot Study

3.6 Image Classification & Post Processing

Upon determining the possible statistical classes, the implementation of the supervised classification was undertaken, using 142 training sites. Class merging was performed and each training site was merged into one of the 4 classes below:

- Sand
- Wet Soil
- Intertidal Zone
- Exposed Bedrock

After which, class sieve was performed to solve the problem of having isolated pixels that occurred after the image classification process. Sieving removes isolated pixels using blob grouping of 4 neighbors to determine if a pixel is grouped

with pixels of the same class, if not, that pixel will be removed and classified as "unclassified."

Then, to fill the newly created "unclassified" class, clump was performed to clump adjacent similar classified areas together using morphological operators. The classes were clumped together, first, by performing a dilate operation, followed by, an erode operation on the classified image using a kernel size of 3 by 3.

3.7 Extracting sand dunes from satellite images (MSS 1992, ETM+ 2002, OLI 2013)

The second main objective of this study is to extract the sand dunes from the three image datasets to analyze the dune movement and change across time, using per pixel maximum likelihood supervised classification algorithm to extract the dunes from the rest of the land cover features. Thereafter, sand features are extracted and transformed into binary maps, resulting in sand and non-sand maps.

3.8 Accuracy Assessment

Accuracy assessment is the next step taken to determine the thematic map's classification accuracy when compared to accuracy assessment sites, which are sites collected separately from the training sites and used for the classification process. In this study, the accuracy assessment sites will be stationary across all three years and will be selected using higher resolution imagery than that of Landsat (*Figure 3.10 & Appendix A Table 3.7*).

To do so, the study uses a RapidEye for the year 2012, and IKONOS for the year 2006, and Spot for the year 1986, each with 5, 1, and 10-meter resolution, respectively (*Appendix A Table 3.8*). These dates will be used to identify the

invariant accuracy assessment sites that will be used to measure how well the classification was performed.

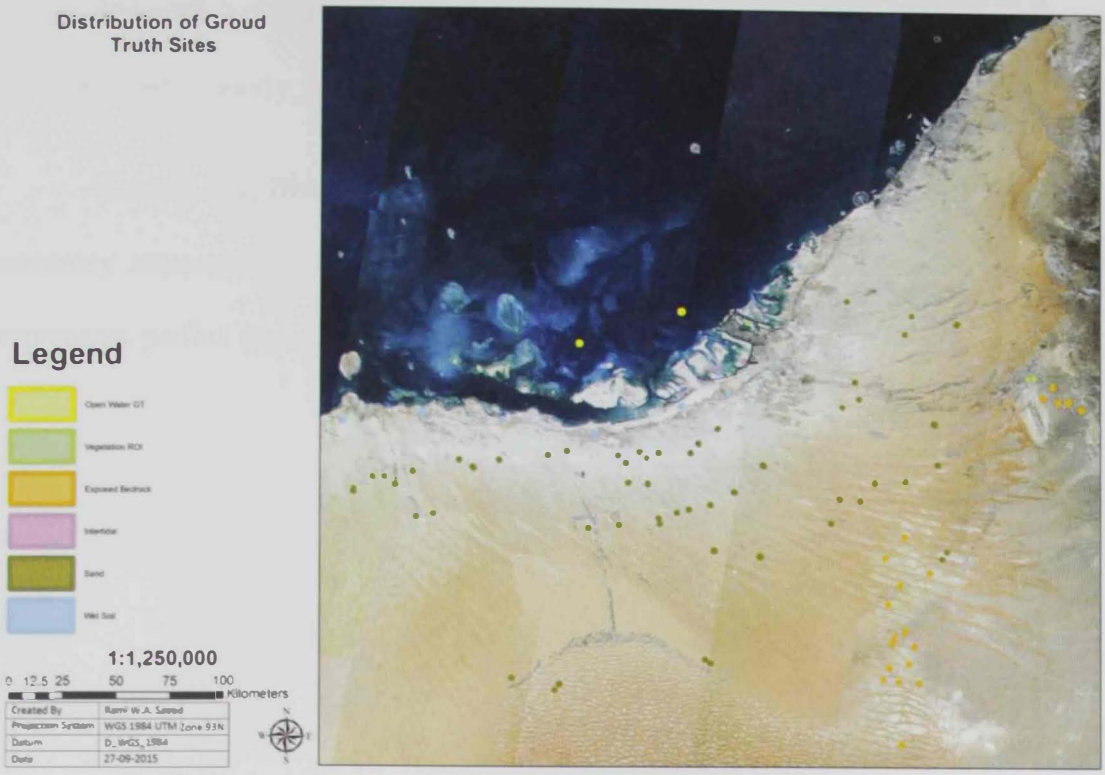

Figure 3.10: Distribution of accuracy assessment sites

There are four types of accuracy that are measured in the confusion matrix calculation:

User's Accuracy: is the error of commission. It measures the probability that a pixel is class "A" given that the classifier has labeled the pixel into class "A". It is calculated by the division of the total number of correctly classified pixels of a certain class by the total number of pixels that were classified in that same class.

Producer's Accuracy: is also referred to as the error of omission. It measures the probability that the classifier labeled an image into class "A" given that the accuracy assessment site is class "A". It is calculated by the division of the total

number of correctly classified pixels of a certain classes by the number of total pixels that actually belong to that same class.

Overall Accuracy: is calculated by summing the total number of pixels that are classified properly, and divided by the total number of pixels.

Kappa Coefficient: measures the agreement between classification and accuracy assessment pixels. It produces an index ranging from 0 to 1, where "1" represents perfect agreement, while "0" represents no agreement.

$$Kappa = \frac{N \sum_{i=1}^{n} m_{i,i} - \sum_{i=1}^{n} C_i G_i}{N^2 - \sum_{i=1}^{n} C_i G_i}$$

Where:

i = class number

N = the total number of classified pixels that are being compared to the accuracy assessment data

$m_{i,i}$ = the number of pixels that belong to the accuracy assessment class in "i" that are also classified with class "i"

C_i = the total number of classified pixels that belong to "i"

G_i = the total number of accuracy assessment pixels that belong to "i"

3.9 Dune change analysis techniques

The post classification change analysis was performed using the flowchart in Figure 3.11. After performing the supervised classification algorithm and verifying its accuracy, the third step was to vectorize the raster image into polygons that held

the classified feature information. Using the union overlay tool from ArcGIS 10.3, we were able to get the following from-to change (Table 3.9) that congregated the three stages of the study into one dataset. Then, in order to map the from–to changes across the three years, an additional field was added and named "From_To" with the following calculation [Class_Name_1992] & " - " & [Class_Name_2002] & " - " & [Class_Name_2013] in order to arrange the class names in order of 1992 to 2002 to 2013, followed by the dissolve in order to remove trajectory duplications. The final results in Table 3.10 could be seen and mapped.

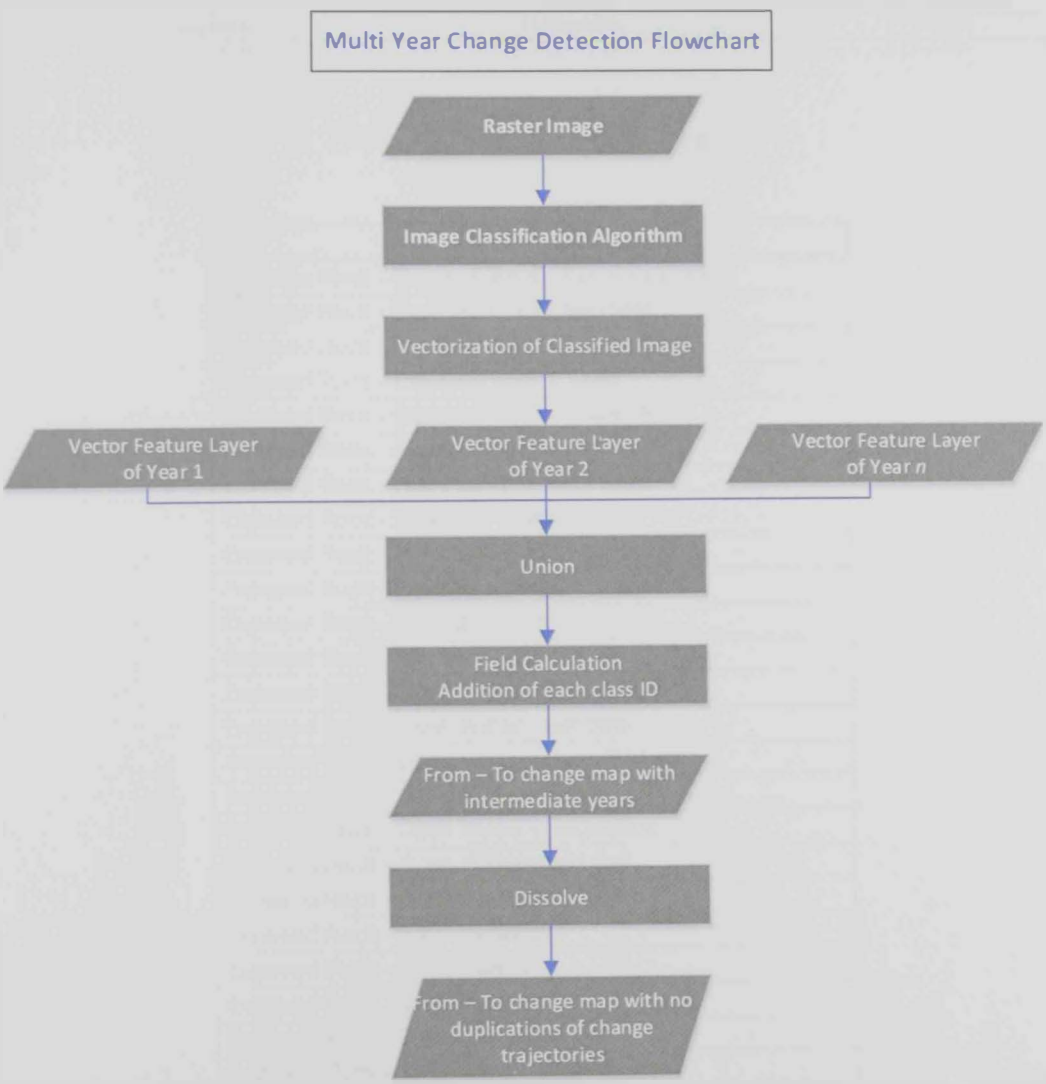

Figure 3.11: Multi Year change detection methodology

FID_Dissolve_1992	Class_Name_1992	FID_Dissolve_2002	Class_Name_2002	FID_Dissolve_2013	Class_Name_2013
1	Vegetation	1	Vegetation	1	Vegetation
2	Open Water	1	Vegetation	1	Vegetation
3	Sand	1	Vegetation	1	Vegetation
4	Exposed Rock	1	Vegetation	1	Vegetation
5	Intertidal	1	Vegetation	1	Vegetation
6	Wet Soil	1	Vegetation	1	Vegetation
1	Vegetation	1	Vegetation	2	Open Water
2	Open Water	1	Vegetation	2	Open Water
4	Exposed Rock	1	Vegetation	2	Open Water
5	Intertidal	1	Vegetation	2	Open Water
6	Wet Soil	1	Vegetation	2	Open Water
1	Vegetation	1	Vegetation	3	Sand
2	Open Water	1	Vegetation	3	Sand
3	Sand	1	Vegetation	3	Sand
4	Exposed Rock	1	Vegetation	3	Sand
5	Intertidal	1	Vegetation	3	Sand
6	Wet Soil	1	Vegetation	3	Sand
1	Vegetation	1	Vegetation	4	Exposed Rock
2	Open Water	1	Vegetation	4	Exposed Rock
3	Sand	1	Vegetation	4	Exposed Rock
4	Exposed Rock	1	Vegetation	4	Exposed Rock
5	Intertidal	1	Vegetation	4	Exposed Rock
6	Wet Soil	1	Vegetation	4	Exposed Rock
1	Vegetation	1	Vegetation	5	Intertidal

Table 3.9: Union of three years

From_To
Exposed Rock - Exposed Rock - Exposed Rock
Exposed Rock - Exposed Rock - Intertidal
Exposed Rock - Exposed Rock - Open Water
Exposed Rock - Exposed Rock - Sand
Exposed Rock - Exposed Rock - Vegetation
Exposed Rock - Exposed Rock - Wet Soil
Exposed Rock - Intertidal - Exposed Rock
Exposed Rock - Intertidal - Intertidal
Exposed Rock - Intertidal - Open Water
Exposed Rock - Intertidal - Sand
Exposed Rock - Intertidal - Vegetation
Exposed Rock - Intertidal - Wet Soil
Exposed Rock - Open Water - Exposed Rock
Exposed Rock - Open Water - Intertidal
Exposed Rock - Open Water - Open Water
Exposed Rock - Open Water - Sand
Exposed Rock - Open Water - Vegetation
Exposed Rock - Open Water - Wet Soil
Exposed Rock - Sand - Exposed Rock
Exposed Rock - Sand - Intertidal
Exposed Rock - Sand - Sand
Exposed Rock - Sand - Vegetation
Exposed Rock - Sand - Wet Soil
Exposed Rock - Vegetation - Exposed Rock

Table 3.10: Final Product of from – to change across three years

This study produced a total of 31 trajectories of possible from-to change between two dates, and they are identified as could be seen below (*Table 3.11*).

From Year 1	To Year 2					
	Class 1	Class 2	Class 3	Class 4	Class 5	Class 6
Class 1	No Change					
Class 2		No Change				
Class 3			No Change			
Class 4				No Change		
Class 5					No Change	
Class 6						No Change

Table 3.11: Change trajectories between two years

When the classes are merged to represent the feature of interest sand to non-sand, we obtain the following three trajectories of possible from-to change across two dates, and they are identified as seen in the table below (*Table 3.12*).

From Year 1	To Year 2	
	Sand	None Sand
Sand	No Change	
None Sand		No Change

Table 3.12: Change trajectories for sand and non-sand between two years

However, overall, there are 212 possible from-to trajectories across all three years of the study (*Figure 3.12*).

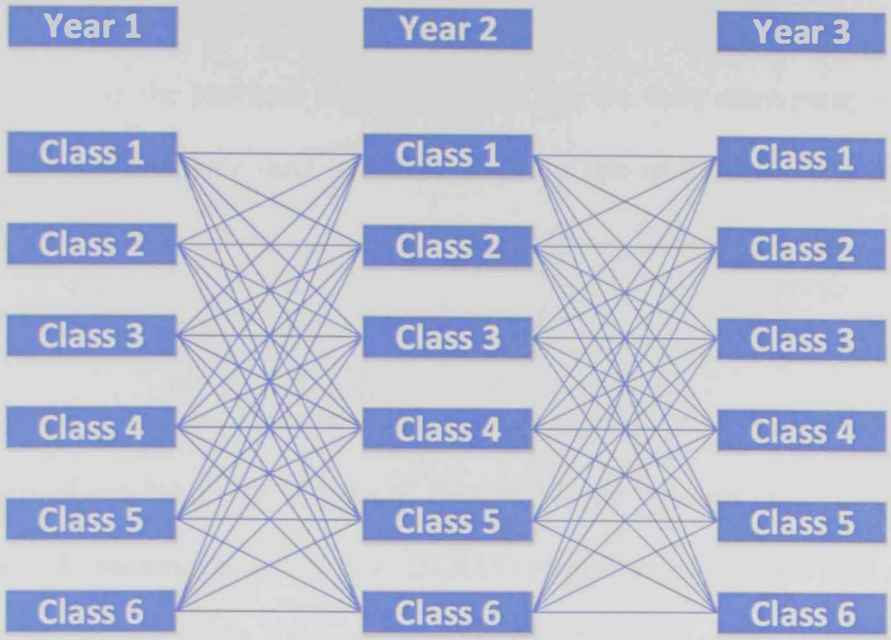

Figure 3.12: Change trajectories across three years

When looking at sand and non-sand changes, we are left with seven across the entire three years of the study (*Table 3.13*).

From Year 1 to Year 2	To Year 3	
	Sand	None Sand
Sand - Sand	No Change	
Sand - None Sand		
None Sand - Sand		
None Sand - None Sand		No Change

Table 3.13: Change trajectories for sand and non-sand across three years

Chapter 4: Results & Discussion

4.1 Training Site Class Identification

As seen in the previous chapter, section 3.6, we were attempting to identify the statistically classifiable land covers through the use of ISODATA unsupervised classification on four different datasets (ISODATA of entropy, Multispectral with high pass filter, multispectral, and PCA) (*Figure 3.9*).

However, after the post classification process of merging the classes into their parent class as per the grouping sites of *Figure 4.1*, the outcome was the same as in *Figure 4.2*. It became apparent that ISODATA performed on the four different datasets, though produced different number of classes in terms of output, still recognized the same features. Statistically speaking, ISODATA is unable to differentiate between Wetlands, Urban, and the Exposed Bedrock features, which indicates that confusion will occur when attempting the supervised classification.

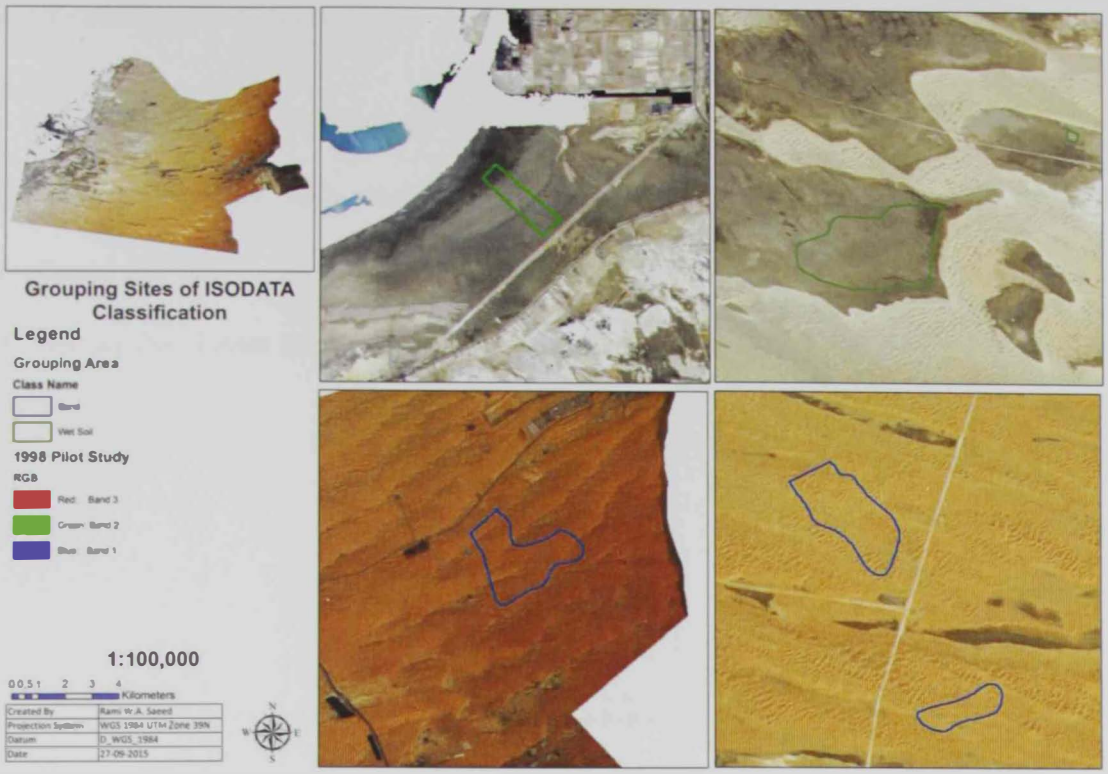

Figure 4.1: Final Outcome after Merge of Classes

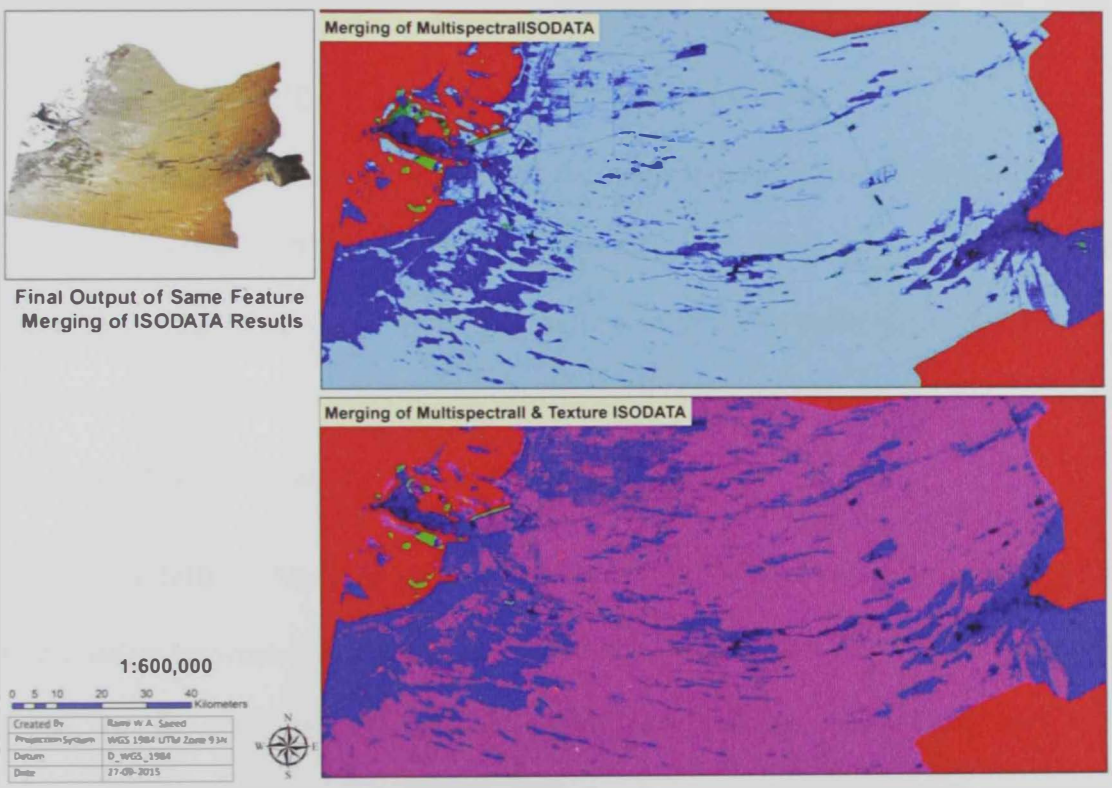

Figure 4.2: Final Outcome after Merge of Classes

4.2 Training Site Selection

Based on the findings of the ISODATA coupled with SAVI mask created from experimenting with various thresholds, it was determined that -1 to -0.2 produced the best results in extracting vegetation across all three years. Thus, *Table 4.1* shows the classes that will be used in this study.

Classes
Vegetation
Surface Water
Sand
Exposed Bedrock
Intertidal
Wet Soil

Table 4.1: Statistical Classifiable Classes

142 invariant training sites that have not changed, were selected across the three years (1992, 2002, and 2013), so as to better represent each year when compared to the other years. Sites that will be used in the supervised classification algorithm were tested for their class separability, to ensure that the selected sites do not get confused with one another statistically.

The Jeffreys-Matusita Distance results for the 1992 dataset concluded that the first conflict between two classes was at 1.938, between class *Sand 38* and *Wet Soil 7*. As for the 2002 dataset, the first conflict between two classes was at 1.897, between *Sand 38 and Wet Soil 10*. As for the final dataset, 2013, it was concluded that the first conflict between two classes appears at 1.980, between *Sand 107 and Exposed Bedrock 11*.

As a result, between all 142 training sites (Sand, Wet Soil, Intertidal, Exposed Bedrock), the JM test proved that there was no considerable class confusion, and upon further examination it was determined that the classes were homogeneous; therefore the use of the Maximum Likelihood algorithm would be suitable.

4.3 1992 LULC Map

Applying the maximum likelihood along with SAVI mask, we produced results that showed the area in km^2 for the initial stage of this study (*Table 4.2*) and two thematic maps; one being all classes as per scheme (*Figure 4.3)* and the other being sand vs non-sand features (*Figure 4.4*).

Class Name	Class Area (Km^2)
Vegetation	146.53
Surface Water	32172.23
Sand	52186.27
Exposed Bedrock	1874.55
Intertidal	3069.62
Wet Soil	5168.40

Table 4.2: 1992 Feature Class Areas

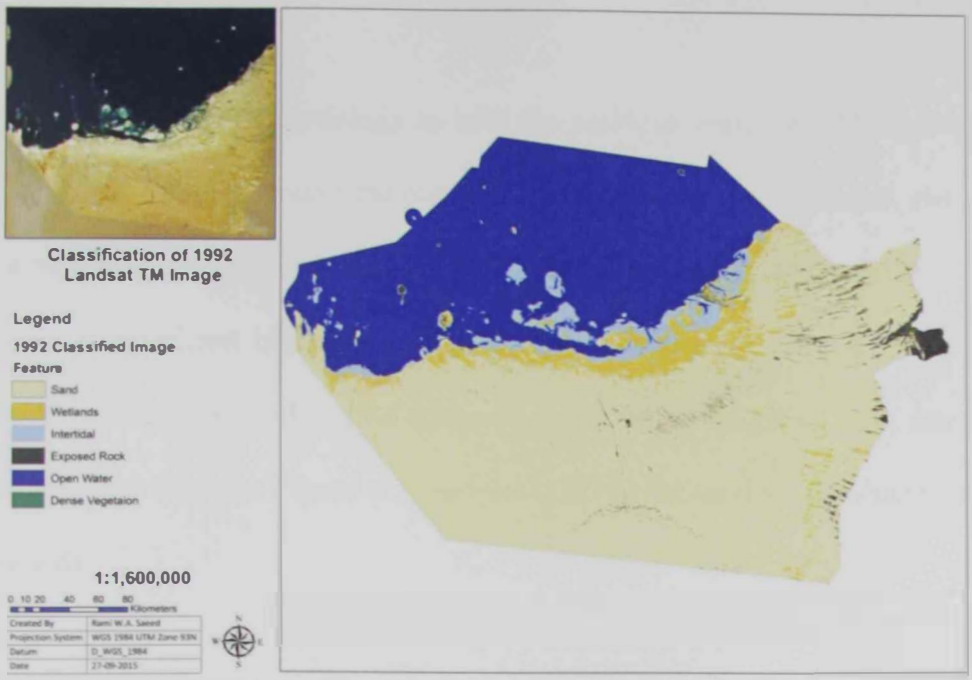

Figure 4.3: Thematic Map of 1992

Figure 4.4: 1992 Thematic Map Showing Sand & Non-Sand Classes

4.4 2002 LULC Map

Using the same methodology as with the previous year, the 1992 dataset, and the study shows changes around the coastal area where sand has expanded, either due to reclamation or due to the change in sensor that it re-classed covers in land. Table 4.3 shows a significant increase in vegetation, a decrease in wet soils, and some changes in sand and intertidal. Two thematic maps are produced as well; one being all classes as per scheme (*Figure 4.5)* and the other being sand vs. non-sand features (*Figure 4.6*).

Class Name	Class Area (Km^2)
Vegetation	518.39
Surface Water	32873.45
Sand	52731.71
Exposed Bedrock	1863.74
Intertidal	2788.27
Wet Soil	4341.34

Table 4.3: 2002 Feature Class Areas

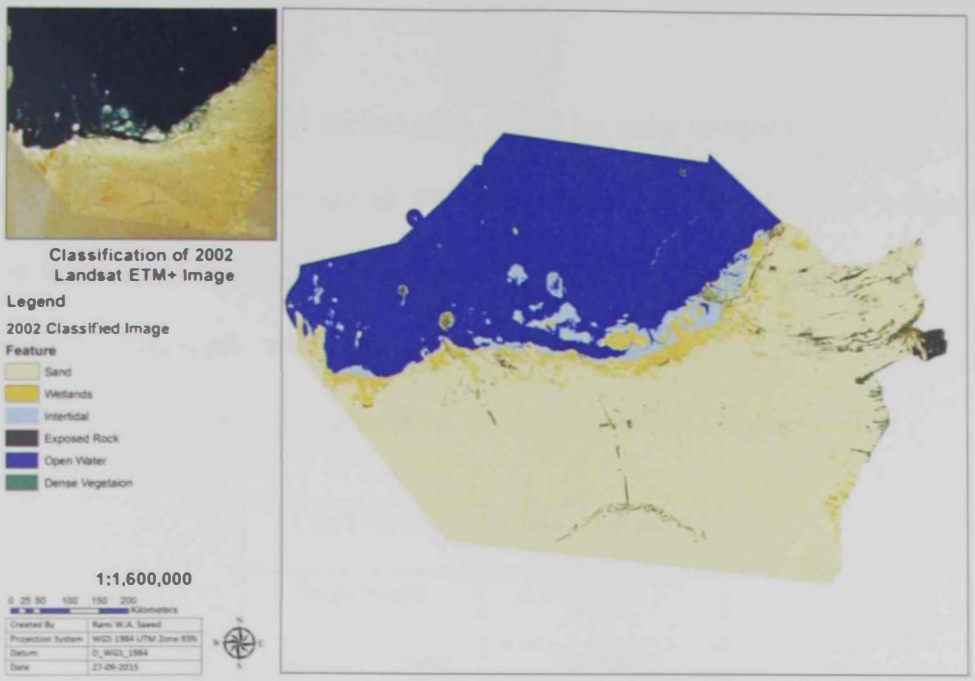

Figure 4.5 - Thematic Map of 2002

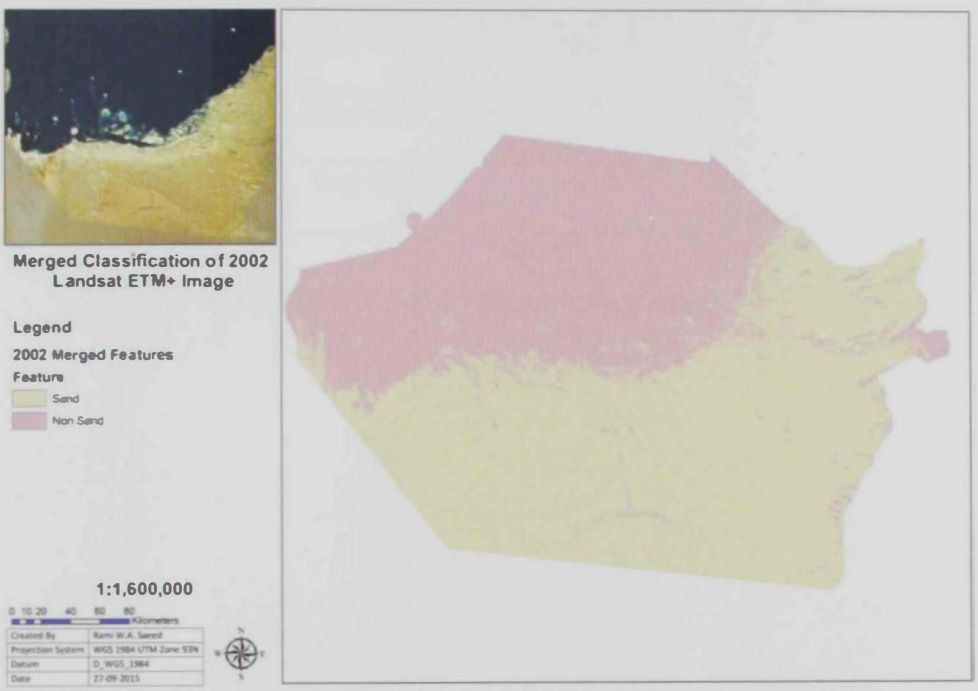

Figure 4.6: 2002 Thematic Map Showing Sand & Non-Sand Classes

4.5 2013 LULC Map

In 2013, further land reclamation could be seen towards the coast, as well urban expansion, and a decrease in vegetation cover. Table 4.4 shows a significant increase in exposed bedrock, a decrease in wet soils, and some changes in sand and intertidal. Two thematic maps are produced; one being all classes as per scheme (*Figure 4.7*) and the other being sand vs. non-sand features (*Figure 4.8*).

Class Name	Class Area (Km^2)
Vegetation	439.78
Surface Water	32678.95
Sand	52848.49
Exposed Bedrock	3821.13
Intertidal	3174.64
Wet Soil	2650.98

Table 4.4: 2013 Feature Class Areas

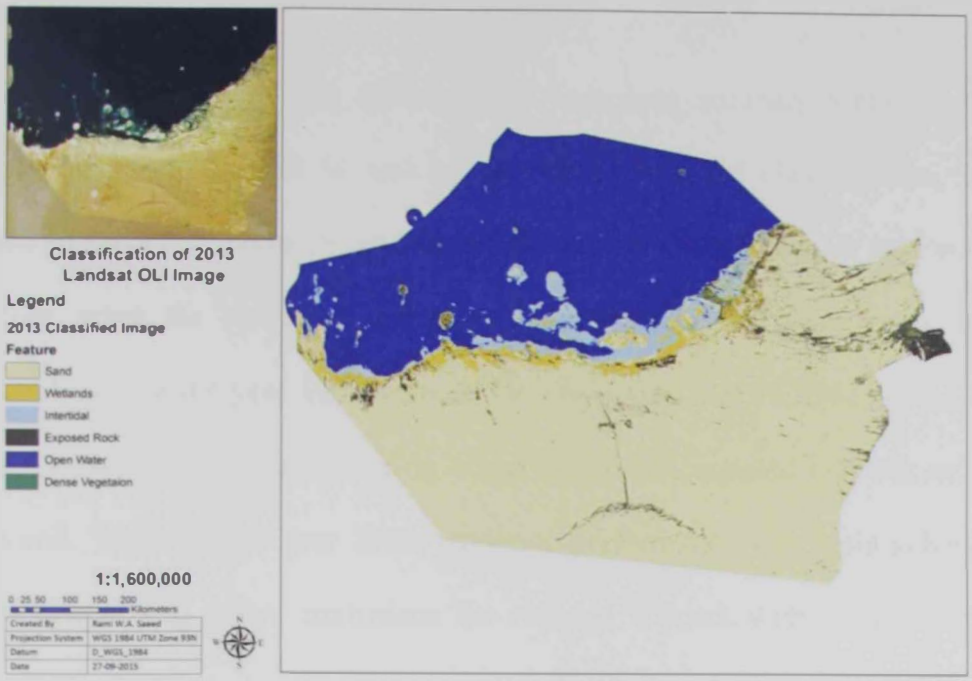

Figure 4.7: Thematic Map of 2013

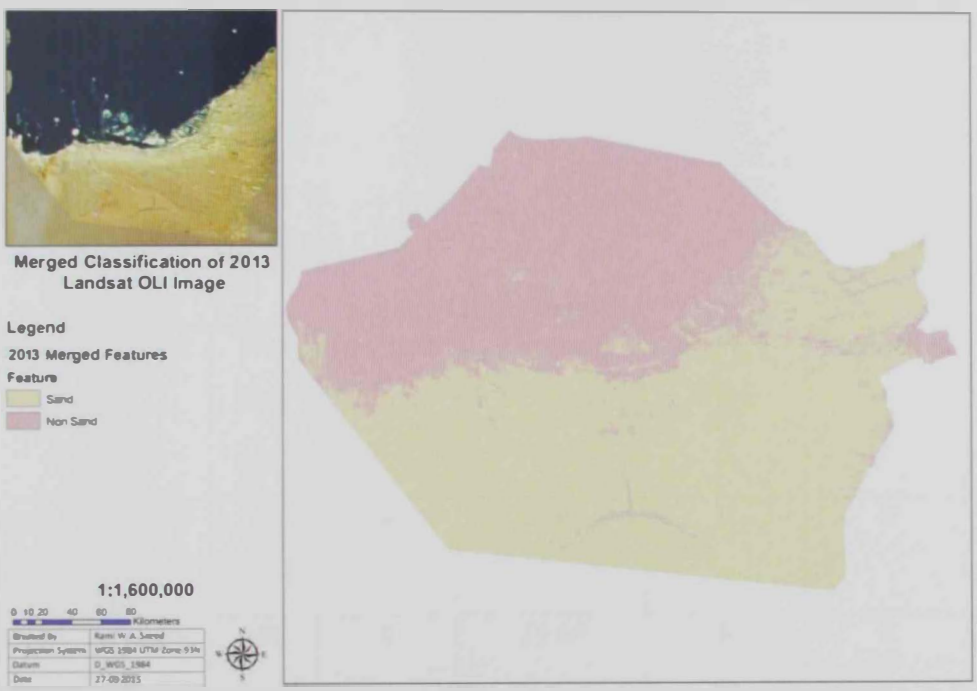

Figure 4.8: 2013 Thematic Map Showing Sand & Non-Sand Classes

4.6 Accuracy Assessment

Following what Jensen (2005) stated regarding accuracy assessment, any Kappa value more than 80 % will be considered of good classification, values between 40 and 80 % moderate, and anything less than 40 % is of poor performance. Therefore, when the confusion matrix was performed on all three years, it was concluded that for the year 1992, a moderate performance at 76.99% was achieved (*Table 4.5*), where the main confusion occurred between exposed bedrock and sand or wet soil. While for the year 2002, moderate performance was again achieved at 78.29% (*Table 4.6*) where confusions for exposed bedrock with sand or wet soil increased, furthermore, in this year wet soil was misclassified with sand, intertidal, and exposed bedrock. As for 2013, good performance was achieved at 81.14% (*Table 4.7*) where the same errors between exposed bedrock and sand or wet soil remained.

Overall Accuracy = 87.81 %

Kappa Coefficient = 76.99 %

Ground Truth (Percent)

Class	Sand	Wet Soil	Intertidal	Exposed Bedrock	Surface Water	Vegetation	Total
Sand	90.98	0	0	23.02	0	0	64.23
Wet Soil	2.88	100	0	25.68	0	0	17.56
Intertidal	0	0	100	0	0	0	1.76
Exposed	6.14	0	0	51.30	0	0	10.56

Bedrock							
Surface Water	0	0	0	0	100	0	4.59
Vegetation	0	0	0	0	0	100	1.29

Class	Commission	Omission	Producers Accuracy	User Accuracy
Sand	4.49	9.02	90.98	95.51
Wet Soil	29.37	0	100	70.63
Intertidal	0	0	100	100
Exposed Bedrock	39.21	48.70	51.30	60.79
Surface Water	0	0	100	100
Vegetation	0	0	100	100

Table 4.5: Accuracy Assessment of 1992 Classification

Overall Accuracy = 89.73 %

Kappa Coefficient = 78.29 %

Ground Truth (Percent)

Class	Sand	Wet Soil	Intertidal	Exposed Bedrock	Surface Water	Vegetation	Total
Sand	99.06	9.76	0	44.60	0	0	73.89
Wet Soil	0.94	80.59	0	16.95	0	0	12.68

Intertidal	0	9.43	100	0	0	0	2.94
Exposed Bedrock	0	0.18	0	38.44	0	0	4.52
Surface Water	0	0	0	0	100	0	4.65
Vegetation	0	0	0	0	0	100	1.31

Class	Commission	Omission	Producers Accuracy	User Accuracy
Sand	8.72	0.94	99.06	91.28
Wet Soil	20.69	19.41	80.59	79.31
Intertidal	39.95	0	100	60.05
Exposed Bedrock	0.51	61.56	38.44	99.49
Surface Water	0	0	100	100
Vegetation	0	0	100	100

Table 4.6: Accuracy Assessment of 2002 Classification

Overall Accuracy = 91.06 %

Kappa Coefficient = 81.14 %

Ground Truth (Percent)

Class	Sand	Wet Soil	Intertidal	Exposed Bedrock	Surface Water	Vegetation	Total
Sand	99.75	0	0	56.15	0	0	74.38
Wet Soil	0.06	85.67	0.85	0.12	0	0	10.63

Intertidal	0	9.97	99.15	0	0	0	2.99
Exposed Bedrock	0.19	4.37	0	43.73	0	0	6.10
Surface Water	0	0	0	0	100	0	4.60
Vegetation	0	0	0	0	0	100	1.30

Class	Commission	Omission	Producers Accuracy	User Accuracy
Sand	9.38	0.25	99.75	90.62
Wet Soil	0.64	14.33	85.67	99.36
Intertidal	41.01	0.85	99.15	58.99
Exposed Bedrock	10.94	56.27	43.73	89.06
Surface Water	0	0	100	100
Vegetation	0	0	100	100

Table 4.7: Accuracy Assessment of 2013 Classification

4.7 Change Analysis

As discussed in the previous chapter, change analysis was performed across the three datasets 1992, 2002, and 2013 using post classification change analysis. Map & statistical results of change between 1992 – 2002 could be seen in *Appendix A Table 4.8 & 4.9 & Figure 4.9, 4.10, and 4.11*. As for the results, between 2002 – 2013, both map and statistics could be seen in *Appendix A Table 4.10& 4.11 & Figure 4.12, 4.13, and 4.14*.

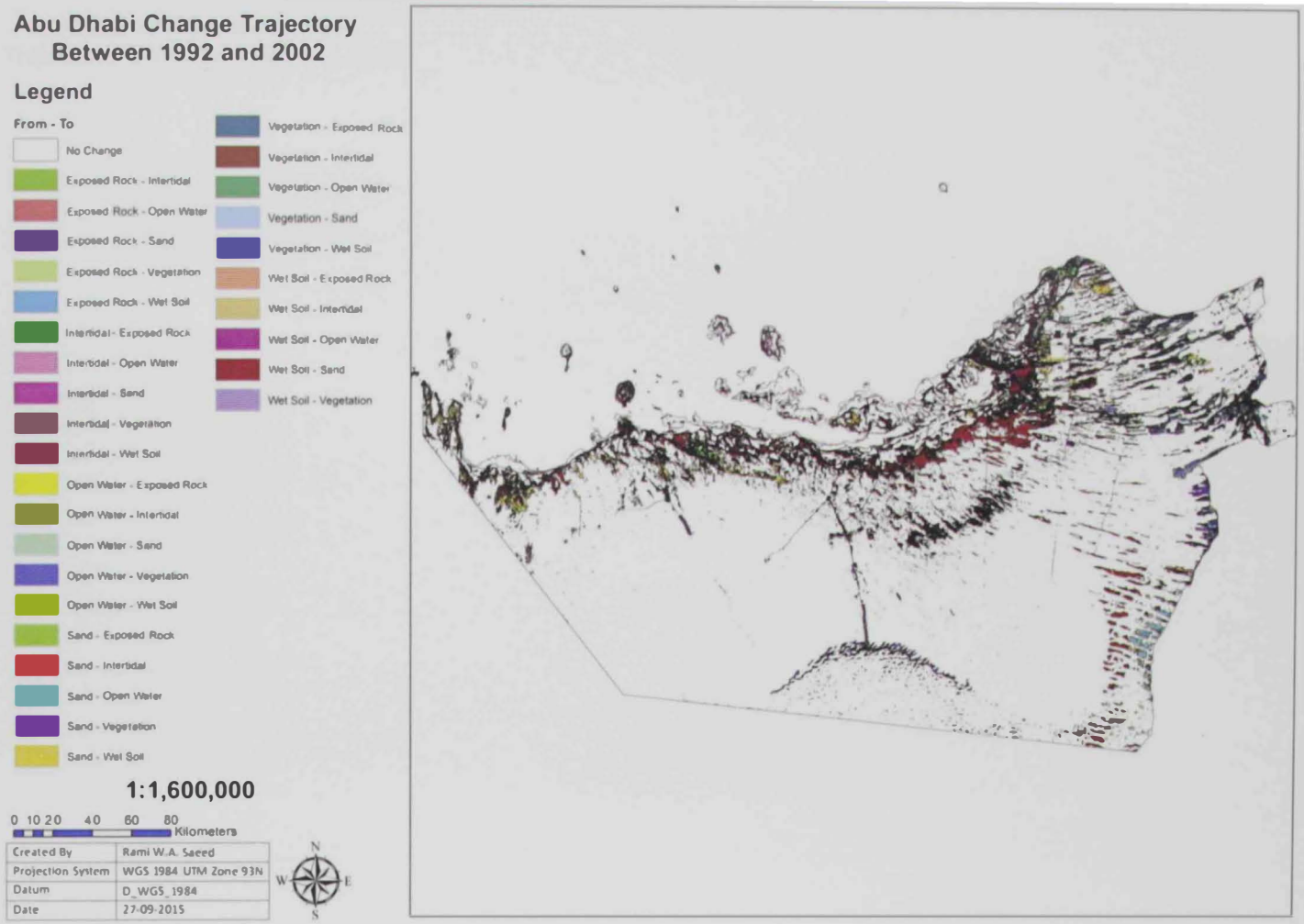

Figure 4.9: Change Trajectory Map from 1992 to 2002

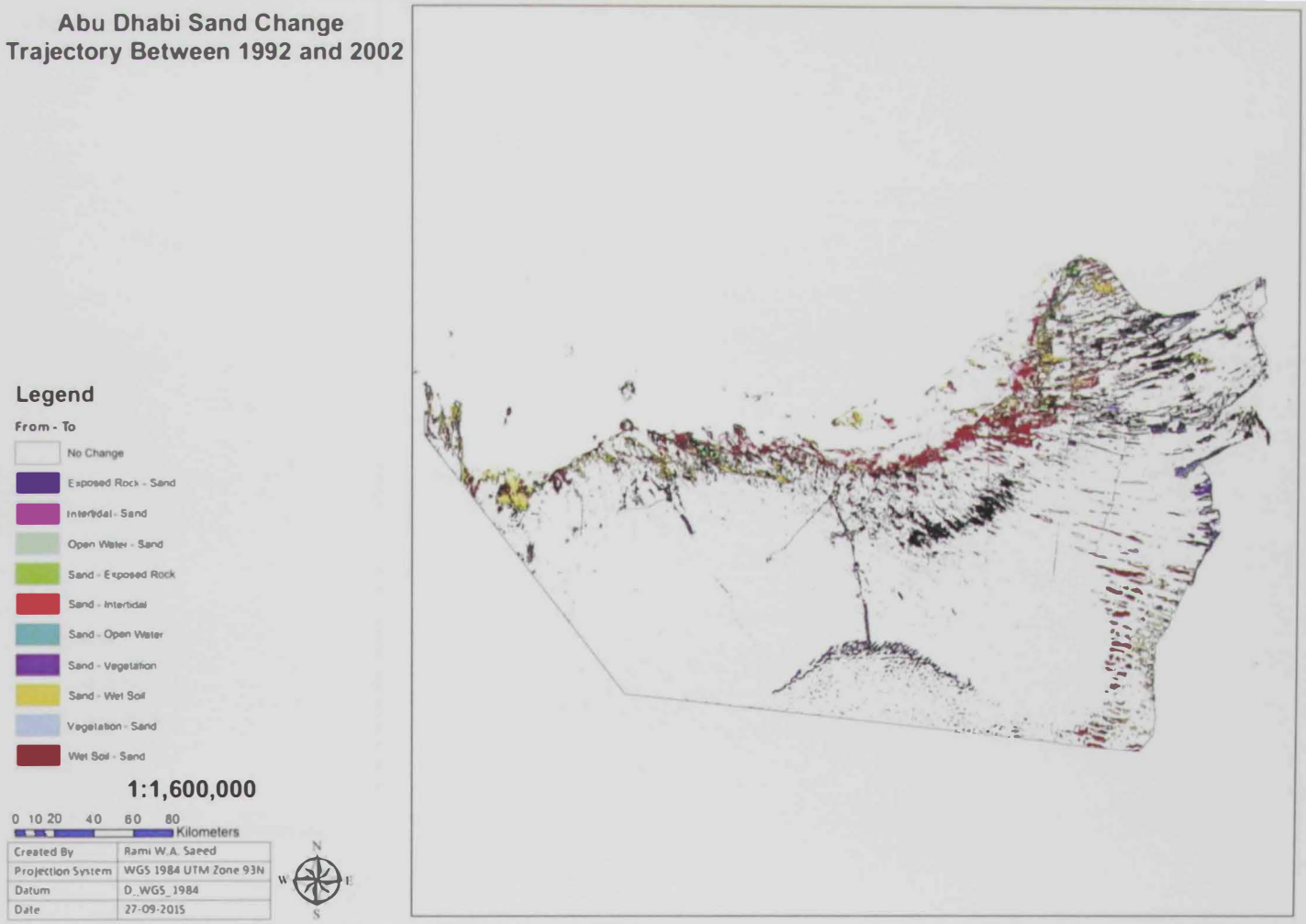

Figure 4.10: Change Trajectory Map of Sand from 1992 to 2002

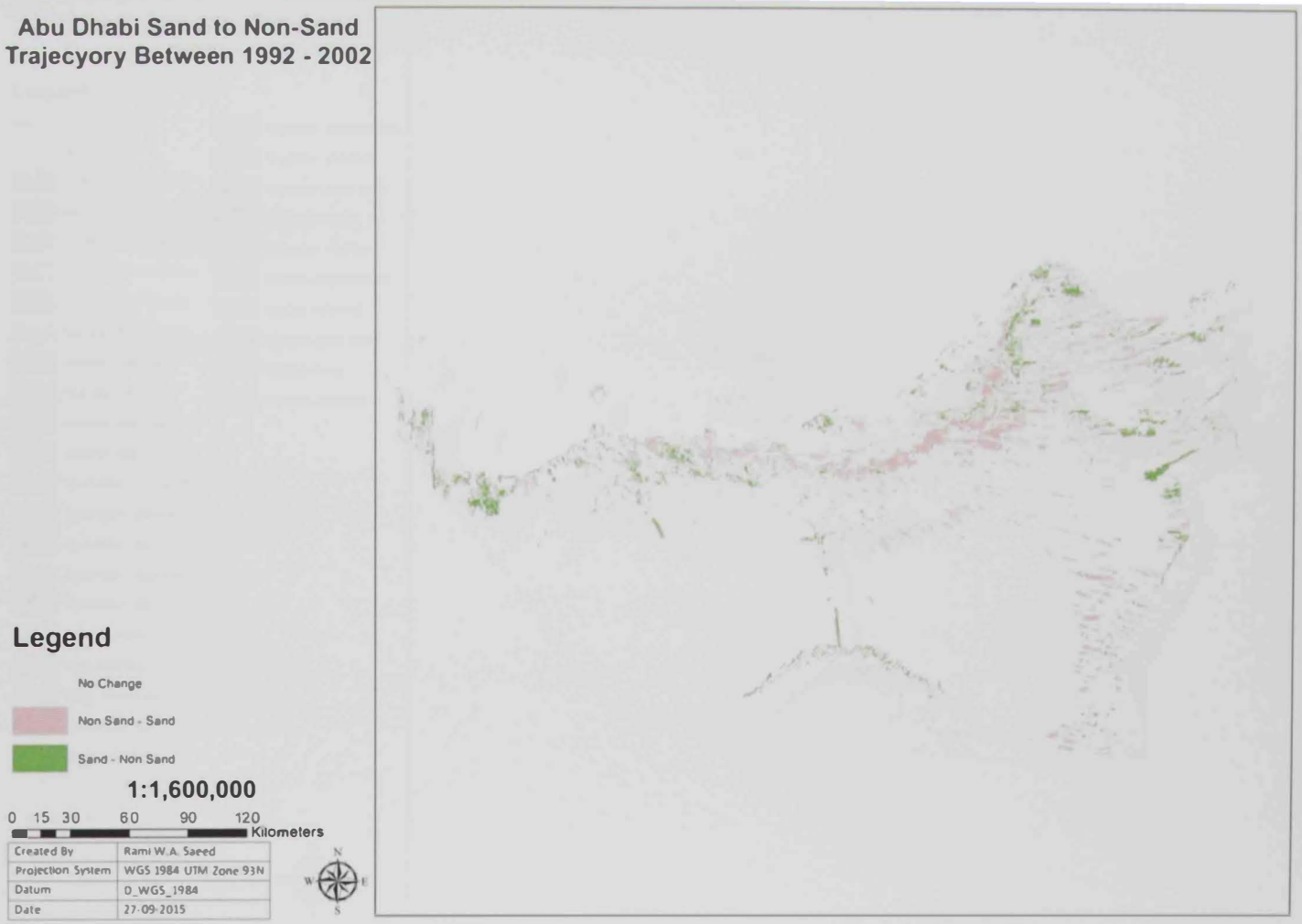

Figure 4.11: Change Trajectory Map of Sand from 1992 to 2002

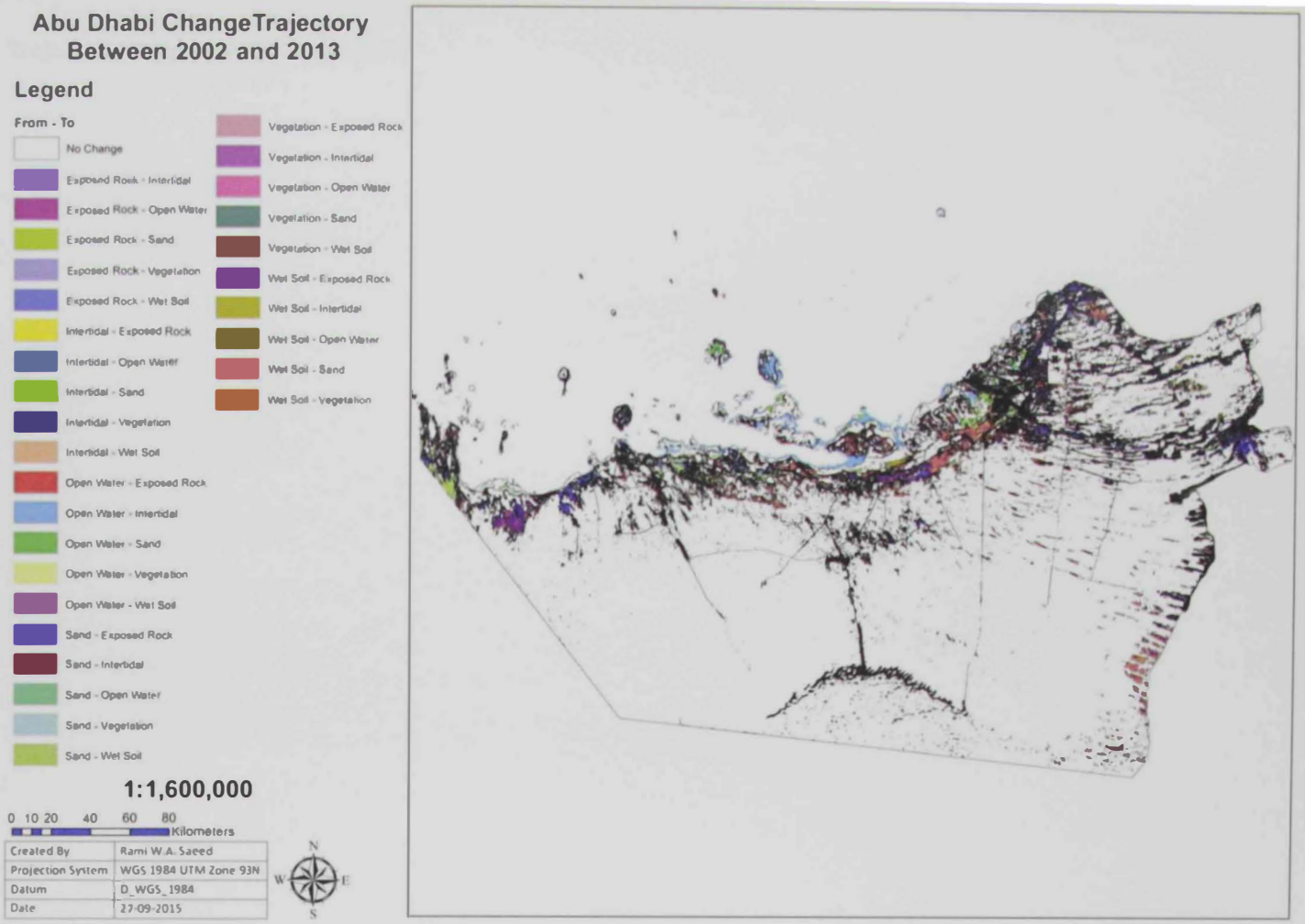

Figure 4.12: Change Trajectory Map from 2002 to 2013

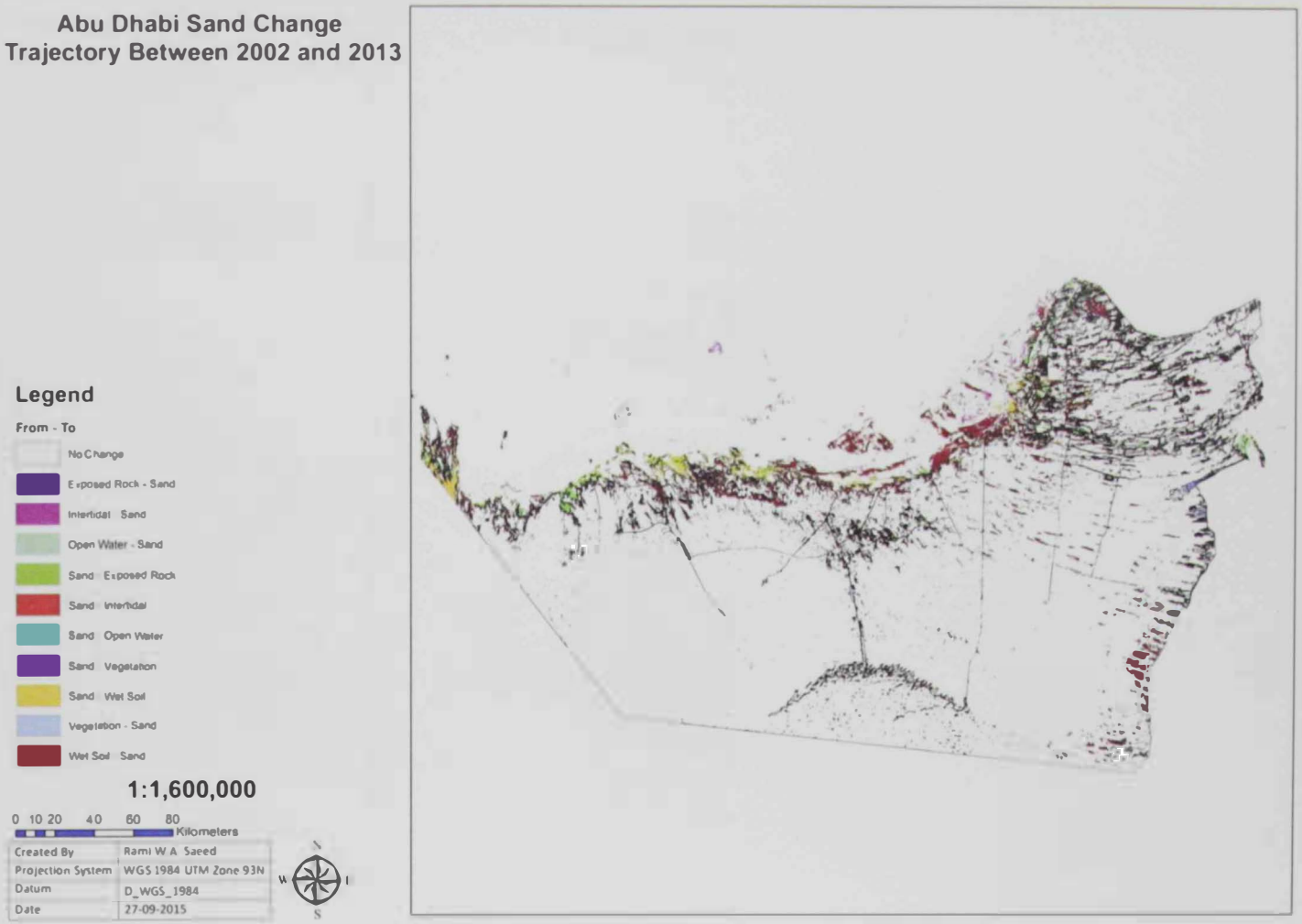

Figure 4.13: Change Trajectory Map of Sand from 2002 to 2013

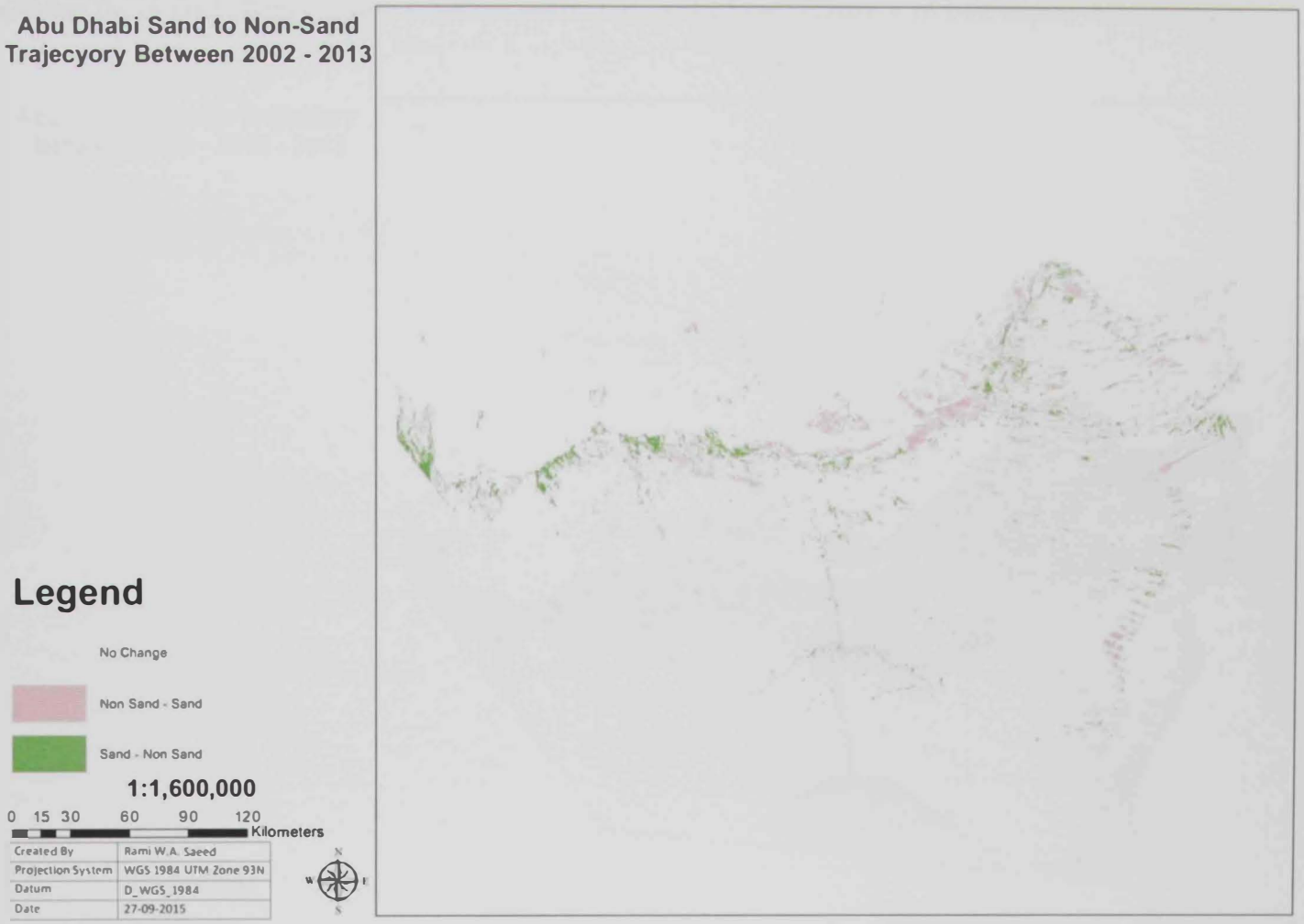

Figure 4.14: Change Trajectory Map of Sand from 1992 to 2002

When considering the overall change across the three years, *Figure 4.15 and Figure 4.16* best depict these changes:

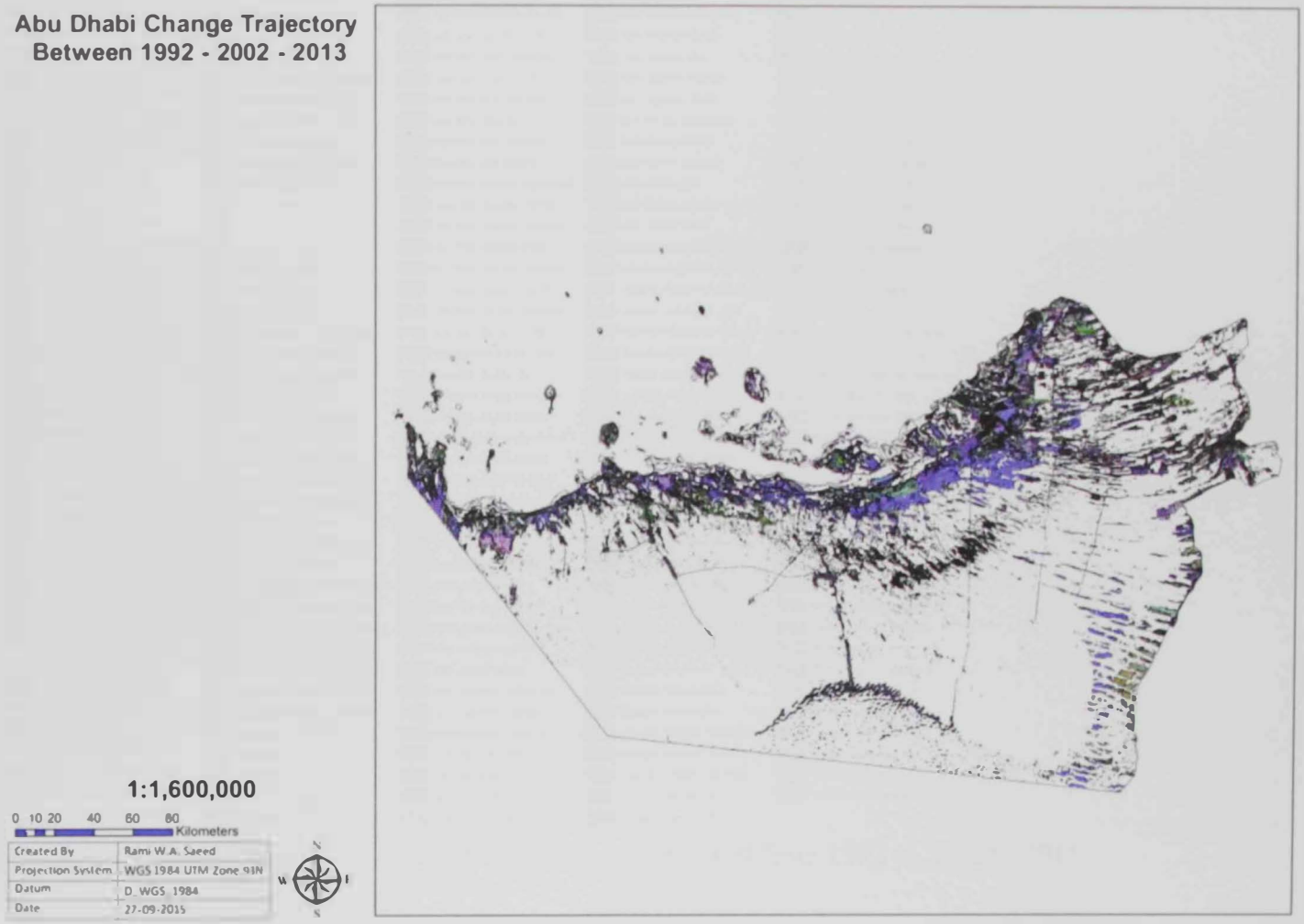

Figure 4.15: Change trajectory from 1992 to 2002 to 2013

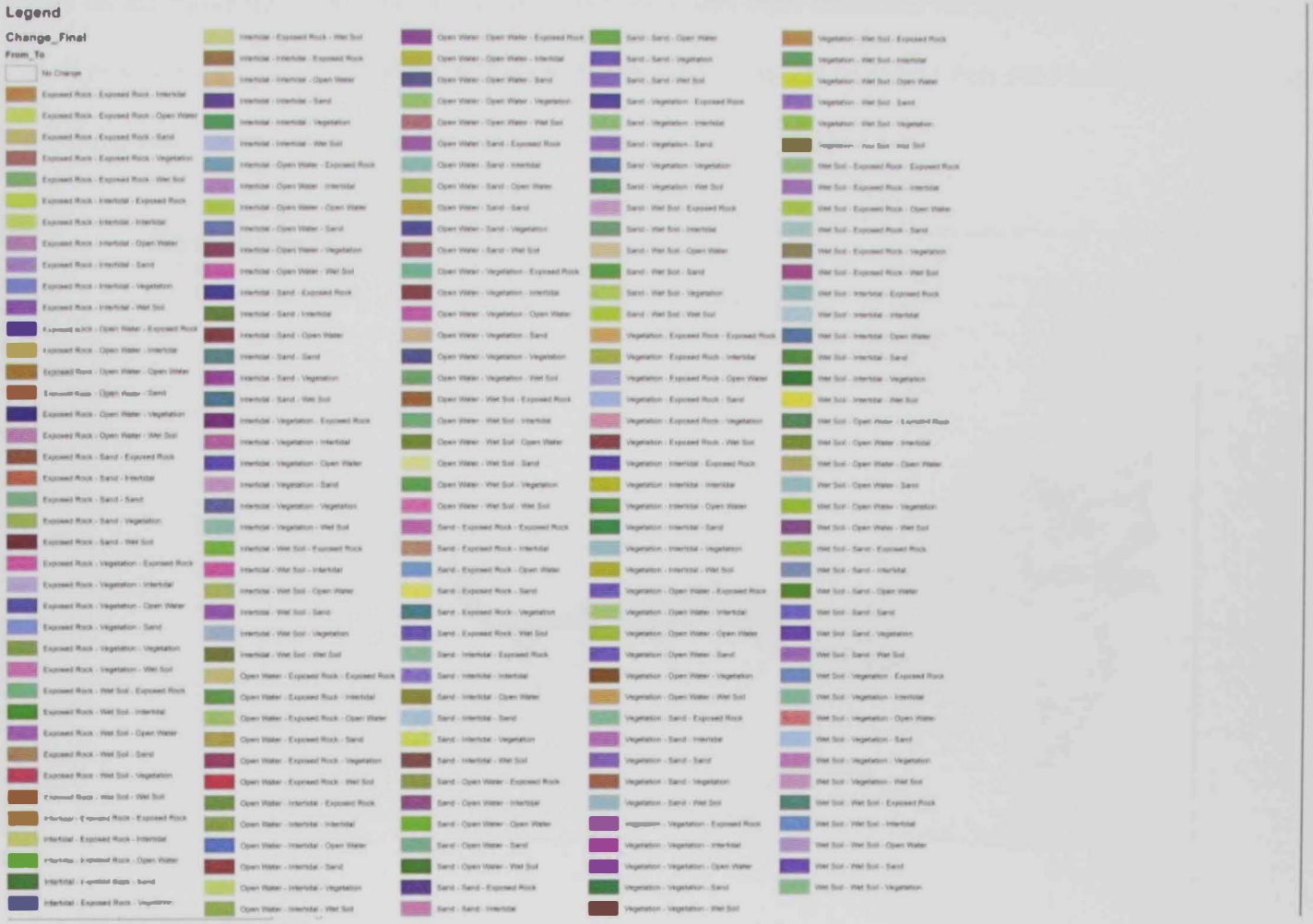

Figure 4.16: Total of 203 change trajectories from 1992 to 2002 to 2013

Since this study focuses on the movement and changes in sand, the resultants were extracted for the feature of interest and the changes can be seen in *Figure 4.17 & Figure 4.18. Figure 4.19* better defines a clearer understanding of sand / non-sand interactions and statistical area change for sand throughout the three years of the study could be seen in *Appendix A Table 4.12.*

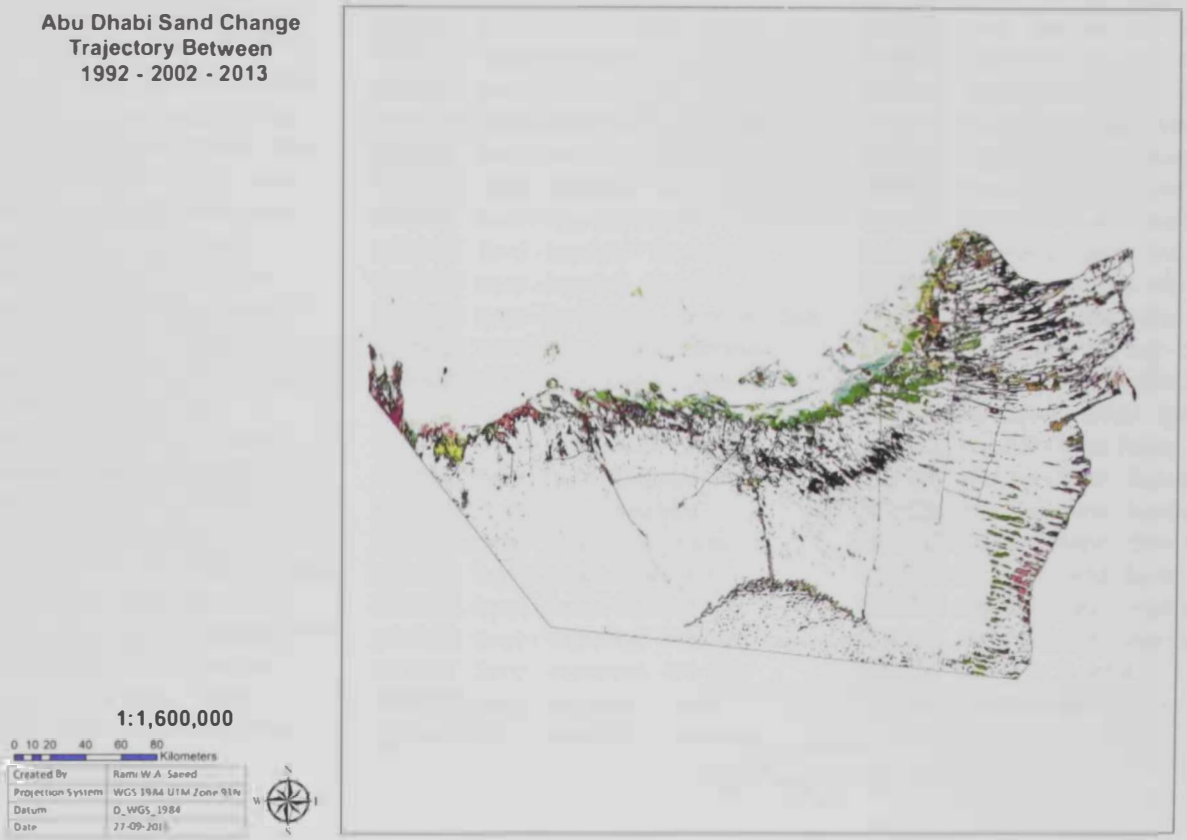

Figure 4.17: Changes in sand trajectories from 1992 to 2002 to 2013

Figure 4.18: Total of 85 change trajectories for sand from 1992 to 2002 to 2013

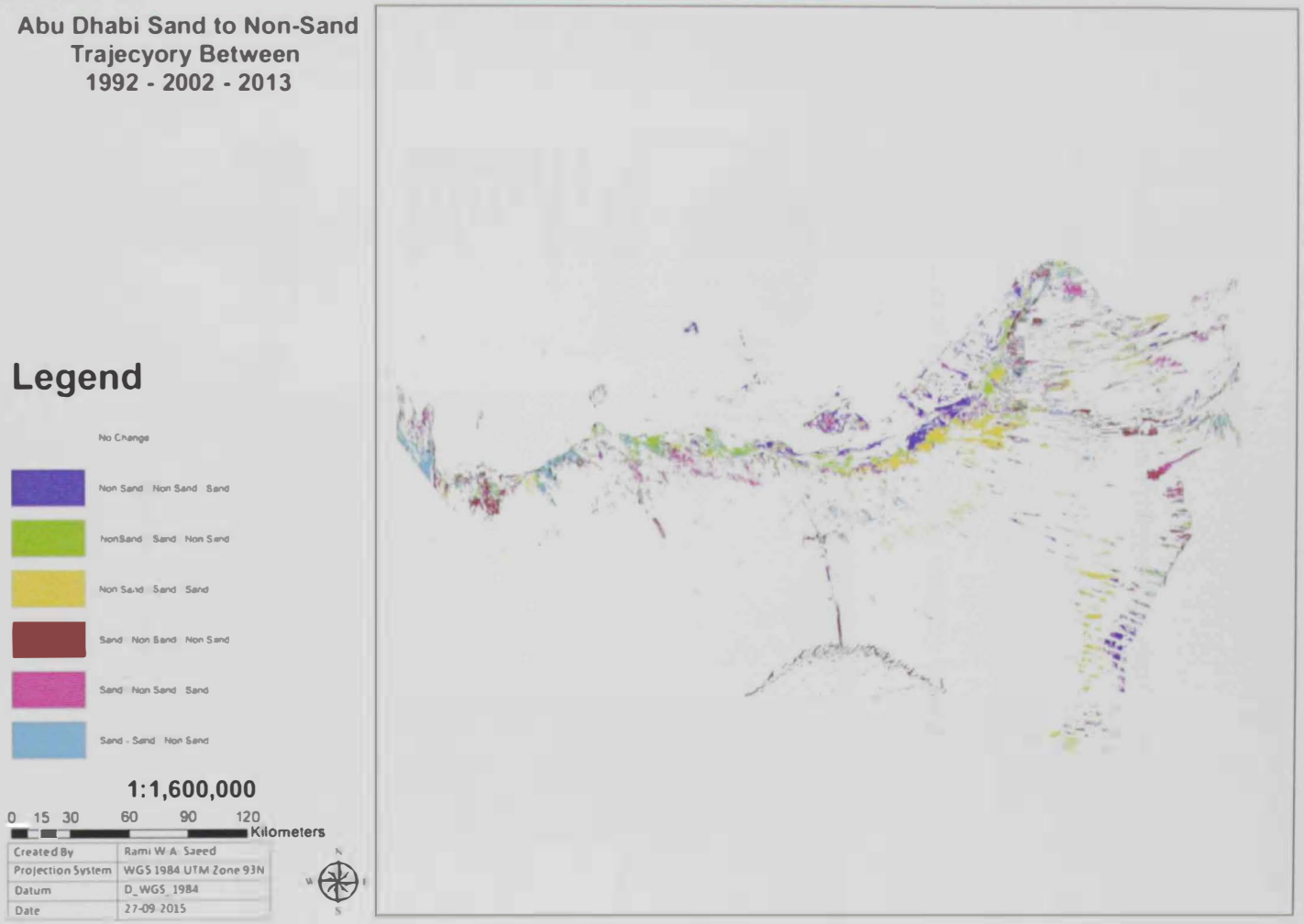

Figure 4.19: Change Trajectory Map of Sand / Non Sand from 1992 to 2002 to 2013

4.8 Discussion

There are apparent and drastic changes between the three years used in this study, due to two factors: the difference between the platforms and the socio-economic growth of the emirate.

Changes attributed to the difference in platforms could be best seen in *Figure 4.20 and Figure 4.21* where areas classified as exposed bedrock in the year 1992 become classified as sand in 2002, although the feature did not change temporally when checked against higher resolution imagery used in this study.

Figure 4.20: Features Classed as Non-Sand

Figure 4.21: Features Classed as Sand

The socioeconomic growth of the Abu Dhabi Emirate is a result of a never ending continuous process of urban and social development that the nation has vowed to undertake to place them as forerunners in the global theater. For the past 40 odd years, the emirate transformed itself from being confined to specific geographical areas, to urban developments across the wide spread desert, all part of a plan to exploit unused land to enhance the emirate's portfolio further. There are many drivers that caused such changes to occur over time, these drivers could be categorized as follows:

- Geographic

  The areas that witnessed the most change are those surrounding the coast. Waterfront properties have always been a selling point, coupled with the fact that the emirate plans to play a more predominant role in world tourism as a holiday and recreation destination, regions surrounding the coast

have seen continuous land reclamation. Meanwhile, as a result of inland dredging to create artificial canals, other areas were being transformed to wet lands due to the change in the water table (*Figure 4.22 & 4.23*).

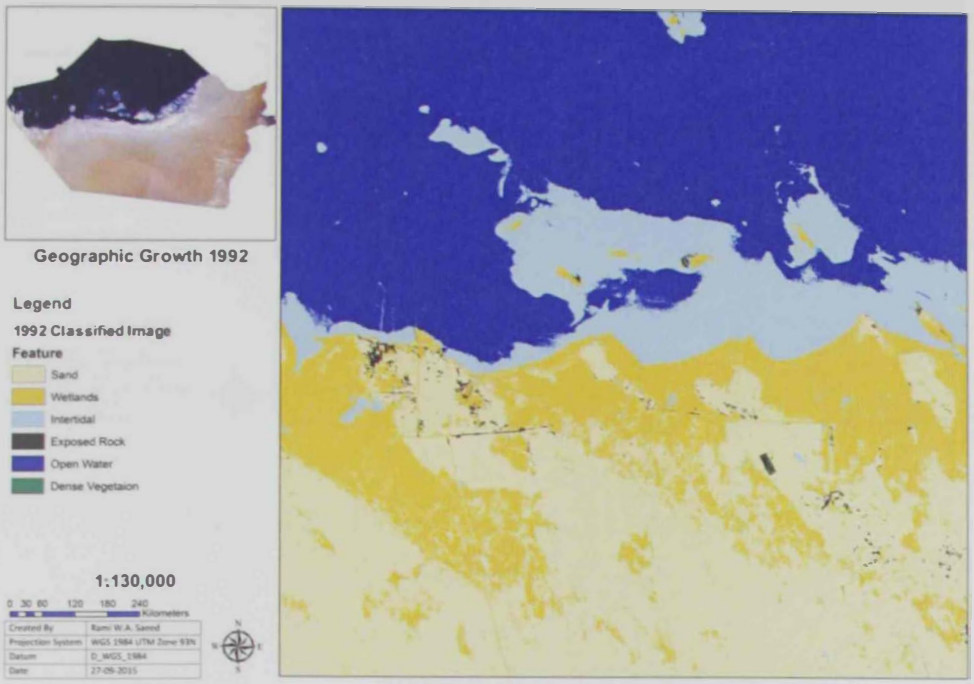

Figure 4.22: Coastal areas in 1992

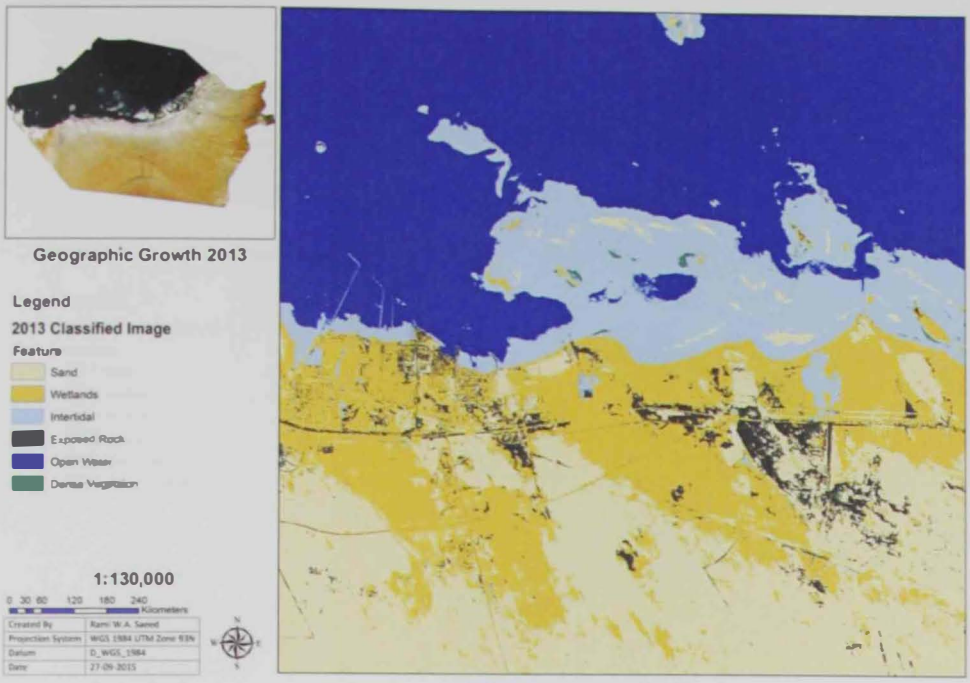

Figure 4.23: Coastal areas in 2013 since 1992

- Socioeconomic

Since the discovery of oil, the emirate has undergone large-scale modernization that resulted in the increase of infrastructures and facilities to cater to the ever increasing desire for better services and social outlets. By that, the increase of vegetation could be seen not just in farm lands the government subsidized to the natives, but also in parks, recreational spaces, international golf courses and green spaces around government, public, and private structures, which contributed to the overall transformation of the desert into a lush green garden. Since all these new developments required empty spaces, much of the desert was transformed into an interconnected city (*Figures 4.24 & 4.25*).

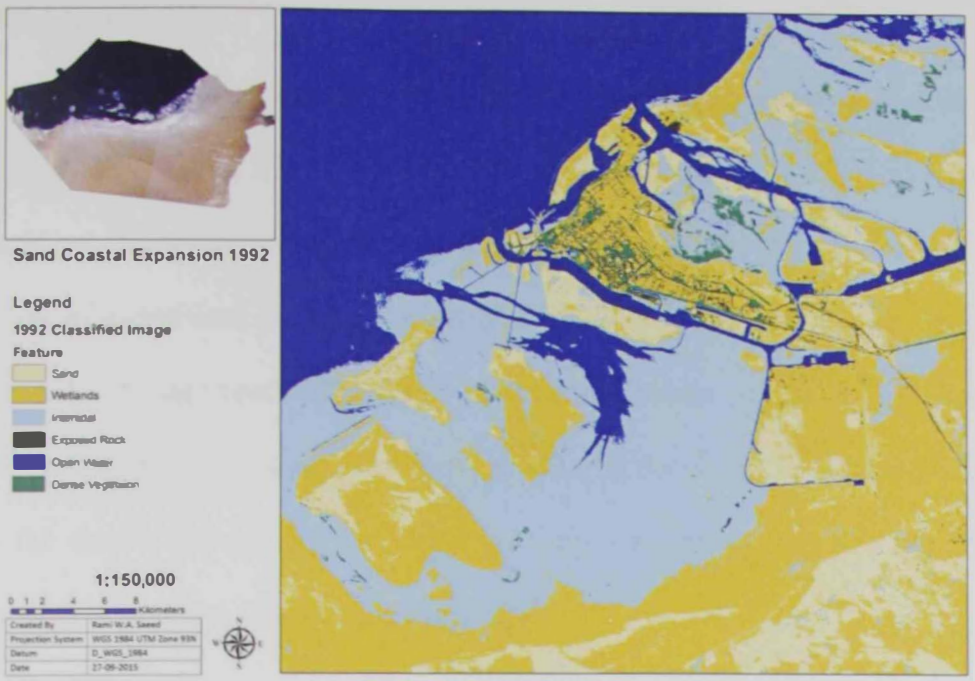

Figure 4.24: Sate of coastal areas in 1992

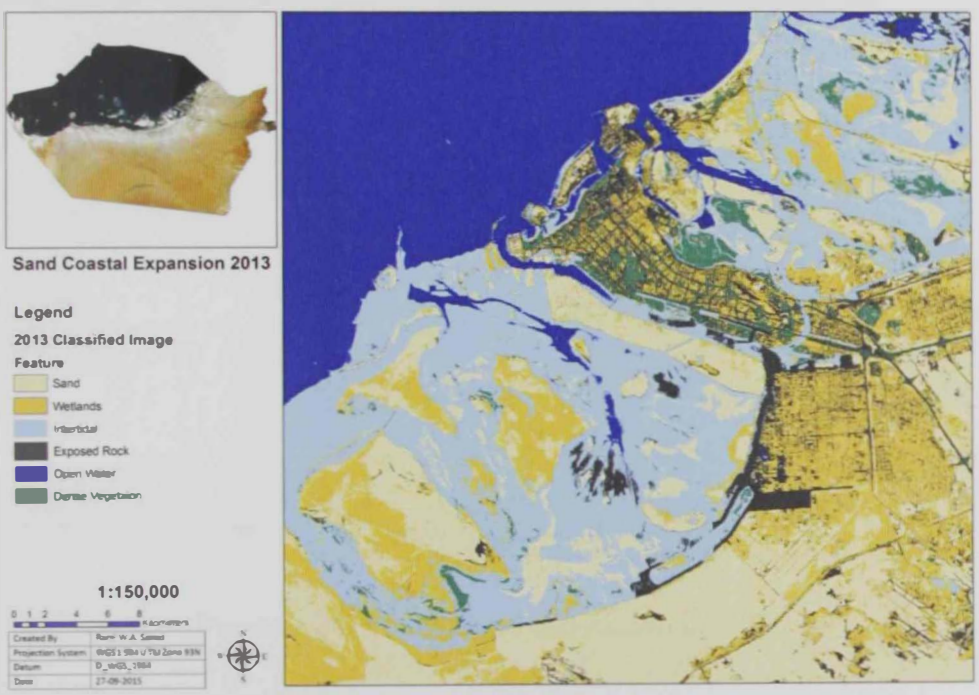

Figure 4.25: Coastal change in 2013 since1992

- Population

The emirate saw a boom in its population in recent years, as there has been an increase in life expectancy and a decrease in child mortality as a result of improved socioeconomic and living standards, coupled with an influx of expatriates looking for better living standards. This growth spurt resulted in further needs of urban development to house, educate, hospitalize, and govern the population. This could be seen by the changes over the years, as the desert surrounding the cities has been urbanized to better suit the growing population (*Figures 4.26 & 4.27*).

Figure 4.26: Population Distribution in 1992

Figure 4.27: Population Change in 2013 since 1992

- Transportation

The expansion of the emirate's road network and the establishment of the motorways permitted the settlement of new frontiers deep in the desert that might have been harder to reach if such infrastructures did not exist. Such success stories include the prospering of the city of Liwa, situated in the southern region of the emirate surrounded by sand dunes, the connecting roads between Al Ain and Abu Dhabi, and the roads connecting Dubai and Abu Dhabi, where a near horizontal expansion could be seen happening across the years of the study. These networks allowed the population to spread and not congregate at certain points in the emirate (*Figures 4.28 & 4.29*).

Figure 4.28: Road Network Limited in 1992

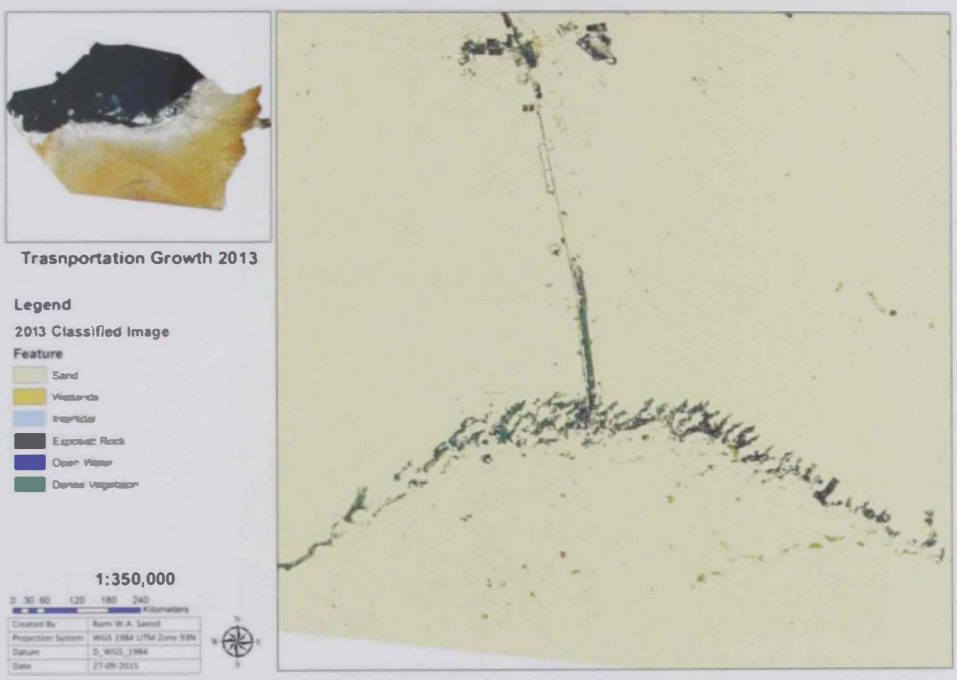

Figure 4.29: Network Enhancement Allowed Growth in 2013 since 1992

- Policies

The emirate's leadership strived to ensure that their populaces are well cared for by ensuring that the policies enacted ensure the benefit and wellbeing of the people. In this study, the most predominant policy that has drastically changed the emirate's LULC is the land grants. Natives who meet the criteria could be awarded a grant in one of four categories: government housing, residential land, commercial land, or farm land. This grant allowed further expansion of the built-up areas across the emirate as more and more eligible persons were able to develop the desert even further (*Figures 4.30 & 4.31*).

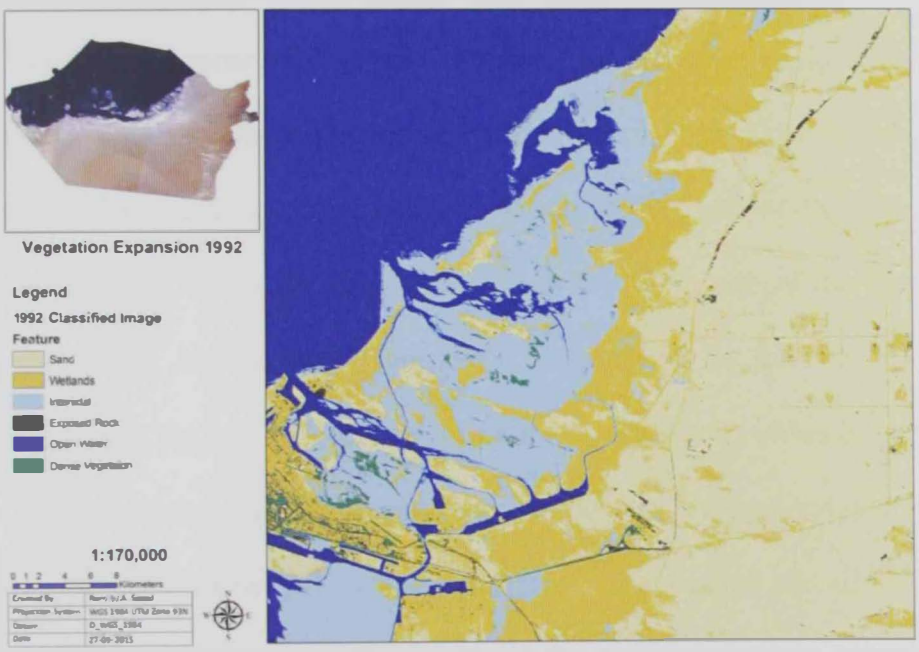

Figure 4.30: Empty Unused Spaces in 1992

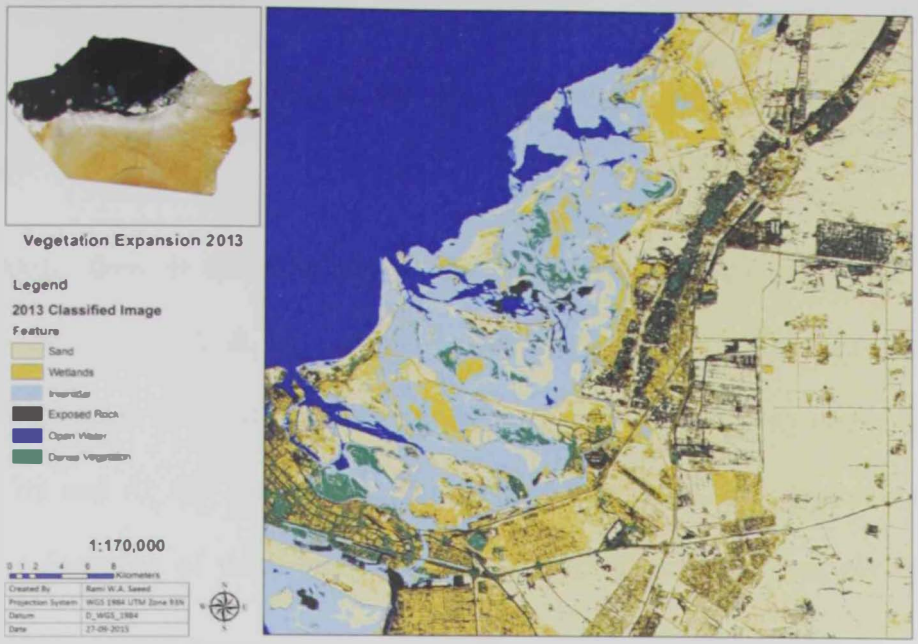

Figure 4.31: Subsides Allowed Expansion in 2013 since 1992

Overall, it is apparent that land development is occurring in several sites causing the total area of dunes to decrease around them. These sites are Abu Dhabi City and the highway leading to Dubai City and Al Ain City, and Al Ain City and the highway leading to Dubai City, thus capsuling the northern part of the Abu Dhabi Emirate. Moreover, land cover change over time could be seen in the region surrounding Liwa City and the highway leading from and to it, which is seen in the southern part of emirate. Lastly, the area with the slowest development, compared to the previous two, is Ruwais City, which is situated in the western part of the emirate the slow development in Ruwais City is due to the fact that it is an industrial city and the development there is mainly related to the emirate's oil & gas development strategic plan.

Although sand area had seen a recession in some parts of the study areas, it was able to gain grounds in other parts. These gains could be attributed to channel dredging that allowed the water table to drop enough causing the drying of the wet

soils, or to land reclamation projects that are part of the Emirate's urban development master plan. Both are factors in the sand growth in the areas surrounding the coastline.

Furthermore, there is the farmland abandonment phenomenon that could be seen between the years 2002 & 2013 in the regions south of Al Ain City near the Omani borders, and other sites such as in Liwa City and along the highway connecting Abu Dhabi City and Al Ain City. Where farmlands where abandoned thus allowing the natural reclamation of these sites by sand that previously the farm owner would prevent from occurring.

Chapter 5: Conclusion & Recommendations

Based on the study performed, the potential of remote sensing is clearly demonstrated when it comes to tracking dune movement across time and space, especially when implemented on a regional level. The study showed that with time, dunes in the Abu Dhabi Emirate are expanding in the sense of its replacement of other land cover features to pave the way for future urban development. This phenomenon will continue as the long as the need for coastal / waterfront properties remains engrained in the population's needs and wants. Nonetheless, it should be mentioned that such changes do not count for desertification, since they are part of a bigger plan that involves preparing the land for urban development. Furthermore, these reclaimed sites classified as sand do not behave in the same manner as dunes, since there are no apparent accumulation or migration of these features. Moreover, it was apparent that even though the increase of vegetation saw a sharp rise between 1992 and 2002, a clear and obvious recession struck between 2002 and 2013, when many farmlands were abandoned, but nonetheless, the overall vegetation land cover showed a continuous increase.

To quantify the change that has occurred to the emirate between 1992 and 2013, this study relied on the use of Landsat imagery to create land use & land cover thematic maps at intermodal stages. The Landsat series is considered to be a wealth of information on global change research since it has been collecting images of Earth since mid-1972. This information permitted the monitoring of dune changes across the past two decades, in this study, to better understand the changes in sand land cover area in the emirate of Abu Dhabi and its trends, and to better predict the future model and what it would look like in the future.

The classification process undertaken in this study is not free from errors, as challenges were confronted including the continuous statistical confusion between land cover features. The use of the unsupervised classification, namely the Iterative Self-Organizing Data Analysis Technique (ISODATA) algorithm, made it apparent what sort of land cover features are expected to be encountered in this study, and what confusions between different features are found, such as between urban and the exposed rock, and urban and wetlands, which led to the grouping of these features as non-sand since the main objective is sand mapping and movement analysis through time. Furthermore, another error that became apparent was that of the sensor being analyzed, where with time, the different sensors mapped land cover features more accurately.

Analyzing the change that occurred throughout this study, it is revealed that the sand cover increased by a total area of 545.44 km^2 between 1992 to 2002, and by 116.78 km^2 between 2002 to 2013. Furthermore, the most notable change is that of the vegetation cover; between 1992 and 2002, we could see a total growth of 371.84 km^2, however, between 2002 and 2013, the total vegetation coverage dropped, and 78.56 km^2 were lost.

Between 1992 and 2013, the land cover features have drastically changed, and though it might appear that dunes are increasing in area, it is mainly attributed to the pre-urban development projects that the government undertakes. The land first has be to be initiated to be better suitable for the construction projects they are being developed for, therefore, reclaiming coastal lands from the wetlands and surface water and intertidal areas are turned into sand fields.

In conclusion, the methodology followed by this study could be adopted and expanded to study and examine various time points to keep track of dune movement and changes in land cover. However, it is less suitable for doing so for other land cover features such as urban, wetlands, exposed rocks since confusion is dominant, thus not allowing a better examination, such cover features would need different sensors at higher resolutions. The Landsat series offer a vast opportunity to better understand the changes that are occurring in the Abu Dhabi Emirate as a whole, and to better map and model its future and possible changes.

Bibliography

AL Ahbabi, 2013.LULC change analysis of Abu Dhabi region between 1986 and 2010: extracted from a mosaic of landsat imageries of Abu Dhabi emirate between 1973 and 2010. *Master's Thesis, United Arab Emirates University*

Abu-Zeid, M.M., Baghdady, A.R., El-Etr, H.A., 2001. Textural attributes, mineralogy and provenance of sand dune fields in the greater Al Ain area, United Arab Emirates. *Journal of Arid Environments*, 475-499

Al Kuwari, N.Y., Kaiser, M.F., 2011. Impact of North Gas Field development on landuse/landcover changes at Al Khore, North Qatar, using remote sensing and GIS. *Applied Geography*, 1144 – 1153

Al-Awadi, J.M.A., 2004. *Sand Flow*, Specialized Book series, First Edition, Kuwait Institute for Scientific Advancement, Directorate of Scientific Culture, state of Kuwait, P. 216

Al-Dabi, H., Koch, M., Al-Sarawi, M., El-Baz, F., 1997. Evolution of sand dune patterns in space and time in north-western Kuwait using Landsat images. *Journal of Arid Environments*, 15-24

Al-Hajri, D., Abahusain, A.A., Abdeh, A.S.A., Sadiq, A.A., 2009. A Study on the movement of sand dunes and its effects on Umm Sa'id Industrial City, Qatar, Using Remote Sensing and GIS. Forth National GIS Symposium in Saudi Arabia, Dammam, Kingdom of Saudi Arabia

Amdev Ren, H., Dem, R.N., Kanik, A., Kesk, N.S., 2005. Use of principal component scores in multiple linear regression models for prediction of Chlorophyll-a in reservoirs. *Ecological Modeling*, 581–589

Bishop, M.A., 2008. COMPARATIVE POINT PATTTERN ANALYSIS OF HYPERBOREAE UNDAE, MARS, AND THE RUB' AL KHALI SAND SEA, EARTH. *Planetary Dunes Workshop: A Record of Climate Change*, Alamogordo, New Mexico

Chang, E.M., Park, K., 2006. Feature Extraction in an Aerial Photography of Gimnyeong Sand Dune Area by Texture Filtering. *Journal of the Korean Geographical Society*, 139-149

Chen, X., Vierling, L., Deering, D., 2005. A simple and effective radiometric correction method to improve landscape change detection across sensors and across time. *Remote Sensing of Environment*, 63-79

El-Sayed, M.I., 1999. Sedimentological characteristics and morphology of the aeolian sand dunes in the eastern part of the UAE: a case study from Ar Rub' Al Khali. *Sedimentary Geology*, 219-238

Embabi, N., El Sharhan, A., Yeiha, A., Abdel Kader, O., Shawki, E., El Badry, K., Kariem, F., 1993. National Atlas of the United Arab Emirates. *Geoprojects Limited*, 198 plates

Embabi, N.S., 1991. Dune types and patterns in the United Arab Emirates using Landsat TM-data. *Proceedings of the 24th International Symposium of Remote Sensing& Environment*. Rio de Janeiro, Brazil, 27-31.

Fung, T., LeDrew, E., 1987. Application of principal components analysis change detection. *Photogrammetric Engineering and Remote Sensing*, 1649 – 1658

Gao, B. C., Heidebrecht, K. B., Goetz, A. F. H., 1993. Derivation of scaled surface reflectances from AVIRIS data. *Remote Sensing of Environment*, 145–163

Gao, J., 2009. *Digital Analysis of Remotely Sensed Imagery*. McGraw-Hill Companies, New York. 689 pp

Gardner AS, Howarth B (2009) Urbanisation in the United Arab Emirates: the challenges for ecological mitigation in a rapidly developing country. In: Krupp F, Musselman LJ, Kotb MMA, Weidig I (Eds) Environment, Biodiversity and Conservation in the Middle East. Proceedings of the First Middle Eastern Biodiversity Congress, Aqaba, Jordan, 20–23 October 2008. BioRisk 3: 27–38.

Gerbermann, A. H., & Neher, D. D., 1979. Reflectance of varying mixtures of a clay soil and sand. *Photogrammetric Engineering and Remote Sensing*, 1145–1151

Ghadiry, M., Koch, B., 2010. Developing a Monitoring System for Sand Dunes Migration in Dakhla Oasis, Western Desert, Egypt. *Remote Sensing for Science, Education, and Natural and Cultural Heritage*, 313-320

Glennie, K.W., 2001. Evolution of the emirates' land surface: an introduction in Al-Abed, I., Hellyr, P., *United Arab Emirates: A New Perspective*, London, Trident Press, 9-27

Gong, P., 1993. Change detection using principal component analysis and fuzzy set theory. *Canadian Journal of Remote Sensing*, 22 – 29

Goodchild M. F., Parks B. O. and Steyaert L. T., 1993. Environmental Modeling with GIS. *Oxford University Press*, New York, 488 p.

Hadeel, A.S., Jabbar, M.T., Chen, X., 2010. Application of remote sensing and GIS in the study of environmental sensitivity to desertification: a case study in Basrah Province, southern part of Iraq. *Appl Geomat*, 101-112

Howari, F.M., Baghdady, A., Goodell, P.C., 2007. Mineralogical and gemorphological characterization of sand dunes in the eastern part of United Arab Emirates using orbital remote sensing integrated with field

investigations. *Geomorphology*. 67-81

Huang. C., Kim. S., Song. K., Townshend. J.R.G. Davis. P., Altstatt. A., Rodas. O., Yanosky. A., Clay.R., Tucker. C.J., Musinsky. J., 2009. Assessment of Paraguay's forest cover change using Landsat observations. *Global and Planetary Change*. 1 – 12

Hunt. G.R., 1982. Spectroscopic properties of rocks and minerals. In Carmichael. R.S., *Handbook of Physical Properties of Rocks*. vol. 1. CRC Press. Boca Raton. FL. 416 P

Hutchison. C.F., 1982. Remote sensing of arid and semi-arid rangeland. *International Geoscience and Remote Sensing symposium*. Munich. Federal Republic of Germany. 5.1-5.6

Ifarraguerri. A., Chang. C.I., 2000. Unsupervised Hyperspectral image analysis with projection pursuit. *IEEE Transactions on Geoscience and Remote Sensing*. 2529–2538

Janke. J.R., analysis of the current stability of the Dune Field at Great Sand Dunes National Monument using temporal TM imagery (1984–1998). *Remote Sensing of Environment*. 488-497

Jensen. J. R. (2005): Introductory digital image processing: a remote sensing perspective. John R. Jensen. 3rd ed., Pearson Education Inc., Upper Saddle River.

Karnieli. A., Tsoar. H., 1995. Spectral Reflectance of biogenic crust developed on desert dune sand along Israel-Egypt border. *International Journal of Remote Sensing*. 369-374

Krishnamurthy. J., Srinivas. G., 1996. Demarcation of the geological and geomorphological features of parts of Dharwar Craton. Karnataka. using IRS LISS-II data. *International Journal of Remote Sensing*. 3271–3288

Kumar. M. , Goossens. E., Goossens. R., 1993. Assessment of sand dune change detection in Rajasthan (Thar) Desert, India. *International Journal of Remote Sensing*. 1689-1703

Lam. D.K., Remmel. T.K., Drezner. T.D., 2011. Tracking Desertification in California Using Remote Sensing: A Sand Dune Encroachment Approach. *Remote Sensing*. 1-13

Larue. E.M., 2004. Using GIS to establish a public library consumer health collection. *Biomedical Digital Libraries*. pp 3

Levin. N., Ben-Dor. E., Karnieli. A., 2004. Topographic information of sand dunes as extracted from shading effects using Landsat images. *Remote Sensing of Environment*. 190-209

Liao, S., Bai Y., 2009. A new grid-cell-based method for error evaluation of vector-to-raster conversion. *Computational Geosciences*

Lillesand, T.M., Kiefer, R.W., 1994. *Remote Sensing and Image Interpretation*. 3rd Edition. John Wiley & Sons, Inc., 230 pp

Lu, D., Mausel, P., Brondizio, E., Moran, E., 2004. Change detection techniques. *International Journal of Remote Sensing*, 2365 – 2407

Masek, J. G., Honzak, M., Goward, S. N., Liu, P., & Pak, E., 2001. Landsat-7 ETM+ as an observatory for land cover: Initial radiometric and geometric comparisons with Landsat-5 Thematic Mapper. *Remote Sensing of Environment*, 118– 130

N.d. Geocaching. Web. 27 Jan. 2016. <https://www.geocaching.com/geocache/GC2VGA8_mesquite-flats-dune-field?guid=c93e835c-617b-4c33-bc61-1e2b484e267a>.

Otazu, X., Arbiol, R., 2000. Land use map production by fusion of multispectral classification of landsat images and texture analysis of high resolution images, international archieved for photogrammetry and remote sensing, Vol. XXXIII, Supplement B7.

Pease, P.P., Bierly, G.D., Tchakerian, V.P., Tindale, N.W., 1999. Mineralogical characterization and transport pathways of dune sand using Landsat TM data. Wahiba Sand Sea, Sultanate of Oman Geomorphology, 235–249.

Pu, R.L., Gong, P., 2000. *Hyperspectral Remote Sensing and Its Application*. High Education Press, Beijing, p. 70

Rajesh, H.M., 2008. Mapping Proterozoic unconformity-related uranium deposits in the Rockhole area, Northern Territory, Australia using Landsat ETM+. *Ore Geology Review*, 382 - 396

Richards, J.A., 2000. *Remote Sensing Digital Image Analysis*, 3rd ed. Springer-Verlag, Berlin, p 190

Richards, J.A., Jia, X., 1999. *Remote Sensing Digital Image Analysis: An Introduction*, 3rd ed. Springer-Verlag, Berlin, 363 p

Sabins, F., 1987. *Remote Sensing: Principles and Interpretation*, 2nd ed. Freeman, New York

Sabins, F.F., 1997. *Remote Sensing: Principles and Interpretation*, W. H. Freeman and Company, New York, 549 pp

Sarnthein, M., 1978. Sand deserts during glacial maximum and climatic optimum. *Nature*, 43–46

Scheidt, S., Ramsey, M., Lancaster, N., 2008. Radiometric normalization and image mosaic generation of ASTER thermal infrared data: An application to extensive sand sheets and dune fields. *Remote Sensing of Environment*, 920-933

Singh, A., 1989. Digital change detection techniques using remotely sensed data. *International Journal of Remote Sensing*, 989 – 1003

Smith, M.O., Ustin, S.L., Adams, J.B., Gillespie, A.R., 1990. Vegetation in deserts: I. A regional measure of abundance from multispectral images. *Remote Sensing of Environment*, 1-26

Sultan, M., Arvidson, R.E., Duncan, I.J., Stern, R., El Kaliouby, B., 1986. Extension of the Najd Fault System from Saudi Arabia to the central Eastern Desert of Egypt based on integrated field and Landsat observations. *Tectonics*, 1291–1306

Summerfield M., 1996. *Global Geomorphology*. Longman Group, Essex, U.K

Teillet, P. M., Barker, J. L., Markham, B. L., Irish, R. R., Fedosejevs, G., & Storey, J. C., 2001. Radiometric cross-calibration of the Landsat-7 ETM+ and Landsat-5 TM sensors based on tandem data sets. *Remote Sensing of Environment*, 39– 54

Tsoar, H., 2001. Types of Aeolian sand dunes and their formation. In Balmforth, N. J., & Provenzale, A., *Lecture Notes in Physics*, 403– 429

Tsoar, H., Blumberg, D.G., Stoler, Y., 2004. Elongation and migration of sand dunes. *Geomorphology*, 293–302.

Tuller, P.T., 1987. Remote Sensing science application in arid environment. *Remote Sensing of Environment*, 143-154

Vincent, R.K., 1997. *Fundamentals of Geological and Environmental Remote Sensing*. Prentice Hall, Upper Saddle River, NJ. 270 pp

Wasson, R. J., & Hyde, R., 1983. Factors determining desert dune type. *Nature*, 337–339

White, K.,Walden, J., Drake, N., Eckardt, F., Settle, J., 1997. Mapping the iron oxide content of dune sands, Namib sand sea, Namibia, using Landsat Thematic Mapper data. *Remote Sensing of Environment*, 30– 39

Yao, Z.Y., Wang, T., Han, Z.W., Zhang, W.M., Zhao, A.G., 2007. Migration of sand dunes on the northern Alxa Plateau, Inner Mongolia, China. *Journal of Arid Environments*, 80-93

Barchan Dunes are crescent shaped and they form in areas where there is a hard ground surface a moderate supply of sand constant wind direction

Transverse Dunes are large fields that resemble sand ripples on a large scale; they form in areas where there is abundant supply of sand and constant wind direction

Barchan Dunes can merge into transvers dunes if the supply of sand increases

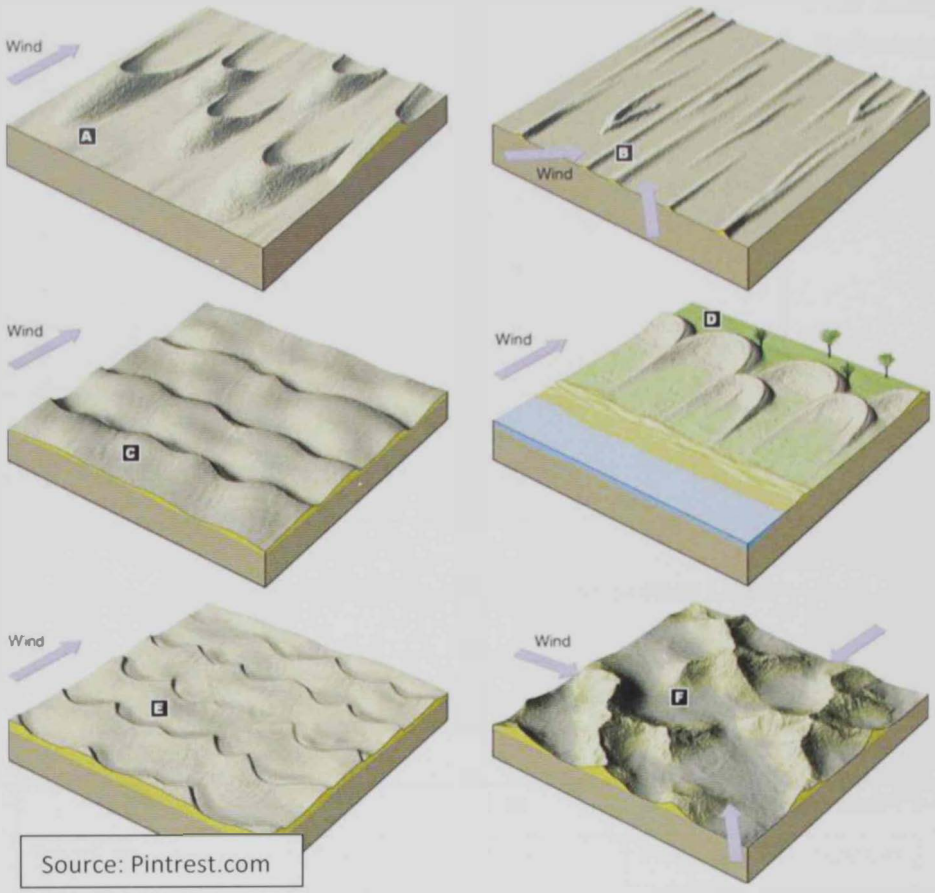

Linear Dunes are long straight dunes that form in areas with limited sand supply and converging wind directions

Parabolic are "U" shaped dunes with an open end facing upwind. They usually stabilized by vegetation, and occur where there is abundant wind direction, a constant wind direction, and an abundant sand supply. They are common in coastal areas

Star dunes are dunes with several arms and variable slip face directions that form in areas where there is abundant sand and variable wind direction

Figure 1.5: Relationship of Dune Pattern & Wind Directions

Row	Path			Resolution	Parameter	Sensor Platform
	162	161	160			
43	04-06-1992	05-06-1992	14-06-1992	30 meters	CDR Surface Reflectance	Landsat 4
	03-07-2002	10-07-2002	12-07-2002			
	01-08-2013	25-07-2013	18-07-2013			Landsat 7
44	04-06-1992	05-06-1992	14-06-1992			
	03-07-2002	10-07-2002	12-07-2002			Landsat 8
	01-08-2013	25-07-2013	18-07-2013			
Datum Projection	WGS 1984 UTM Zone 39 N	WGS 1984 UTM Zone 39 N	WGS 1984 UTM Zone 40 N			

Table 3.1: Summary of Dates and Scenes Used

Data Type	Date	Spatial Resolution	Purpose
Rapid Eye	2013	5 m	Accuracy assessment
IKONOS	2003	1 m	Accuracy Assessment
SPOT Panchromatic	1986	10 m	Accuracy Assessment

Table 3.8: Imagery used for accuracy assessment

Basic Stats	Min	Max	Mean	Stdev
Band 1	-9999	16000	-6252.606775	5504.63962
Band 2	-9999	6170	-5980.524268	5904.184034
Band 3	-9999	6906	-5732.788246	6269.470532
Band 4	-9999	7800	-5505.377137	6605.096761
Band 5	-9999	16000	-5196.9497	7083.101278
Band 6	-9999	16000	-5375.882562	6805.800292

Table 3.5: Original Image

Basic Stats	Min	Max	Mean	Stdev
Band 1	-9998.404297	11334.28711	-6252.606446	5504.383371
Band 2	-9999.154297	10335.90527	-5980.524461	5904.081714
Band 3	-9999.510742	8558.262695	-5732.787964	6269.313087
Band 4	-9999.255859	8426.101563	-5505.376756	6604.653347
Band 5	-9998.989258	16014.30566	-5196.949671	7083.101044
Band 6	-9998.638672	13575.10645	-5375.882695	6805.655311

Table 3.6: Inverse PCA

Number	Class Name	Area (m^2)	Longitude X	Latitude Y
1	Exposed Bedrock	239400	55.85790	24.17674
2	Exposed Bedrock	272700	55.80807	24.12984
3	Exposed Bedrock	329400	55.92488	24.10874
4	Exposed Bedrock	219600	55.87740	24.11057
5	Exposed Bedrock	213300	55.98582	24.07560
6	Exposed Bedrock	78300	55.05485	23.45851

7	Exposed Bedrock	54000	55.14645	23.55011
8	Exposed Bedrock	90000	55.25873	23.38995
9	Exposed Bedrock	57600	55.06358	23.26041
10	Exposed Bedrock	40500	55.08874	23.11769
11	Exposed Bedrock	18900	55.07350	23.09072
12	Exposed Bedrock	56700	55.12020	23.34016
13	Exposed Bedrock	102600	55.13896	23.14545
14	Exposed Bedrock	39600	55.05860	22.99041
15	Exposed Bedrock	36900	55.02905	22.93987
16	Exposed Bedrock	59400	55.17806	23.07842
17	Exposed Bedrock	69300	55.14979	23.00472
18	Exposed Bedrock	20700	55.10206	22.92965
19	Exposed Bedrock	45000	55.19510	22.92255
20	Exposed Bedrock	73800	55.10592	22.66125
21	Intertidal	212400	54.42082	24.31528
22	Intertidal	78300	54.30486	24.29348
23	Intertidal	126000	54.13290	24.17732
24	Sand	39600	54.90911	24.56342
25	Sand	24300	55.20990	24.49442
26	Sand	230400	54.93839	24.21582
27	Sand	496800	55.41940	24.45562
28	Sand	80100	55.17505	24.41627
29	Sand	277200	54.20540	23.96498

30	Sand	162000	54.29597	24.02682
31	Sand	55800	54.95474	24.14206
32	Sand	54900	54.87611	24.10853
33	Sand	781200	55.30071	24.02830
34	Sand	121500	51.83614	23.89597
35	Sand	27000	52.02787	23.80108
36	Sand	900	52.04082	23.76266
37	Sand	98100	52.03862	23.75991
38	Sand	54000	52.10286	23.74464
39	Sand	37800	52.10627	23.69375
40	Sand	900	52.10412	23.69340
41	Sand	234000	52.69980	23.84309
42	Sand	77400	52.61254	23.78852
43	Sand	103500	52.61076	23.77605
44	Sand	233100	52.88266	23.86424
45	Sand	208800	52.75354	23.84472
46	Sand	232200	52.80203	23.80996
47	Sand	90900	52.97576	23.68664
48	Sand	343800	53.28420	23.90807
49	Sand	225900	53.09927	23.91057
50	Sand	359100	53.16407	23.87686
51	Sand	432000	53.50831	23.92628
52	Sand	285300	53.83196	23.92158

53	Sand	369000	53.86812	23.88984
54	Sand	140400	53.87799	23.80317
55	Sand	171000	53.93159	23.93518
56	Sand	181800	54.16804	23.92578
57	Sand	206100	54.02015	23.92853
58	Sand	107100	53.96309	23.90842
59	Sand	309600	53.96782	23.79683
60	Sand	178200	54.15475	23.68377
61	Sand	161100	54.09939	23.67099
62	Sand	665100	54.50263	23.86638
63	Sand	393300	54.36611	23.75372
64	Sand	188100	54.25477	23.70131
65	Sand	203400	55.01988	23.78133
66	Sand	277200	54.85270	23.71927
67	Sand	200700	54.94555	23.70860
68	Sand	219600	55.31098	23.85337
69	Sand	160200	55.15812	23.78481
70	Sand	70200	52.13726	23.53918
71	Sand	181800	52.89853	23.67225
72	Sand	153900	53.83042	23.62315
73	Sand	172800	53.68902	23.61130
74	Sand	179100	54.01496	23.64829
75	Sand	164700	54.02013	23.62419

76	Sand	496800	54.26765	23.50464
77	Sand	748800	54.47902	23.47654
78	Sand	230400	54.81004	23.61255
79	Sand	63000	55.34124	23.47955
80	Sand	68400	55.31925	23.44978
81	Sand	190800	53.32713	22.97557
82	Sand	199800	53.54490	22.94772
83	Sand	162000	53.52320	22.92214
84	Sand	128700	54.21428	23.04178
85	Sand	162900	54.23936	23.02597
86	Sand	243000	53.59601	23.94774
87	Wet Soil	360000	54.69626	24.72054
88	Wet Soil	167400	51.88118	23.97313
89	Wet Soil	593100	52.56356	24.08089
90	Wet Soil	221400	52.93105	24.11449
91	Wet Soil	547200	53.30494	24.07995
92	Wet Soil	360900	53.72570	24.01713
93	Wet Soil	541800	54.13168	24.12557
94	Wet Soil	148500	54.34816	24.17384

Table 3.7: List of accuracy assessment sites

From - To	Area (Km^2)
No Change	53775.08
Exposed Rock - Intertidal	5.34
Exposed Rock - Surface Water	1.72
Exposed Rock - Sand	617.22
Exposed Rock - Vegetation	72.20
Exposed Rock - Wet Soil	212.83
Intertidal - Exposed Rock	13.23
Intertidal - Surface Water	271.24
Intertidal - Sand	33.42
Intertidal - Vegetation	48.89
Intertidal - Wet Soil	122.54
Surface Water- Exposed Rock	0.34
Surface Water- Intertidal	73.84
Surface Water- Sand	8.06
Surface Water- Vegetation	0.03
Surface Water- Wet Soil	10.54
Sand - Exposed Rock	684.87
Sand - Intertidal	10.29
Sand - Surface Water	0.12
Sand - Vegetation	310.57
Sand - Wet Soil	1208.96
Vegetation - Exposed Rock	54.78
Vegetation - Intertidal	6.21
Vegetation - Surface Water	1.94
Vegetation - Sand	8.46

Vegetation - Wet Soil	1.95
Wet Soil - Exposed Rock	159.92
Wet Soil - Intertidal	112.57
Wet Soil - Surface Water	1.84
Wet Soil - Sand	2095.20
Wet Soil - Vegetation	13.48

Table 4.8: Changes from 1992 to 2002 statistics

From - To	Area (Km^2)
No Change	49967.90
Exposed Rock - Sand	617.22
Intertidal - Sand	33.42
Surface Water- Sand	8.06
Sand - Exposed Rock	684.87
Sand - Intertidal	10.29
Sand - Surface Water	0.12
Sand - Vegetation	310.57
Sand - Wet Soil	1208.96
Vegetation - Sand	8.46
Wet Soil - Sand	2095.20

Table 4.9: Changes for sand features from 1992 to 2002 statistics

From - To	Area (Km^2)
No Change	53689.72
Exposed Rock - Intertidal	7.43
Exposed Rock - Surface Water	0.30

Exposed Rock - Sand	421.40
Exposed Rock - Vegetation	132.50
Exposed Rock - Wet Soil	43.88
Intertidal - Exposed Rock	71.34
Intertidal - Surface Water	20.55
Intertidal - Sand	179.47
Intertidal - Vegetation	46.35
Intertidal - Wet Soil	79.54
Surface Water- Exposed Rock	41.23
Surface Water- Intertidal	648.32
Surface Water- Sand	8.00
Surface Water- Vegetation	0.32
Surface Water- Wet Soil	5.09
Sand - Exposed Rock	1408.30
Sand - Intertidal	8.23
Sand - Surface Water	7.30
Sand - Vegetation	51.14
Sand - Wet Soil	765.01
Vegetation - Exposed Rock	219.40
Vegetation - Intertidal	25.89
Vegetation - Surface Water	0.09
Vegetation - Sand	82.14
Vegetation - Wet Soil	1.63
Wet Soil - Exposed Rock	797.72
Wet Soil - Intertidal	94.61
Wet Soil - Surface Water	6.04
Wet Soil - Sand	1665.73

Wet Soil - Vegetation	19.90

Table 4.10: Changes from 2002 to 2013 statistics

From - To	Area (Km^2)
No Change	50488.08
Exposed Rock - Sand	421.40
Intertidal - Sand	179.47
Surface Water- Sand	8.00
Sand - Exposed Rock	1408.30
Sand - Intertidal	8.23
Sand - Surface Water	7.30
Sand - Vegetation	51.14
Sand - Wet Soil	765.01
Vegetation - Sand	82.14
Wet Soil - Sand	1665.73

Table 4.11: Changes for sand features from 2002 to 2013 statistics

From 1992 to 2002 to 2013	Km^2
No Change	48467.49
Exposed Rock - Exposed Rock - Sand	134.1106
Exposed Rock - Intertidal - Sand	0.287151
Exposed Rock - Surface Water- Sand	0.0027
Exposed Rock - Sand - Exposed Rock	116.5672
Exposed Rock - Sand - Intertidal	0.036308
Exposed Rock - Sand - Sand	491.2252
Exposed Rock - Sand - Vegetation	4.983226

Exposed Rock - Sand - Wet Soil	4.343693
Exposed Rock - Vegetation - Sand	4.497708
Exposed Rock - Wet Soil - Sand	122.1677
Intertidal - Exposed Rock - Sand	0.738053
Intertidal - Intertidal - Sand	154.1987
Intertidal - Surface Water- Sand	2.711898
Intertidal - Sand - Exposed Rock	5.080186
Intertidal - Sand - Intertidal	0.861521
Intertidal - Sand - Surface Water	0.008743
Intertidal - Sand - Sand	20.34425
Intertidal - Sand - Vegetation	0.412198
Intertidal - Sand - Wet Soil	6.685668
Intertidal - Vegetation - Sand	5.144544
Intertidal - Wet Soil - Sand	37.92144
Surface Water- Exposed Rock - Sand	0.006712
Surface Water- Intertidal - Sand	0.75412
Surface Water- Sand - Exposed Rock	0.232169
Surface Water- Sand - Intertidal	0.011572
Surface Water- Sand - Sand	0.338892
Surface Water- Sand - Vegetation	0.046158
Surface Water- Sand - Wet Soil	0.159404
Surface Water- Vegetation - Sand	0.0018
Surface Water- Wet Soil - Sand	1.131525
Sand - Exposed Rock - Exposed Rock	371.2412
Sand - Exposed Rock - Intertidal	0.111265
Sand - Exposed Rock - Surface Water	0.050273
Sand - Exposed Rock - Sand	252.3309

Sand - Exposed Rock - Vegetation	51.22143
Sand - Exposed Rock - Wet Soil	9.705026
Sand - Intertidal - Exposed Rock	1.412122
Sand - Intertidal - Intertidal	0.76174
Sand - Intertidal - Surface Water	0.007277
Sand - Intertidal - Sand	6.568865
Sand - Intertidal - Vegetation	0.118052
Sand - Intertidal - Wet Soil	1.413691
Sand - Surface Water- Exposed Rock	0.021575
Sand - Surface Water- Intertidal	0.030419
Sand - Surface Water- Open Water	0.029469
Sand - Surface Water- Sand	0.0189
Sand - Surface Water- Wet Soil	0.01566
Sand - Sand - Exposed Rock	1058.593
Sand - Sand - Intertidal	1.470492
Sand - Sand - Surface Water	0.00882
Sand - Sand - Vegetation	40.24828
Sand - Sand - Wet Soil	397.9692
Sand - Vegetation - Exposed Rock	158.3852
Sand - Vegetation - Intertidal	0.125357
Sand - Vegetation - Sand	66.16132
Sand - Vegetation - Vegetation	85.52665
Sand - Vegetation - Wet Soil	0.210803
Sand - Wet Soil - Exposed Rock	293.8213
Sand - Wet Soil - Intertidal	2.563589
Sand - Wet Soil - Surface Water	0.134048
Sand - Wet Soil - Sand	642.4969

Sand - Wet Soil - Vegetation	5.43866
Sand - Wet Soil - Wet Soil	264.1563
Vegetation - Exposed Rock - Sand	12.77711
Vegetation - Intertidal - Sand	0.300238
Vegetation - Surface Water- Sand	2.57E-05
Vegetation - Sand - Exposed Rock	3.165749
Vegetation - Sand - Intertidal	0.0144
Vegetation - Sand - Sand	4.137737
Vegetation - Sand - Vegetation	1.105305
Vegetation - Sand - Wet Soil	0.035177
Vegetation - Vegetation - Sand	5.916207
Vegetation - Wet Soil - Sand	0.198693
Wet Soil - Exposed Rock - Sand	21.38466
Wet Soil - Intertidal - Sand	17.3575
Wet Soil - Surface Water- Sand	0.001003
Wet Soil - Sand - Exposed Rock	224.6085
Wet Soil - Sand - Intertidal	5.829352
Wet Soil - Sand - Surface Water	0.011211
Wet Soil - Sand - Sand	1504.255
Wet Soil - Sand - Vegetation	4.33453
Wet Soil - Sand - Wet Soil	355.7941
Wet Soil - Vegetation - Sand	0.407027
Wet Soil - Wet Soil - Sand	861.7374

Table 4.12: Sand / Non Sand change analysis statistics from 1992 -2002 -2013

Digitally signed by Shrieen
DN: cn=Shrieen, o=UAE University, ou=UAEU Libraries Deanship, email=shrieen@uaeu.ac.ae, c=US
Date: 2016.06.14 13:40:56 '+02'00'

UAEU Libraries Deanship